

**Contract No:**

This document was prepared in conjunction with work accomplished under Contract No. DE-AC09-08SR22470 with the U.S. Department of Energy (DOE) Office of Environmental Management (EM).

**Disclaimer:**

This work was prepared under an agreement with and funded by the U.S. Government. Neither the U. S. Government or its employees, nor any of its contractors, subcontractors or their employees, makes any express or implied:

- 1 ) warranty or assumes any legal liability for the accuracy, completeness, or for the use or results of such use of any information, product, or process disclosed; or
- 2 ) representation that such use or results of such use would not infringe privately owned rights; or
- 3) endorsement or recommendation of any specifically identified commercial product, process, or service.

Any views and opinions of authors expressed in this work do not necessarily state or reflect those of the United States Government, or its contractors, or subcontractors.



# Defense Waste Processing Facility (DWPF) Viscosity Model: Revisions for Processing High $\text{TiO}_2$ Containing Glasses

C.M. Jantzen

T.B. Edwards

AUGUST 2016

SRNL-STI-2016-00115, Revision 0



## **DISCLAIMER**

This work was prepared under an agreement with and funded by the U.S. Government. Neither the U.S. Government or its employees, nor any of its contractors, subcontractors or their employees, makes any express or implied:

1. warranty or assumes any legal liability for the accuracy, completeness, or for the use or results of such use of any information, product, or process disclosed; or
2. representation that such use or results of such use would not infringe privately owned rights; or
3. endorsement or recommendation of any specifically identified commercial product, process, or service.

Any views and opinions of authors expressed in this work do not necessarily state or reflect those of the United States Government, or its contractors, or subcontractors.

**Printed in the United States of America**

**Prepared for  
U.S. Department of Energy**

**Keywords:** *DWPF, process control, viscosity, Salt Waste Processing Facility, Monosodium Titanate, Crystalline Silicon Titanate*

**Retention:** *Permanent*

## **Defense Waste Processing Facility (DWPF) Viscosity Model: Revisions for Processing High TiO<sub>2</sub> Containing Glasses**

C.M. Jantzen  
T.B. Edwards

August 2016

---

Prepared for the U.S. Department of Energy under contract number DE-AC09-08SR22470.



## REVIEWS AND APPROVALS

### AUTHORS:

---

C.M. Jantzen, Engineering Process Development	Date
---	------

---

T.B. Edwards, Engineering Process Development	Date
---	------

### TECHNICAL REVIEW:

---

D.L. McClane, Engineering Process Development	Date
---	------

---

K.M. Fox, Hanford Mission Programs	Date
------------------------------------	------

---

C.L. Trivelpiece, Engineering Process Development, Reviewed per E7 2.60	Date
---	------

### APPROVAL:

---

E.N. Hoffman, Manager Engineering Process Development	Date
--	------

---

D.E. Dooley, Director Environmental & Chemical Process Technology Research Programs	Date
--	------

---

E.J. Freed, Manager DWPF Engineering	Date
---	------

## **ACKNOWLEDGEMENTS**

The research presented in this document was sponsored by the Savannah River Defense Waste Processing Facility (DWPF) in connection with work done under Contract No. DE-AC09-96SR18500 with the U.S. Department of Energy. The development of the 1991 and 2005 viscosity models was completed and the associated validation data were accumulated from 1988 to present under DOE Contracts No. DE-AC09-89SR18035 with E.I. DuPont deNemours & Co., Contract No. DE-AC09-96SR18500 with Westinghouse Savannah River Co. (WSRC) and Washington Group Inc. (WGI), and Contract No. DE-AC09-08SR22470 with Savannah River Nuclear Solutions (SRNS).

## EXECUTIVE SUMMARY

Radioactive high level waste (HLW) at the Savannah River Site (SRS) has successfully been vitrified into borosilicate glass in the Defense Waste Processing Facility (DWPF) since 1996. Vitrification requires stringent product/process (P/P) constraints since the glass cannot be reworked once it is poured into ten foot tall by two foot diameter canisters. A unique “feed forward” statistical *process* control (SPC) was developed for this control rather than statistical *quality* control (SQC). In SPC, the feed composition to the DWPF melter is controlled *prior* to vitrification. In SQC, the glass product would be sampled *after* it is vitrified. Individual glass property-composition models form the basis for the “feed forward” SPC. The models transform constraints on the melt and glass properties into constraints on the feed composition going to the melter in order to guarantee, at the 95% confidence level, that the feed will be processable and that the durability of the resulting waste form will be acceptable to a geologic repository.

The DWPF SPC system is known as the Product Composition Control System (PCCS). One of the process models within the PCCS is the viscosity model which was developed in 1991 with as-batched compositions and revised in 2005 with as-measured compositions which made the model more accurate. The form and terms in the viscosity model did not change between 1991 and 2005, only the fitted coefficients changed. The 2005 model will be referred to as the “historic” PCCS viscosity model throughout this document.

The DWPF viscosity model is based on bond counting of bridging oxygen (BO) and non-bridging oxygen (NBO) bonds and melt temperature. Bridging oxygen bonds polymerize the glass and NBO's depolymerize the glass. A larger NBO term indicates a very fluid melt with a low viscosity while a smaller NBO term indicates a more viscous melt, i.e. one with a higher viscosity. In 2005 it was also shown that the viscosity model did not need a uranium term as the impact of BO's and NBO's around a uranium atom in glass cancel each other out in the model.

The DWPF PCCS modeling approach for each property model, is parsimonious in that the oxide terms in each model are only those which are necessary and sufficient to describe the glass property of interest. This approach excludes composition terms that are unnecessary to the implementation of the DWPF flowsheets and helps to minimize the sources of error in the PCCS models. Another aspect of the PCCS process models, that minimizes the sources of error, is that oxide terms that have a similar impact on the glass property being modeled can be grouped, i.e.  $\text{Na}_2\text{O}$ ,  $\text{Li}_2\text{O}$ ,  $\text{K}_2\text{O}$  and  $\text{Cs}_2\text{O}$  are grouped in the viscosity model as they each create two NBO bonds per mole of alkali present. These parsimonious models have successfully operated the DWPF vitrification process over the last 20 years.

The DWPF will soon be receiving wastes from the Salt Waste Processing Facility (SWPF) containing increased concentrations of  $\text{TiO}_2$ ,  $\text{Na}_2\text{O}$ , and  $\text{Cs}_2\text{O}$ . The SWPF is being built to pretreat the high-curie fraction of the salt waste to be removed from the HLW tanks in the F- and H-Area Tank Farms at the SRS. The SWPF contains unit operations that remove and concentrate the radioactive cesium ( $^{137}\text{Cs}$ ), strontium ( $^{90}\text{Sr}$ ), and actinides from the bulk salt solution feed. Separation processes planned at SRS include caustic side solvent extraction (CSSX), for  $^{137}\text{Cs}$  removal, and ion exchange/sorption of  $^{90}\text{Sr}$  and alpha-emitting radionuclides with monosodium titanate (MST which is  $\text{NaHTi}_2\text{O}_5 \cdot 2.8\text{H}_2\text{O}$ ). The predominant alpha-emitting radionuclides in the highly alkaline waste solutions include plutonium isotopes  $^{238}\text{Pu}$ ,  $^{239}\text{Pu}$  and  $^{240}\text{Pu}$ . The MST is the source of the  $\text{TiO}_2$  and  $\text{Na}_2\text{O}$  enriched wastes while the  $\text{Cs}_2\text{O}$  is derived from the CSSX stream that will be coming to the DWPF from the SWPF.

The SWPF process will replace the current Actinide Removal Process (ARP)/Modular CSSX Unit (MCU) process currently in use. The ARP already sends MST to the DWPF for vitrification but the volume of the ARP product, including the associated MST component, is less than the volume anticipated with the SWPF MST wastes. Currently, the DWPF is operating under a  $\text{TiO}_2$  solubility constraint of 2 wt%  $\text{TiO}_2$  in the final glass. At the 2.0 wt% solubility concentration, a  $\text{TiO}_2$  term was not needed in the PCCS viscosity model and the existing  $\text{TiO}_2$  terms in the PCCS durability and liquidus models had not been validated at  $\text{TiO}_2$  concentrations greater than 2.0 wt%.

In order to process  $\text{TiO}_2$  concentrations >2.0 wt% in the DWPF, new viscosity data were developed over the range of 1.90 to 5.85 wt%  $\text{TiO}_2$  (measured compositions for glasses that were considered acceptable for modeling) and evaluated against the 2005 historic viscosity model. The viscosities measured for the SWPF study glasses were designed to cover the anticipated concentrations of  $\text{TiO}_2$ ,  $\text{Na}_2\text{O}$ , and  $\text{Cs}_2\text{O}$  based on the projected volumes of SWPF. These glasses were also designed to cover any gaps in  $\text{TiO}_2$  content above the 2.0 wt% solubility limit and the 6.0 wt% maximum  $\text{TiO}_2$  anticipated during coupled (sludge + SWPF product) processing at DWPF. At the same time, the adequacy of the  $\text{Na}_2\text{O}$  and  $\text{Cs}_2\text{O}$  viscosity terms were evaluated over the SWPF target range, i.e. 8 to 18 wt%  $\text{Na}_2\text{O}$  and 0.3 to 1.0 wt%  $\text{Cs}_2\text{O}$  since the historic DWPF viscosity model only covers 5.8-15.8 wt%  $\text{Na}_2\text{O}$  and 0-0.33 wt%  $\text{Cs}_2\text{O}$ .

As part of the PCCS durability model and Reduction of Constraints (ROC)  $\text{TiO}_2$  assessment, a 4.0 wt%  $\text{Al}_2\text{O}_3$  restriction had to be placed on the ROC for SWPF high  $\text{TiO}_2$  containing glasses. The durability and ROC assessment will be documented in a separate study, but the impact of the change in the ROC meant that several SWPF study glasses were removed from viscosity modeling which altered the ranges for  $\text{TiO}_2$  in the glass to 1.9-5.85 wt%. Within measurement error, the 5.85 wt%  $\text{TiO}_2$  limit can be rounded up to 6.0 wt%  $\text{TiO}_2$ , the projected upper limit for the SWPF study, and the mechanistic  $\text{TiO}_2$  viscosity model will adequately predict. Conversely, the analyzed high  $\text{TiO}_2$  glasses were higher in  $\text{Na}_2\text{O}$  and  $\text{Cs}_2\text{O}$  than the target concentrations giving a range of 8.03-18.14 wt%  $\text{Na}_2\text{O}$  and 0.48-1.62 wt%  $\text{Cs}_2\text{O}$ . It was determined that the  $\text{Na}_2\text{O}$  and  $\text{Cs}_2\text{O}$  terms in the historic viscosity model were adequate up to these high concentrations and that a  $\text{TiO}_2$  term was needed in the model to adequately describe the impact of higher  $\text{TiO}_2$  concentrations on melt viscosity. This model will be called the SWPF  $\text{TiO}_2$ -only viscosity model throughout this study.

This study documents the development of a  $\text{TiO}_2$  term, as a depolymerizing agent in the glass (creating NBO's), for the historic PCCS viscosity model. The  $\text{TiO}_2$ -only viscosity model spans from 0.00 to 5.85 wt%  $\text{TiO}_2$  since the historic and SWPF datasets were pooled to develop the model and the  $\text{TiO}_2$ -only viscosity model was validated up to 5.90 wt%  $\text{TiO}_2$ . At  $\text{TiO}_2$  concentrations up to ~6.0 wt%, Ti is octahedral (6-coordinated) and acts as a depolymerizing agent in the glass based on literature studies. Note that validation limits are not model limits and they are not solubility limits.

Several additional SRNL viscosity studies were examined at  $\text{TiO}_2$  concentrations up to 8.38 wt%. These studies indicate that  $\text{TiO}_2$  acts as a polymerizing agent and is tetrahedrally coordinated (4-coordinated) in waste glasses at these higher concentrations. The literature indicates that the switch in the role of  $\text{TiO}_2$  from NBO to BO varies with the complexity of the overall glass composition. The exact  $\text{TiO}_2$  concentrations at which  $\text{TiO}_2$  switches from a network modifier to a network former lies somewhere between ~6.00 and 8.00 wt%  $\text{TiO}_2$  and additional studies would have to be performed to determine this limit. These higher  $\text{TiO}_2$  studies are not evaluated in this modeling report as this would change the sign of the  $\text{TiO}_2$  term in the viscosity model from a depolymerizing agent (positive term) to a polymerizing agent (negative term).



Therefore the TiO<sub>2</sub>-only SWPF viscosity model takes the following form:

$$\log \eta(\text{poise}) = -0.606597 + \left( \frac{4587.5797}{T(^{\circ}\text{C})} \right) - (1.711755 * NBO)$$

where 
$$NBO \equiv \frac{2(Na_2O + K_2O + Cs_2O + Li_2O) + 2(Fe_2O_3 - Al_2O_3) + B_2O_3 + TiO_2}{SiO_2}$$

With an adjusted R<sup>2</sup> = 0.9541 and a root mean square error of 0.1012 in log (poise) units.

Since the TiO<sub>2</sub>-only viscosity model contained glasses with Cs<sub>2</sub>O up to 1.62 wt%, the new SWPF data validated the Cs<sub>2</sub>O term used in the historic and TiO<sub>2</sub>-only DWPF viscosity models. The TiO<sub>2</sub>-only model was also shown to be valid up to 4.14 wt% CaO and 2.92 wt% MgO. This means that CaO and/or MgO can be added to frit compositions up to these concentrations since CaO is known to suppress nepheline crystallization and MgO is known to improve glass durability and reduce DWPF refractory corrosion and wear.

An alternate viscosity model is also derived for potential future use, should the DWPF ever need to process other titanate containing ion exchange materials, such as crystalline silicotitanate (CST - Na<sub>1.5</sub>Nb<sub>0.5</sub>Ti<sub>1.5</sub>O<sub>3</sub>SiO<sub>4</sub>•2H<sub>2</sub>O). The CST viscosity model is not being implemented currently as the DWPF is not processing CST nor does it appear likely that CST will be processed in the near future. The CST contains Nb<sub>2</sub>O<sub>5</sub> and Nb would then become an element in the glass that is reportable to the geologic repository. This would require a revision to the DWPF Waste Acceptance Product Specifications (WAPS). In addition, the measurement uncertainty needed to implement an Nb term in PCCS is currently not available. Therefore, the CST viscosity model is being provided for future use should the DWPF have to process CST. When CST processing becomes necessary, the other implementation requirements associated with a CST viscosity model will be addressed. The CST viscosity model takes the following form:

$$\log \eta(\text{poise}) = -0.629934 + \left( \frac{4547.3573}{T(^{\circ}\text{C})} \right) - (1.622574 * NBO)$$

where

$$NBO \equiv \frac{2(Na_2O + K_2O + Cs_2O + Li_2O + Fe_2O_3 + Nb_2O_5 - Al_2O_3) + B_2O_3 + TiO_2 - ZrO_2}{SiO_2}$$

With an adjusted R<sup>2</sup>=0.9397 and a RMSE=0.1033 which are somewhat lower and higher, respectively, than the values for the TiO<sub>2</sub>-only model.

The CST, also known as IE-911, is remarkable for its ability to separate parts-per-million concentrations of cesium from highly alkaline solutions (pH>14) containing high sodium concentrations (>5M). It is also highly effective for removing cesium from neutral and acidic solutions, and for removing strontium from basic and neutral solutions. Therefore, the DWPF may receive CST generated by an alternate flowsheet if used to pretreat the high-curve fraction of the SRS salt waste. The CST not only contains TiO<sub>2</sub> but also contains Nb<sub>2</sub>O<sub>5</sub> and a ZrO<sub>2</sub> binder where TiO<sub>2</sub> and Nb<sub>2</sub>O<sub>5</sub> act to depolymerize the glass (create NBO's) and ZrO<sub>2</sub> polymerizes the glass (creates BO's). The MST would still be used for <sup>90</sup>Sr removal so this viscosity model would cover future DWPF processing of CST alone or coupled CST-

MST flowsheet additions. When the SWPF model glasses ( $\text{TiO}_2=1.90\text{-}5.85$  wt%) and the CST model and validation glasses ( $\text{TiO}_2=3.03\text{-}6.62$ ,  $\text{Nb}_2\text{O}_5=0.03\text{-}2.30$  wt% and  $\text{ZrO}_2=0.15\text{-}2.09$  wt%) are combined with the historic DWPF viscosity database ( $\text{TiO}_2=0\text{-}1.78$  wt%), the MST glass data cover a wider range of  $\text{TiO}_2$  than the CST or historic viscosity data. The  $\text{Nb}_2\text{O}_5$  and  $\text{ZrO}_2$  terms are derived solely from the CST data as neither the SWPF viscosity data nor the historic viscosity data contain these species.

While the SWPF  $\text{TiO}_2$ -only viscosity model has been modeled/validated up to  $\sim 6$  wt% (actual of 5.85 wt%  $\text{TiO}_2$ ) and the CST viscosity model has been modeled/validated up to 6.62 wt%  $\text{TiO}_2$ . The role of  $\text{TiO}_2$  as a network breaker switches to a network former somewhere between 6.62 and 8.38 wt%  $\text{TiO}_2$ . The exact region at which this switch occurs has not been investigated so the usage of the SWPF  $\text{TiO}_2$ -only viscosity model is  $\sim 6$  wt%  $\text{TiO}_2$  and the CST model is  $\sim 6.5$  wt%  $\text{TiO}_2$ .

The ultimate limit on the amount of  $\text{TiO}_2$  that can be accommodated from SWPF will be determined by the three PCCS models, the waste composition of a given sludge batch, the waste loading of the sludge batch, and the frit used for vitrification. Once a component like  $\text{TiO}_2$  is present at larger concentrations than 1-2 wt%, the interactions of that component with other components in the melter feed must be considered simultaneously, i.e. an individual solubility limit cannot be defined to globally account for the interactions with all the remaining sludge/frit composition variables. It is known that  $\text{Ti}^{4+}$  competes with  $\text{Al}^{3+}$  for alkali bonding and it is known that  $\text{Ti}^{4+}$  and  $\text{Fe}^{3+}$  have a coupled impact on their joint solubility in a glass.

## TABLE OF CONTENTS

EXECUTIVE SUMMARY .....	vi
LIST OF TABLES .....	xii
LIST OF FIGURES .....	xiii
LIST OF ABBREVIATIONS .....	xiv
1.0 Introduction .....	1
1.1 The DWPF PCCS Historical Viscosity Model .....	2
1.2 Quality Assurance .....	8
2.0 DWPF Process/Product (P/P) Modeling Constraints .....	8
2.1 Modeling Constraints Common to PCCS Models .....	8
2.2 Modeling Constraints Unique to the PCCS Viscosity Model .....	9
3.0 Defining Future DWPF Processing Ranges .....	10
4.0 Experimental .....	11
4.1 Historic Viscosity Model and Validation Databases [from Reference 17] .....	11
4.2 SWPF (TiO <sub>2</sub> -only) Viscosity Model Database .....	15
4.3 SWPF (TiO <sub>2</sub> -only) Viscosity Validation Database .....	16
4.4 CST Viscosity Model Database .....	16
4.5 CST Viscosity Validation Database .....	17
5.0 SWPF (TiO <sub>2</sub> -only) Viscosity Model .....	18
5.1 Evaluation of the SWPF Glasses Against the Historic DWPF Viscosity Model .....	18
5.2 Structural Role of TiO <sub>2</sub> in DWPF Glasses .....	19
5.3 Development of the SWPF (TiO <sub>2</sub> -only) Viscosity Model .....	19
5.4 Property Acceptable Region (PAR) Assessments for the SWPF (TiO <sub>2</sub> -only) Viscosity Model .....	20
5.5 Validation of the SWPF (TiO <sub>2</sub> -only) Viscosity Model .....	27
6.0 CST TiO <sub>2</sub> -Nb <sub>2</sub> O <sub>5</sub> -ZrO <sub>2</sub> Viscosity Model .....	28
6.1 Evaluation of the CST Model Glasses Against the Historic DWPF Viscosity Model .....	28
6.2 Structural Role of TiO <sub>2</sub> , Nb <sub>2</sub> O <sub>5</sub> and ZrO <sub>2</sub> in DWPF Glasses .....	28
6.3 Development of the CST (TiO <sub>2</sub> -Nb <sub>2</sub> O <sub>5</sub> -ZrO <sub>2</sub> ) Viscosity Model .....	29
6.4 Property Acceptable Region (PAR) Assessments for the CST (TiO <sub>2</sub> -Nb <sub>2</sub> O <sub>5</sub> -ZrO <sub>2</sub> ) Viscosity Model .....	30
6.5 Validation of the CST (TiO <sub>2</sub> -Nb <sub>2</sub> O <sub>5</sub> -ZrO <sub>2</sub> ) Viscosity Model .....	35
7.0 Conclusions .....	36
8.0 Acknowledgements .....	37

APPENDIX A. Historic Glass Model Database .....	38
APPENDIX B. Modeling Constraints .....	42
B.1 The Homogeneity and Low $\text{Al}_2\text{O}_3$ Constraint.....	42
B.2 High $\text{P}_2\text{O}_5$ Constraint .....	43
B.3 High $\text{B}_2\text{O}_3$ Constraint.....	43
APPENDIX C. SWPF ( $\text{TiO}_2$ -only) Glass Database .....	44
APPENDIX D. SWPF ( $\text{TiO}_2$ -only) Validation Database .....	48
APPENDIX E. CST ( $\text{TiO}_2$ - $\text{Nb}_2\text{O}_5$ - $\text{ZrO}_2$ ) Glass Model Database .....	57
APPENDIX F. CST Glass Validation Database (KT-04 to KT-10 Studies) .....	66
9.0 References.....	73

## LIST OF TABLES

Table 1. Waste Glass Product and Process (P/P) Constraints.....	1
Table 2. Composition, Temperature, and Viscosity Range of DWPF Viscosity Model.....	7
Table 3. Oxide Intervals for Reduction of Constraints Study for Coupled Operations with ARP and MCU .....	10
Table 4. Oxide Intervals for SWPF Gap Analysis Study.....	11
Table 5. Temperature, Viscosity and Composition Ranges for the Historical DWPF Viscosity Model (see Appendix A for individual analyses) .....	12
Table 6. References for Viscosity Model and Validation .....	13
Table 7. CST Model Data vs. Validation Data Randomly Selected .....	17
Table 8. a Vectors and Offsets for the TiO <sub>2</sub> -Only Viscosity Model Constraints .....	26
Table 9. a Vectors and Offsets for the CST Viscosity Model Constraints.....	34

## LIST OF FIGURES

Figure 1-1. DWPF viscosity model showing the relationship between composition (NBO), viscosity and temperature. ....	5
Figure 2-1. Graphical Representation of the Constraints Applied to the Choice of Model and Validation Data for the Durability, Viscosity, and Liquidus P/P Models for glasses with 0-2.00 wt% TiO <sub>2</sub> . The Al <sub>2</sub> O <sub>3</sub> term in the inhomogeneous by visible crystallization is 2.99 wt% to accommodate the WCP Purex glass which contains 2.99 wt% Al <sub>2</sub> O <sub>3</sub> . ....	9
Figure 2-2. Graphical Representation of the Constraints Applied to the Choice of Model and Validation Data for the Durability, Viscosity, and Liquidus P/P Models for glasses with 0-2.00 wt% TiO <sub>2</sub> and glasses with ≥ 2.00 wt% TiO <sub>2</sub> . The Al <sub>2</sub> O <sub>3</sub> term in the “inhomogeneous by visible crystallization” box is 2.99 wt% to accommodate the WCP Purex glass. ....	9
Figure 5-1. Comparisons of the Historic and SWPF Database Glasses Using the Historic DWPF Viscosity Model (Equations 1 and 3). ....	19
Figure 5-2. New SWPF TiO <sub>2</sub> -only Model fit to Pooled SWPF and Historic Databases and Fit Separately. ....	20
Figure 5-3. Validation Data from Appendix D (116 viscosity-temperature-NBO combinations) overlain on the SWPF (TiO <sub>2</sub> -only) model developed from the SWPF and Historic glass Databases in Appendices B and C (334 viscosity-temperature-NBO combinations). Vertical lines indicate DWPF processing limits. ....	28
Figure 6-1. CST Viscosity Model with terms for TiO <sub>2</sub> , Nb <sub>2</sub> O <sub>5</sub> , and ZrO <sub>2</sub> . Note that there were 5 different KT studies and so there are 5 different symbols on the figure but all the KT studies are shaded gray. ....	30
Figure 6-2. Validation Data from Appendix F (201 viscosity-temperature-NBO combinations) overlain on the CST viscosity model developed from the CST, KT (5 different studies shown with 5 different symbols), SWPF, and Historic glass Databases in Appendices B, C, and E (577 viscosity-temperature-NBO combinations). ....	36

## LIST OF ABBREVIATIONS

AD	Analytic Development
APS	Amorphous Phase Separation
ARP	Actinide Removal Process
ASME	American Society of Mechanical Engineers
ASTM	American Society for Testing and Materials
BO	Bridging Oxygen
CELS	Corning Engineering Laboratory Services
OCF	Owens Corning Fiberglass
CPS	Crystalline Phase Separation
CSSX	Caustic-Side Solvent Extraction
CST	Crystalline SilicoTitanate
DCP	Direct Current Plasma Emission Spectrometry
DOE	Department of Energy
DSS	Dissolved Salt Solution
DWPF	Defense Waste Processing Facility
EPA	Environmental Protection Agency
EPAR	Expected Property Acceptable Region
ES-VSL	Energy Solutions – Vitreous State Laboratory
HLW	High Level Waste
IC	Ion Chromatography
ICP-ES	Inductively Coupled Plasma-Emission Spectroscopy
IDMS	Integrated DWPF Melter System
L95	Lower 95% confidence interval
MAR	Measurement Acceptable Region
MAS NMR	Magic Angle Spinning Nuclear Magnetic Resonance
MCU	Modular CSSX Unit
MST	MonoSodium Titanate
NBO	Non-Bridging Oxygen
NBS	National Bureau of Standards
NQA	Nuclear Quality Assurance
OCF-SS	Owens Corning Fiberglass-Sharp Shurtz
P/P	Product/Process
PAR	Property Acceptable Region
PCCS	Product Composition Control System
PHA	Precipitate Hydrolysis Aqueous
PNNL	Pacific Northwest National Laboratory
PSAL	Process Science Analytic Laboratory
QAP	Quality Assurance Program
RCRA	Resource Conservation and Recovery Act
REDOX	REDuction/OXidation
ROC	Reduction of Constraints
RMSE	Root Mean Square Error
SB	Sludge Batch
SEM	Scanning Electron Microscopy
SG	Study Glasses
SGM	Scale Glass Melter
SME	Slurry Mix Evaporator
SPC	Statistical Process Control

SQC	Statistical Quality Control
SRNL	Savannah River National Laboratory
SRNS	Savannah River Nuclear Solutions
SRS	Savannah River Site
SS	Sharp-Shurtz
SWPF	Salt Waste Processing Facility
TCLP	Toxic Characteristic Leaching Procedure
TEM	Transmission Electron Microscopy
THERMO™	Thermodynamic Hydration Energy Reaction MOdel
TTQAP	Technical Task and Quality Assurance Plan
TTR	Technical Task Request
T <sub>L</sub>	Liquidus Temperature
U95	Upper 95% confidence interval
VFT	Vogel-Fulcher-Tammann
V <sub>r</sub>	Viscosity ratio
WAPS	Waste Acceptance Product Specifications
WCP	Waste Form Compliance Plan
WGI	Washington Group Inc.
WQR	Waste Qualification Report
WL	Waste Loading
WSRC	Westinghouse Savannah River Co.
XANES	X-ray Absorption Near Edge Spectroscopy
Z/r	Atomic charge/Atomic radius



## 1.0 Introduction

Borosilicate glasses have been used in the United States and in Europe to immobilize radioactive high level waste (HLW) for ultimate geologic disposal. Waste glass formulations should maximize the concentration of waste in the vitrified waste form so that waste glass volumes and the associated storage and disposal costs are reduced. Moreover, the optimization of HLW glass formulations [1,2,3] must simultaneously balance multiple product/process (P/P) constraints (Table 1).

**Table 1. Waste Glass Product and Process (P/P) Constraints**

Product Constraints	Process Constraints
chemical durability	melt viscosity/resistivity
glass homogeneity	liquidus
thermal stability	waste solubility
regulatory compliance	melt temperature/corrosivity
mechanical stability	radionuclide volatility
	REDuction/Oxidation (REDOX)*

\* controls foaming and thus improves melt rate and controls metal nodule formation and thus improves melter longevity

The chemical durability, which includes glass homogeneity, the melt viscosity, and the liquidus constraints from Table 1 are the only parameters controlled during HLW processing. Thermal and mechanical stability were measured during development of the HLW processing flowsheet.[ 4 ] Regulatory compliance using the Toxic Characteristic Leach Test (TCLP) was bounded by using 1X and 10X the Environmental Protection Agency (EPA) Resource Conservation and Recovery Act (RCRA) hazardous constituents anticipated to be in glasses made from the range of wastes found in the Savannah River Site (SRS) tank farm.[5,6] Melt temperature, was balanced against volatilization of radionuclides and materials of construction corrosivity during extensive pilot scale testing at the SRS before the Defense Waste Processing Facility (DWPF) startup. The melt temperature was optimized at 1150°C to minimize radionuclide volatility, afford an adequate viscosity to the melt for convection and at the same time minimize corrosion of melter materials of construction, i.e. Inconel®690 and Monofrax™ K-3 refractory.[7,8,9] Melter REDOX is controlled at an  $\text{Fe}^{2+}/\Sigma\text{Fe}$  target of ~0.2 and in the range of  $\text{Fe}^{2+}/\Sigma\text{Fe} = 0.09\text{-}0.33$ . [10,11,12,13,14] Waste solubility is handled in PCCS as limits of the individual species in wt% in the glass.

Radioactive HLW has successfully been vitrified into borosilicate glass during HLW processing at the DWPF since 1996. The DWPF must measure melt/glass acceptability a priori to the melter, since no remediation of the glass composition to ensure durability and processability is possible except in the vessel (i.e., in the Slurry Mix Evaporator (SME) vessel) in which frit and waste are blended. Therefore, the acceptability decision is made on the upstream process (specifically, at the SME), rather than on the downstream *melt* or glass product. That is, it is based on “feed forward” statistical *process* control<sup>†</sup> (SPC) rather than statistical *quality* control (SQC).<sup>††</sup> The DWPF SPC control system is known as the Product Composition Control System (PCCS). Individual property-composition models enable the monitoring and process control strategies embedded in the DWPF PCCS.[15] These models transform constraints on the melt and glass properties such as viscosity, liquidus, and durability into constraints on feed composition.

<sup>†</sup> This controls the slurry feed to the melter *prior* to vitrification.

<sup>††</sup> Which would adjudicate product release by sampling the glass *after* it's been made.

The DWPF property-composition models have been under development and validation since the late 1980's. Since the 1980's, the individual property models for each feed/glass constraint have been developed over wider property ranges than the feeds that were anticipated to be fed to the DWPF. The property models that have been developed are mechanistic<sup>t</sup> in nature and depend on known relationships between glass structure/bonding (viscosity)[16,17], thermodynamics of melt structures and components (durability)[18,19], and quasicrystalline melt species (liquidus).[20,21,22] The P/P models group terms with very similar effects so that each model only contains the terms that are necessary and sufficient (parsimonious) to model the P/P property of interest.

The PCCS historic viscosity model currently in use at DWPF will be assessed in this document against newly generated data covering the future composition region defined by SWPF processing (see Section 3.0 for discussion). Specifically, this document will assess the impact of enriched TiO<sub>2</sub> waste streams from SWPF on viscosity. The TiO<sub>2</sub> and Na<sub>2</sub>O enriched waste streams are generated by decontamination of the HLW salt waste stream using MonoSodiumTitanate (MST) to remove <sup>90</sup>Sr and <sup>137</sup>Cs. If needed, a TiO<sub>2</sub> term will be added to the historic viscosity model. A solubility limit has been placed on TiO<sub>2</sub> additions to DWPF glass, i.e., 2 wt% TiO<sub>2</sub>, based on an evaluation of the tendency of TiO<sub>2</sub> to induce crystallization in DWPF glasses.[23] Therefore, a TiO<sub>2</sub> term was not included in the historic viscosity model. While the current assessment of the historic viscosity model is addressing higher concentrations of TiO<sub>2</sub> and the impact on melt viscosity at 1150°C, a revision of the PCCS liquidus model will address the crystallization issue and may limit the amount of SWPF waste that can be added to any one batch of DWPF glass.

In the future, the DWPF may also receive Crystalline SilicoTitanate (CST) that may be used to decontaminate the <sup>137</sup>Cs from the salt waste or from tank cleanout. The CST is remarkable for its ability to separate parts-per-million concentrations of cesium from highly alkaline solutions (pH>14) containing high sodium concentrations (>5M). It is also highly effective for removing cesium from neutral and acidic solutions, and for removing strontium from basic and neutral solutions.[24] The CST is comprised primarily of: Na, Si, Ti, and Nb (formerly referred to as proprietary material one, or PM-1) plus an exchangeable monovalent cation. The binder is based on a technology that employs zirconium (formerly PM-2).[25]

### 1.1 The DWPF PCCS Historical Viscosity Model

The viscosity of a waste glass melt as a function of temperature is one of the most important variables affecting the melt rate,<sup>τ</sup> the pourability of the glass, and the electrical resistivity of the glass, thus inhibiting Joule heating. The viscosity determines the rate of melting of the raw feed, the rate of gas bubble release (foaming and fining), the rate of homogenization, the adequacy of heat transfer, the devitrification rate, and thus, the homogeneity of the final glass product. If the viscosity is too low, excessive convection currents can occur, increasing corrosion/erosion of the melter materials (refractories and electrodes) and making control of the waste glass melter more difficult. The lowest glass viscosities set for the DWPF waste glass melter are, therefore, conservatively set at ~20 poise at T<sub>melt</sub>. Waste glasses are usually poured continuously into stainless steel canisters for ultimate storage. Glasses with viscosities above 500 poise do not readily pour. Moreover, too high a viscosity can reduce glass quality by causing voids in the final glass. A conservative maximum viscosity of 110 poise at T<sub>melt</sub>,

<sup>t</sup> Mechanistic models can be applied to composition regions outside of the regions for which they were developed. The DWPF mechanistic models allow more flexibility for process control than empirical models which are (1) restricted to the compositional region over which they were developed and (2) require glass formulations near the center of a pre-qualified glass composition region instead of in regions where waste loading can be maximized.

<sup>τ</sup> Melt rate is also related to melt pool resistivity, which is highly correlated to melt pool viscosity: melt rate is also related to the REDOX of the melt pool as an oxidizing melt pool can cause O<sub>2</sub> foaming from manganese oxide reduction, and the foam can form an insulating layer on the melt pool and inhibit heat transfer from the lid heaters; so that neither the fresh batch nor the cold cap melt as efficiently.

was, therefore, established for DWPF production.[26]

The approach taken in the development of the historic viscosity and electrical resistivity process models [2,16,17] was based on glass structural considerations, expressed as a calculated non-bridging oxygen (NBO) parameter. This NBO parameter represents the amount of structural depolymerization in the glass (Equation 1). A larger NBO indicates a very fluid melt while a smaller NBO indicates a more viscous melt, i.e. with a higher viscosity. The same approach is used in this study to incorporate other oxide terms.

$$\text{Equation 1} \quad \text{NBO} \equiv \frac{2(\text{Na}_2\text{O} + \text{K}_2\text{O} + \text{Cs}_2\text{O} + \text{Li}_2\text{O} + \text{Fe}_2\text{O}_3 - \text{Al}_2\text{O}_3) + \text{B}_2\text{O}_3}{\text{SiO}_2}$$

Oxide species in the DWPF viscosity models are expressed in mole fraction and related to the viscosity-temperature dependence of the Fulcher equation [16,17], also known as the Vogel-Fulcher-Tammann (VFT)<sup>‡</sup> equation. The VFT relates the viscosity ( $\eta$ ) of a glass to temperature (Equation 2) for Newtonian fluids. Therefore, non-Newtonian fluids, such as crystallized glasses [27] are not included in the viscosity model or validation data. Phase separated glasses of the glass-in-glass (amorphous phases) type are also not included in the viscosity models or validation data as phase separated glasses give anomalous viscosity vs. temperature plots. [36]

$$\text{Equation 2} \quad \log_{10} \eta = A + \frac{B}{T - T_o}$$

In Equation 2,  $\eta$  is viscosity (poise, P, or Pa•s<sup>\*</sup>), T is temperature in °C, and A, B, and T<sub>o</sub> are fitted constants. It is well documented that the overall fit of the Fulcher equation is excellent for glasses but that it also overestimates viscosity at lower temperatures in the range of viscosities >10<sup>11</sup> poise.[28] In addition, viscosities less than 10 poise are not modeled as ASTM C965 [29] indicates that the measurement is not accurate in this low viscosity range.

Calculation of the NBO term from molar compositions was combined with quantitative statistical analyses of response surfaces to express glass viscosity and resistivity as a function of melt temperature and glass composition. The DWPF historic viscosity model was originally developed in 1991 [2,16] based on “as-batched” glass compositions, and the coefficients were revised in 2005 based on “as-measured” glass compositions.[17] The 2005 version of the DWPF viscosity model, referred to in this study as the “historic DWPF viscosity model” is given by:

$$\text{Equation 3} \quad \log \eta(\text{poise}) = -0.519571 + \left( \frac{4453.87}{T(^{\circ}\text{C})} \right) - (1.690326 * \text{NBO}).$$

with an adjusted R<sup>2</sup> = 0.966, and a root mean square error (RMSE) of 0.0832. Equation 3 is based on 175 viscosity-temperature data points from 33 different glasses.

<sup>‡</sup> Fulcher derived this expression to model viscosity of inorganic glasses in 1925. In 1921, Vogel (Phys. Zeit., 22, 645-646) derived a similar expression for the viscosity of water, mercury, and oils and Tammann and Hesse generated a similar equation for organic liquids in 1926 (Z. Anorg. Allg. Chem. 156, 245-257). So all three are credited with the derivation of the mathematical expression, and it is often referred to as the VFT equation. Throughout this document the VTF equation is noted as the Fulcher equation.

<sup>\*</sup> The unit of viscosity is the dyne second per square centimeter, which is called the poise. The SI unit for viscosity is the Newton second per square meter, or pascal second (Pa.s); one of these units equals 10 poise.

The form of the NBO parameter did not change between 1991 and 2005 but the coefficients to the NBO and  $1/T(^{\circ}\text{C})$  parameters and intercept were refit. The viscosity model data and the associated validation data comprise the VISCOMP™ database of ~500 HLW glasses. Additional viscosity data have been generated since the 2005 viscosity model was refit, and specifically viscosity and composition data have been developed over the future compositional processing range that DWPF is expected to experience until the end of its mission.

The DWPF viscosity model assumes that a pure  $\text{SiO}_2$  glass is fully polymerized; i.e. there are no NBO and 4 bridging oxygen (BO) bonds per silicon atom. Addition of other species known as network modifiers depolymerizes the glass while network formers polymerize the glass. A larger NBO term indicates a very fluid melt with a low viscosity while a smaller NBO term indicates a more viscous melt, i.e. one with a higher viscosity. This approach was a simplification of an NBO term developed by White and Minser [30] to describe the structural features observed in Raman spectroscopy data of complex natural glasses (obsidians and tektites), which had no  $\text{B}_2\text{O}_3$  and almost all FeO instead of  $\text{Fe}_2\text{O}_3$ . Equation 3 is also consistent with the usage of a viscosity ratio ( $V_r$ ) to model the viscosity of slags [31]. The  $V_r$  is defined as the sum of the  $Z/r$  (atomic charge/atomic radius) of the network formers multiplied by the atomic % of the network formers divided by the sum of the  $Z/r$  of the network modifiers multiplied by the atomic % of the network modifiers.

In the DWPF historic viscosity model, it is assumed that each mole of alkali oxide added creates two NBO bonds by forming metasilicate  $((\text{Rb,Cs,K,Na,Li})_2\text{SiO}_3)$  structural units; thus depolymerizing the glass. While the exact number of NBO atoms depends on the molar ratio of all of the species in a waste glass to  $\text{SiO}_2$ , most DWPF glasses have a  $\text{O}^{2-}/\text{Si}^{4+}$  ratio of 2.6 to 3.3 which implies that disilicate and metasilicate structural units predominate for the alkali species in the waste glasses. Calculation of the  $\text{O}^{2-}/\text{Si}^{4+}$  ratio for DWPF glasses included contributions from Na, K, Li, and Cs alkali species and a  $\text{Si}^{4+}$  concentration that was depleted by the amount associated with  $\text{B}_2\text{O}_3$  structural units.

The DWPF historic viscosity model further assumes that each mole of  $\text{Al}_2\text{O}_3$  creates two BO bonds (polymerizes the glass structure) by creating tetrahedral alumina groups that bond as  $(\text{Rb,Cs,K,Na,Li})\text{AlO}_2$  structural groups. In  $\text{Al}_2\text{O}_3$  and/or  $\text{SiO}_2$  deficient glasses,  $\text{Fe}_2\text{O}_3$  can take on a tetrahedral coordination and polymerize a glass by forming  $(\text{Rb,Cs,K,Na,Li})\text{FeO}_2$  structural groups. However, if sufficient  $\text{Al}_2\text{O}_3$  and  $\text{SiO}_2$  are present in a glass such as DWPF waste glasses that contain >3 wt%  $\text{Al}_2\text{O}_3$  and >40 wt%  $\text{SiO}_2$ , then  $\text{Fe}_2\text{O}_3$  is octahedral and creates two NBO bonds, i.e., it depolymerizes the glass matrix as assumed in the DWPF viscosity model (Equation 3). This is consistent with the work of Mysen [32] who demonstrated that high iron magmas (iron silicate glasses) that contained levels of 10 wt%  $\text{Fe}_2\text{O}_3$  decreased the melt viscosity. Mysen concluded that  $\text{NaFeO}_2$  structural groups were not incorporated into the silicate network to the same degree as  $\text{NaAlO}_2$  structural groups [32]. Therefore,  $\text{Fe}_2\text{O}_3$  is considered a network modifier (or depolymerizer) in the DWPF viscosity model.

Lastly, the DWPF historic viscosity model assumes that each mole of  $\text{B}_2\text{O}_3$  creates one NBO bond. This is based on data by Smets and Krol [33], and Konijnendijk [34] who demonstrated that for sodium silicate glasses with low  $\text{B}_2\text{O}_3$  content the  $\text{B}_2\text{O}_3$  enters the glass network as  $\text{BO}_4^-$  tetrahedral. At higher  $\text{B}_2\text{O}_3$  concentrations, these tetrahedra are converted into planar  $\text{BO}_3^-$  groups. Tetrahedral  $\text{BO}_4^-$  contributes no NBO while planar  $\text{BO}_3^-$  groups contribute one NBO atom.[35]

In 1991, the viscosity model was developed on as-batched compositions [2,16] and revised in 2005 [17] based on analyses of the same non-radioactive glasses and frits (220 viscosity-temperature measurements for 41 glasses). Eight of the 1991 glasses were determined to be phase separated during the development

of the PCCS historic durability model in 1995 (see discussion in Section 2.0). These glasses were removed from the earlier viscosity model during the 2005 revision leaving a data pool of 175 viscosity-temperature measurements for 33 glasses. During the 2005 revision, the model was validated [17] on an additional 200 glasses (radioactive and non-radioactive and 1004 viscosity-temperature pairs). Uranium was shown to have no impact on glass viscosity as U has as many BO's as NBO's and they cancel each other out in the NBO parameter.[17] Likewise,  $\text{ThO}_2$  at <1 wt% had no impact on glass viscosity. The viscosity model was developed over wider composition space and temperature regions (873-1491°C), than DWPF operation. This allows for high leverage points during modeling, improves the model fit, and helps ensure that any individual terms are adequately accounted for. The viscosity constraint is applied in PCCS at the DWPF melt temperature of 1150°C.

Equation 3 was implemented in PCCS at the DWPF melt temperature of 1150°C. However, the equation represents a three dimensional plane in composition (NBO), viscosity, and temperature space as shown in Figure 1-1. Therefore, the viscosity model could easily be applied at a variety of glass temperatures in a variety of different melter designs. The historic viscosity model covers temperatures from 873-1491°C but was validated to as low as 808°C. The model covers glasses from 10.2 poise to 122 poise (see Appendix A) but was validated up to 1,100 poise (validation data are given in Reference 17). The composition range over which the 2005 DWPF viscosity model was developed is given in Table 2.

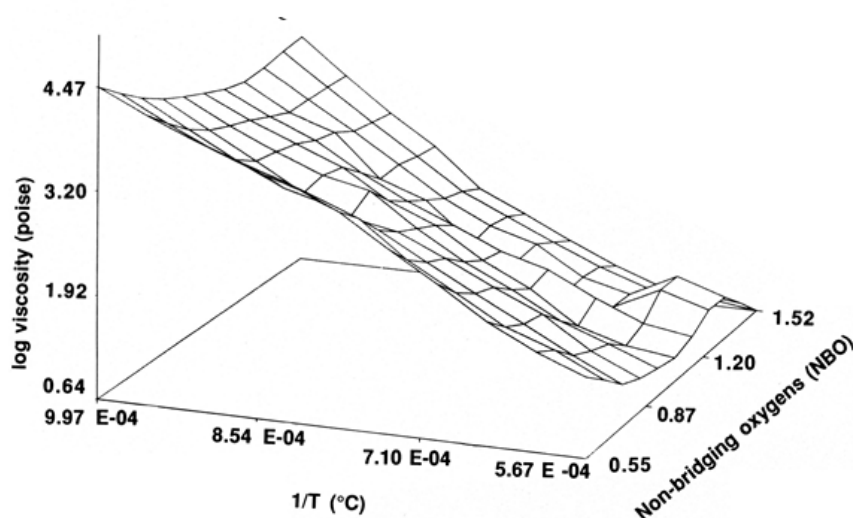


Figure 1-1. DWPF viscosity model showing the relationship between composition (NBO), viscosity and temperature.

Radioactive glasses were not included in the development of the 1991 DWPF viscosity model because the commercial glass laboratories that were performing the measurements could not handle radioactive glasses. The SRNL developed radioactive viscosity measurement capability in 1998. The 1991 viscosity model was re-examined in 2005 [17] to determine whether radioactive components were needed in the model and to determine the impact of having used the as-batched instead of as-measured glass compositions. The following was concluded:

- the 1991 DWPF PCCS viscosity model was found to be biased due to six as-batched glass compositions that were in error and two glasses that were determined to be phase separated: phase separated glasses can give anomalous viscosity response [36]

- the magnitude of the bias in the 1991 DWPF viscosity model based on as-batched glass compositions over the 7-1,000 poise range relative to the non-radioactive as-measured glasses was the same as the bias observed between the as-batched model and radioactive glasses
- the coefficients of the 1991 DWPF viscosity model were revised in 2005 using the as-measured glass compositions and eliminating the inhomogeneous glass responses and this corrected the 1991 model bias
- once the bias in the 1991 DWPF viscosity model was corrected, it was shown that a  $U^{+6}$  term was not needed and a  $Th^{+4}$  term was not needed as long as the  $Th^{+4}$  concentrations in the glass were  $\leq 1\text{wt}\%$
- a  $Th^{+4}$  term may be necessary for DWPF glasses containing  $Th^{+4} > 1\text{ wt}\%$  ( $ThO_2 = 1.14\text{ wt}\%$ ) if such concentrations are processed in the future. Subsequently, a study [37] showed that 1.8 wt%  $ThO_2$  could be processed adequately with the historic viscosity model.

**Table 2. Composition, Temperature, and Viscosity Range of DWPF Viscosity Model.**

Parameter	Viscosity “ Model Data” (33 glasses; 175 viscosity-temperature pairs)
	<b>2005 MODEL DATA</b>
Temperature (°C)	873-1491
Viscosity (poise)	10.23-1122.02
Fe <sup>+2</sup> /ΣFe	0.00-0.47
Al <sub>2</sub> O <sub>3</sub> (wt%)	0.00-13.90
B <sub>2</sub> O <sub>3</sub> (wt%)	6.41-12.20
BaO(wt%)	0.00-0.20
CaO(wt%)	0.00-1.47
Cr <sub>2</sub> O <sub>3</sub> (wt%)	0.00-0.09
Cs <sub>2</sub> O(wt%)	0.00-0.15
CuO(wt%)	0.00-0.33
Cu <sub>2</sub> O(wt%)	0.00-0.30
FeO(wt%)	0.00-7.14
Fe <sub>2</sub> O <sub>3</sub> (wt%)	0.00-14.20
K <sub>2</sub> O(wt%)	0.00-5.73
La <sub>2</sub> O <sub>3</sub> (wt%)	0.00-0.36
Li <sub>2</sub> O(wt%)	2.59-6.96
MgO(wt%)	0.49-2.92
MnO(wt%)	0.00-3.26
Na <sub>2</sub> O(wt%)	5.80-15.80
Nb <sub>2</sub> O <sub>5</sub> (wt%)	0.00
NiO(wt%)	0.00-2.97
P <sub>2</sub> O <sub>5</sub> (wt%)	0.00
SiO <sub>2</sub> (wt%)	45.60-77.04
SrO(wt%)	0.00-0.07
ThO <sub>2</sub> (wt%)	0.00
TiO <sub>2</sub> (wt%)	0.00-1.78
U <sub>3</sub> O <sub>8</sub> (wt%)	0.00
ZnO(wt%)	0.00
ZrO <sub>2</sub> (wt%)	0.00-0.99

In the current study, the PCCS viscosity model is assessed against the future composition region of interest to DWPF for the implementation of the fully coupled flowsheet, i.e. when the SWPF comes on line to decontaminate salt solution at much higher throughputs than the current ARP and (MCU) process. This in-depth assessment is presented in Section 5.0 of this study and demonstrates that the PCCS viscosity model requires an additional parameter<sup>f</sup> in order to cover the SWPF composition space.

The assessment of the PCCS viscosity model also examined whether additional species or parameters were needed to encompass any changes in frit formulation that may be necessary, i.e. MgO and/or CaO to prevent nepheline crystallization.[38,39,40] The specific compositional regions assessed in Reference 41 will be the focus of the main body of this document, and this will be discussed in Section 2.0.

<sup>f</sup> Where a parameter can be an individual oxide component or a group of oxides, like the alkali oxides of Cs, Na, K, and Li, that act as a grouped or lumped parameter in a model.

## 1.2 Quality Assurance

All the model assessments presented in this study were performed in accordance with DOE/RW-0333P and a Quality Assurance Program (QAP) that meets the Quality Assurance criteria specified in DOE O. 414.1, *Quality Assurance*, 10 CFR 830, *Nuclear Safety Management*, Subpart A, “*Quality Assurance Requirements*”, paragraph 830.122 and also meets the requirements of ASME Nuclear Quality Assurance (NQA)-1, *Quality Assurance Requirements for Nuclear Facility Applications*.

The customer for this work is DWPF/SALTSTONE Facility Engineering. The point of contact is E.W. Holtzscheiter. The request is detailed in X-TTR-S-00012 and is in accordance with the Task Technical and Quality Assurance Plan (TTQAP) given in Reference 42. This work involved research and development that is considered technical baseline. The TTR requires DOE/RW-0333P to be invoked for specific tasks associated with waste form affecting properties (such as durability). All other scopes do not require RW-0333P procedures.

Requirements for performing reviews of technical reports and the extent of review are established in manual E7 2.60. SRNL documents the extent and type of review using the SRNL Technical Report Design Checklist contained in WSRC-IM-2002-00011, Rev. 2. All of the viscosity property-composition models presented in this report were conducted using JMP Version 11.1.1 (CMJ), validated using JMP Pro Version 11.2.1 (TBE), and checked by E7 2.60 using JMP Version 11.2.0 (CLT).[43]

## 2.0 DWPF Process/Product (P/P) Modeling Constraints

### 2.1 Modeling Constraints Common to PCCS Models

For all the PCCS models and validation data, various constraints are applied on the data. The first requires that the chemical composition of the glass, on an oxide basis, be within 100±5 weight percent (wt%).[44] The “sum of oxides” constraint minimizes the impact of analytic errors during modeling and validation.

Moreover, a given glass must be homogeneous, i.e. not phase separated by liquid-liquid amorphous phase separation (APS). Regions of APS are known to form due to low  $\text{Al}_2\text{O}_3$  ( $\leq 3.00$  wt%), high  $\text{P}_2\text{O}_5$  ( $\geq 2.25$  wt%), or high  $\text{B}_2\text{O}_3$  ( $\geq 14.00$  wt%) concentrations in HLW glasses, and so these compositions are excluded from modeling (see Figure 2-1). Sometimes an XRD of an as-quenched glass will show a double amorphous hump rather than a single amorphous hump which is also an indication of APS. Occasionally, Scanning Electron Microscopy (SEM) or Transmission Electron Microscopy (TEM) is necessary to make the determination of whether a glass is phase separated or not.[18,19] In References 18 and 19, a “homogeneity constraint” based on glass composition was developed to distinguish between homogeneous and phase separated glasses. Likewise, glasses for modeling should not be crystallized because phase separated and/or crystallized glasses can give anomalous durability [18,19,45,46,47], viscosity [36], and liquidus [48] responses.

The glass REDOX, expressed as the  $\text{Fe}^{2+}/\Sigma\text{Fe}$  ratio, must be  $<0.33$ , which is the upper limit of processability in the DWPF melter. This is because REDOX values  $<0.33$  have been shown not to impact glass durability [49,50,51], glass viscosity, or glass liquidus values, while higher REDOX ratios (more reducing values) can impact these properties.

The alkali ( $\Sigma\text{R}_2\text{O}$  where  $\text{R}=\text{Rb}, \text{Cs}, \text{Na}, \text{Li}, \text{or K}$ ) and alumina ( $\text{Al}_2\text{O}_3$ ) constraints shown in Figure 2-1 were developed after the DWPF durability model (THERMO™) was developed to ensure that the durability response of a glass could be modeled. The alkali and alumina constraint replaced the “homogeneity constraint” and became known as the “reduction of constraints (ROC)” as discussed in Appendix B.1. The ROC within PCCS determines whether a glass can be processed in DWPF. The ROC



as shown in Figure 2-1 has worked for DWPF glasses with 0-2.00 wt%  $\text{TiO}_2$ . Recent investigations [52] have shown that for glasses such as the SWPF glasses with  $\text{TiO}_2 > 2.00$  wt% that the ROC constraint has to be  $\text{Al}_2\text{O}_3 \geq 4.00$  wt% which alters the Figure 2-1 constraints to those shown in Figure 2-2.

The constraints, without the uncertainties factored into the values shown, are summarized graphically in Figure 2-1 and discussed in detail in Appendix B. These constraints are applied to the modeling data (composition and property) so that model accuracy is maximized and model error is minimized by ensuring complete glass analyses and no anomalous property responses.

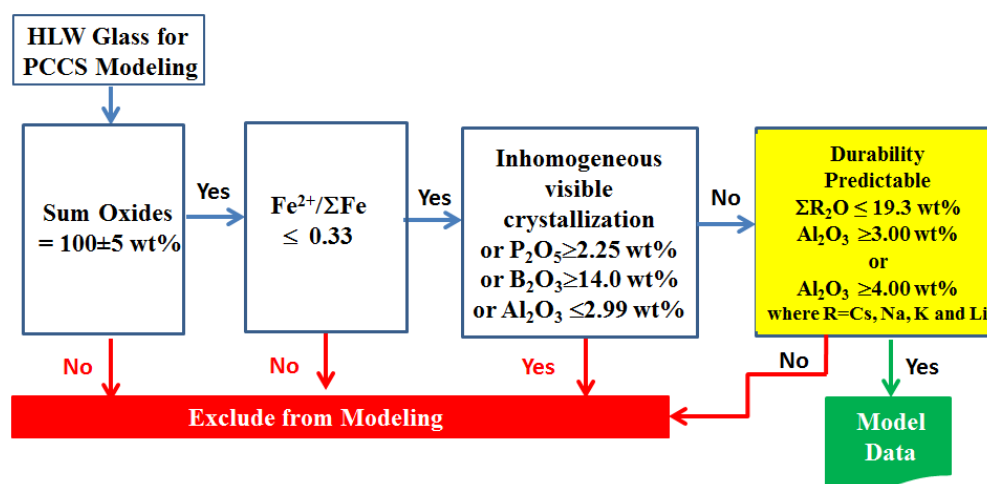


Figure 2-1. Graphical Representation of the Constraints Applied to the Choice of Model and Validation Data for the Durability, Viscosity, and Liquidus P/P Models for glasses with 0-2.00 wt%  $\text{TiO}_2$ . The  $\text{Al}_2\text{O}_3$  term in the inhomogeneous by visible crystallization is 2.99 wt% to accommodate the WCP Purex glass which contains 2.99 wt%  $\text{Al}_2\text{O}_3$ .

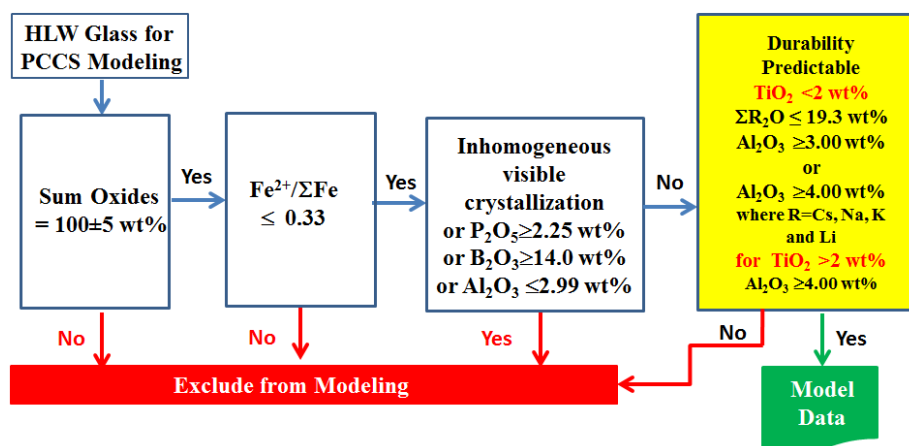


Figure 2-2. Graphical Representation of the Constraints Applied to the Choice of Model and Validation Data for the Durability, Viscosity, and Liquidus P/P Models for glasses with 0-2.00 wt%  $\text{TiO}_2$  and glasses with  $\geq 2.00$  wt%  $\text{TiO}_2$ . The  $\text{Al}_2\text{O}_3$  term in the “inhomogeneous by visible crystallization” box is 2.99 wt% to accommodate the WCP Purex glass.

## 2.2 Modeling Constraints Unique to the PCCS Viscosity Model

Melt viscosity is a unique property and the measurement of this property invokes additional modeling constraints in addition to those discussed in Section 2.1. The unique constraints are:

- no crystallized glasses nor glasses that crystallized during viscosity measurement, i.e. anomalous hysteresis curves, were used as the viscosity of crystallized glasses is non-Newtonian (Note: not all the viscosity measurement vendors provided hysteresis curves. Specifically, OCF and CELS determined that glasses had crystallized during viscosity measurement if there was a sharp break in the viscosity-temperature curves and ES-VSL was not required to perform hysteresis as it is not a requirement in ASTM C965 and it was not specified in the statement of work).
- if the measured temperature was  $\leq 800^{\circ}\text{C}$ , the data were excluded to avoid bias due to potential non-Newtonian viscosity behavior caused by crystallization of the glass below  $800^{\circ}\text{C}$  (for viscosity measurements where hysteresis curves were not provided by the vendor).
- no viscosities below 10 poise as the ASTM 965 procedure can be inaccurate in this range of viscosity
  - o if more than 2 out of 5 measurement points at different temperatures violated the 10 poise criteria then the entire set of glass viscosities was not considered for validation.

### 3.0 Defining Future DWPF Processing Ranges

With the initiation of the ARP and MCU at SRS in 2008, there was a need to revisit the DWPF homogeneity constraint shown in Figure 2-1 and discussed in Appendix A for coupled operations. This constraint was specifically addressed through the variability study for Sludge Batch 5 (SB5).[53] Table 3 defines the compositional region of interest for coupled operations at DWPF with  $\text{TiO}_2$  levels up to 2 wt%.[53]

**Table 3. Oxide Intervals for Reduction of Constraints Study for Coupled Operations with ARP and MCU**

Oxide	Minimum (wt%)	Maximum (wt%)
$\text{Al}_2\text{O}_3$	3.25	18
$\text{B}_2\text{O}_3$	4.5	14
$\text{CaO}$	0	4
$\text{Cr}_2\text{O}_3$	0	0.2
$\text{Fe}_2\text{O}_3$	5	21
$\text{Li}_2\text{O}$	4	7
$\text{MgO}$	0	1.5
$\text{MnO}$	0.3	5.5
$\text{Na}_2\text{O}$	10	18
$\text{NiO}$	0	2.5
$\text{SiO}_2$	30	55
$\text{TiO}_2$	0.5	2.0
$\text{U}_3\text{O}_8$	0	9.5
Others	0	2.0

The information in Table 3 was then used to support an effort to define any potential gaps in the compositional range of the current PCCS models when compared to the compositional region projected for the SWPF flowsheet. In addition to addressing this issue for the PCCS models, the SWPF gap analysis study [41,42,54] extended the reduction of constraints coverage to the glass composition region

anticipated for the DWPF and SWPF coupled flowsheet. From Reference 54, the compositional region of interest is defined by the oxides and wt% intervals given in Table 4. In this table, the shaded oxide rows define the “others” component for this compositional region.

Thus, one may look to the glass regions of Table 3 and Table 4 to define the region of interest for assessing the applicability of the historic viscosity-composition model for SWPF processing. The DWPF viscosity model data [16], augmented by the validation data given in Reference 17, was used to investigate the applicability of the existing viscosity data to the SWPF space defined by Table 3 and Table 4 (see Reference 55). Additional viscosity validation data have been generated at SRNL since Reference 17 was published. The sources of the viscosity model and validation data as a function of measurement temperature and glass composition are discussed in Section 4.1. These additional data were also used to assess how valid the historic DWPF viscosity model is over the future DWPF compositional regions defined by Table 3 and Table 4 (see Reference 55).

**Table 4. Oxide Intervals for SWPF Gap Analysis Study**

<b>Oxide</b>	<b>Minimum (wt%)</b>	<b>Maximum (wt%)</b>
Al <sub>2</sub> O <sub>3</sub>	3.5	13
B <sub>2</sub> O <sub>3</sub>	4.5	10
BaO	0	0.25
CaO	0.2	2
Ce <sub>2</sub> O <sub>3</sub>	0	0.2
CoO	0	0.1
Cr <sub>2</sub> O <sub>3</sub>	0	0.2
Cs <sub>2</sub> O	0.3	1
CuO	0	0.1
Fe <sub>2</sub> O <sub>3</sub>	5	16
K <sub>2</sub> O	0	0.2
La <sub>2</sub> O <sub>3</sub>	0	0.1
Li <sub>2</sub> O	1	7
MgO	0	2
MnO	0.2	4
Na <sub>2</sub> O	8	18
NiO	0	2
PbO	0	0.25
SO <sub>4</sub>	0	0.3
SiO <sub>2</sub>	40	55
ThO <sub>2</sub>	0	1
TiO <sub>2</sub>	2	6
U <sub>3</sub> O <sub>8</sub>	0	6
ZnO	0	0.2
ZrO <sub>2</sub>	0	0.25

## 4.0 Experimental

### 4.1 Historic Viscosity Model and Validation Databases [from Reference 17]

Forty one glasses of varying, expected extreme DWPF compositions were fabricated between 1984 and 1996. The range of the individual oxides and the sum of oxides is given in Table 5 and the number of

glasses and the studies from which they were derived are given in Table 6. During 1984-1996, viscosity, liquidus temperature ( $T_L$ ), and replicate chemical analyses were performed on these glasses by commercial glass laboratories such as Corning Engineering Laboratory Services (CELS) and Owen Corning Fiberglass (OCF) analytic division known as Sharp Shurtz (SS). Often duplicate glass compositions were re-made and sent to the laboratories for replicate measurements. Thus, there are two Frit 131 average sludge-only glasses that were made in 1985 (designated AH131AV-1985 and 1985-2) and another Frit 131 average sludge-only glass made in 1988 (designated AH131AV-1988). The laboratory performing >90% of the chemical analyses was CELS as indicated in Appendix A. The viscosity was measured by both OCF-SS and CELS but the data that were used in modeling were the data generated by SS using ASTM C965A which eliminated bias due to unwanted crystallization at the lower temperatures used by CELS during viscosity measurement using ASTM 965B.

**Table 5.** Temperature, Viscosity and Composition Ranges for the Historical DWPF Viscosity Model (see Appendix A for individual analyses)

Parameter	Maximum Value	Minimum Value
Temperature (°C)	1491	873
Viscosity (poise)	1122.02	10.23
$\text{Fe}^{+2}/\Sigma\text{Fe}$	0.47	0.00
$\text{Al}_2\text{O}_3(\text{wt}\%)$	13.90	0.00
$\text{B}_2\text{O}_3(\text{wt}\%)$	12.20	6.41
$\text{BaO}(\text{wt}\%)$	0.20	0.00
$\text{CaO}(\text{wt}\%)$	1.47	0.00
$\text{Cr}_2\text{O}_3(\text{wt}\%)$	0.09	0.00
$\text{Cs}_2\text{O}(\text{wt}\%)$	0.15	0.00
$\text{CuO}(\text{wt}\%)$	0.33	0.00
$\text{Cu}_2\text{O}(\text{wt}\%)$	0.30	0.00
$\text{FeO}(\text{wt}\%)$	7.14	0.00
$\text{Fe}_2\text{O}_3(\text{wt}\%)$	14.20	0.00
$\text{K}_2\text{O}(\text{wt}\%)$	5.73	0.00
$\text{La}_2\text{O}_3(\text{wt}\%)$	0.36	0.00
$\text{Li}_2\text{O}(\text{wt}\%)$	6.96	2.59
$\text{MgO}(\text{wt}\%)$	2.92	0.49
$\text{MnO}(\text{wt}\%)$	3.26	0.00
$\text{Na}_2\text{O}(\text{wt}\%)$	15.80	5.80
$\text{NiO}(\text{wt}\%)$	2.97	0.00
$\text{SiO}_2(\text{wt}\%)$	77.04	45.60
$\text{SrO}(\text{wt}\%)$	0.07	0.00
$\text{TiO}_2(\text{wt}\%)$	1.78	0.00
$\text{ZnO}(\text{wt}\%)$	0.00	0.00
$\text{ZrO}_2(\text{wt}\%)$	0.99	0.00
Sum Oxides	100.28	98.23

**Table 6. References for Viscosity Model and Validation**

<b>Sample Study</b>	<b>Model or Validation</b>	<b>Number of Viscosity-Temperature Measurements</b>	<b>Viscosity Data Year</b>	<b>Reference</b>
Model Data	HISTORIC MODEL – CELS and OCF-SS	160	2005	17
DWPF Startup Frit	HISTORIC MODEL (OCF-SS)	15	2005	17, 56
DWPF Startup Frit	HISTORIC VALIDATION (Round Robin) Standards used in other studies	164 + 40	2005	17, 57, 58
Waste Form Compliance Plan (WCP) Glasses	HISTORIC VALIDATION	129	2005	17, 59, 60, 61, 62, 66, 69, 71
PNNL Studies (Chemical Variability Study; CVS-1 and CVS-2)	HISTORIC VALIDATION	699	2005	63
SRNL Integrated DWPF Melter System (IDMS) glass (Hanford, PX and HM)	HISTORIC VALIDATION	195	2005	17, 62
SRNL SGM	HISTORIC VALIDATION	331	2005	62
SRNL Soper (1982)	HISTORIC VALIDATION	124	2005	17, DPSTN-3345, DPSTN-4025, DPSTN-4416, 64
Crystalline SilicoTitanate (CST) Glasses	HISTORIC U VALIDATION AND CST MODEL	70	2005	17, 65, 66, 67, 68, 69
Precipitate Hydrolysis Aqueous (PHA)	HISTORIC U VALIDATION	74		17, 70, 71, 72, 73, 74
Environmental Assessment (EA) Glass	HISTORIC VALIDATION	7	2005	17, 95,96
West Valley (WVCM and WVUTh, AL,CR,FE,MN, NI,P glasses)	URANIUM-THORIUM VALIDATION	228	2005	17, 75, 76
M-Area	HISTORIC U VALIDATION	80	2005	77
U and U/Th Glasses (RC, RCTH,Tank 40, rchwl, Glass 1-5 and U std)	HISTORIC U and Th VALIDATION	466	2005	17, 58, 61, 78
M-Area (compositions revised in 2014)	HISTORIC U VALIDATION	80	2014	79
PNNL Study Glasses (SG)	VALIDATION NOT USED	60	2014	80
Sulfate Glasses	VALIDATION NOT USED	90	2014	81
High Loaded HLW Glasses	SWPF MODEL VALIDATION	264	2014	82, 83
CST/MST Glasses	CST MODEL AND VALIDATION	587	2014	84, 85, 86, 87
DWPF Non-Rad Startup Glasses (WP-14, 15, 16) as a Function of REDOX	VALIDATION NOT USED	48	2014	88

CELS dissolved the glasses and analyzed the compositions of the AH glasses in quadruplicate<sup>†</sup> by Inductively Coupled Plasma-Emission Spectroscopy (ICP-ES) using ASTM C1463 so that any effects of short term instrument bias on the whole element chemistry would be observable. CELS analyzed the various black frits six to ten times as indicated in Appendix A. All CELS composition analyses are traceable to the NBS 777 standard glass. These data indicate little random or systematic variation for these analyses. The white frits were dissolved and analyzed by SRNL's Analytic Development Directorate (ADD) and analyzed by ICP-ES in duplicate.

The historical model validation data are given in the appendices of Reference 17 and the references cited therein. These studies are summarized in Table 6. Most of the historical validation glasses were measured at SRNL using ASTM C965A. However, the historic validation data also included ~200 replicate viscosity measurements on the DWPF startup frit, a round robin, by six different laboratories [89]. The DWPF startup frit data round robin was performed so that the DWPF startup frit could be used to calibrate viscometers for performing ASTM C965A or B since the SRM711 standard called for in ASTM C965 has a measured viscosity at 1150°C of 4390 poise whereas a typical HLW glass is between 20 and 100 poise at 1150°C. After the DWPF round robin, this startup frit was used to calibrate the SRNL viscometers instead of SRM711. Therefore, there are multiple measurements available for the DWPF startup frit as indicated in Table 6. Additional references with validation data are shown in Table 6 and include ~130 measurements on the Waste Compliance Plan (WCP) glasses by OCF-SS, ~10 measurements of the Environmental Assessment (EA) glass by OCF-SS, ~140 glasses from West Valley measured at Alfred University, ~125 measurements from SRNL testing in the early 1980's, ~700 measurements from Pacific Northwest National Laboratory (PNNL) on two different statistically designed matrices of simulated waste glasses (Composition Variability Study I and II), and ~530 measurements made by OCF-SS on glasses made in the SRNL Integrated DWPF Melter System (IDMS) and the Scale Glass Melter (SGM).

A data set of 192 radioactive viscosity-temperature pairs containing only U<sup>+6</sup> was also used as validation data for the historical viscosity model. The historic uranium validation data reference is given in Table 6 and can also be found in Reference 17. Uranium appeared to have little to no impact on glass viscosity. An additional 26 glasses for which 98 viscosity-temperature measurements were available indicate disparate roles for ThO<sub>2</sub> depending on the U<sub>3</sub>O<sub>8</sub> concentration and the Al<sub>2</sub>O<sub>3</sub> concentration of the glasses measured.

In addition, glasses from DWPF Waste Qualification Runs (WQR) WP-14, WP-15, and WP-17 taken from DWPF canisters S00009, S00179, and S00310 [90] were used as validation data. The viscosities of the WQR glasses were measured at the SRNL in 1997 during non-radioactive startup testing of the SRNL radioactive viscometer. The radioactive viscosity measurement capability was set up in SRNL in 1998 with a Harrop viscometer [91, 92]. The ASTM C965A procedure was modified for use at SRNL to use only 6-7 grams of glass compared to the 200-700 grams required by the commercial laboratories. The use of the WQR glasses as historic validation data is given in Reference 17.

In order to constrain the historical validation data to a composition range that overlapped the DWPF composition range but was, in general broader, while not having to develop new composition terms for ZrO<sub>2</sub>, CaO, and MgO which are all known to impact glass viscosity strongly, the following boundary conditions were set:

- if the ZrO<sub>2</sub> was  $\geq 2.00$  wt%, which was twice the ZrO<sub>2</sub> content of the data on which the DWPF model is based (see Table 5), the data were excluded

---

<sup>†</sup> That is, two dissolutions were performed—one on each day—with each dissolution being analyzed in duplicate.

- if the CaO was  $\geq 3.5$  wt%, which was more than twice the CaO content of the data on which the DWPF model is based (see Table 5), the data were excluded
- if the MgO was  $\geq 6.00$  wt%, which was twice the MgO content of the data on which the DWPF model is based (see Table 5), the data were excluded
- if the  $B_2O_3$  was  $\geq 14.00$  wt%, which was over the  $B_2O_3$  content of the data on which the DWPF model is based (see Table 5) by 2 wt% but clearly in the range of phase separated glasses as defined by Tovenia [45], the data were excluded.

Altogether, 1805 waste glass viscosity-temperature pairs and measured glass compositions were used for validation of the historic viscosity model (Table 6). However, the historic validation data from Reference 17 only went to 1.43 wt%  $TiO_2$  while the historical model data went to 1.78 wt%  $TiO_2$ . The limitation of  $TiO_2$  concentrations in the historic model and validation data is due primarily to the 2 wt%  $TiO_2$  solubility limit that has been imposed for DWPF since 2003 [23] and the previous 1 wt%  $TiO_2$  solubility limit that had been imposed for DWPF between 1990-2003.[93]

#### 4.2 SWPF ( $TiO_2$ -only) Viscosity Model Database

The SWPF glasses were made and analyzed by Energy Solutions-Vitreous State Laboratory (ES-VSL). The details of the glass fabrication are given in Reference.94 The chemical compositions were measured by X-ray Fluorescence (XRF) and other methods. Since XRF cannot measure light elements such as B and Li, the glasses were dissolved and analyzed by Direct Current Plasma Emission Spectrometry (DCP) for these two elements. For each glass, two XRF and two DCP preparations were performed and two reads on each were performed on different days. Therefore, each glass had four replicate measurements. A glass standard, the SRNL EA glass was used. The EA glass had been manufactured and analyzed by CELS ten replicate times and the analyses were validated by ten additional analyses by SRNL ADD.[95,96] The details of the SWPF glass measurements and bias correction to the EA glass standards are discussed elsewhere.[97] The biased corrected glass compositions are given in Appendix C.

The SWPF glass viscosities were measured by ES-VSL using ASTM C965A and documented in Reference 98. The relative torque of a rotating spindle immersed in molten glass was measured as a function of rotational velocity (revolutions per minute, rpm) at regular temperature intervals between  $\approx 950^\circ C$  and  $\approx 1250^\circ C$ ; the melt viscosity was calculated from the torque data versus rpm. Measurements were checked against a NIST traceable standard reference glass (SRM711) since the DWPF startup frit had not been specified as the standard in the scope of work provided to ES-VSL. Among the problems with the SRM711 standard is the fact that there are only two calibration points in the region of viscosity of interest to DWPF processing. Only one SRM711 calibration curve was provided by ES-VSL and there is some deviation from the SRM711 calibration curve where the ES-VSL data are biased low at higher temperatures and biased high at lower temperatures. However, the amount of bias is difficult to quantify since there are only two calibration data points in the DWPF temperature range of interest. Therefore, no statement regarding the bias in the ES-VSL data can be made.

The ES-VSL did not check for the hysteresis of the viscosity curves, i.e. whether the viscosity curves measured during heat up were the same as those measured during cool down. This is not required in ASTM C965A and was not specified in the scope of work provided to ES-VSL. It is a methodology used at SRNL to provide additional data as to whether the samples crystallized during the heat up of the sample for the viscosity measurement as this can be used to screen out viscosity measurements that were impacted by crystallization per the modeling criteria given in Figure 2-1 and Figure 2-2. Viscosity measurements on crystallized glasses can be non-Newtonian in behavior which is undesirable when a Newtonian viscosity model is being developed.

The SWPF viscosity measurements are given in Appendix C. Data that were excluded from modeling is shaded in Appendix C. Data that were excluded from modeling included SWPF-08 which was visually inhomogeneous, SWPF-12 which appears to have crystallized during the viscosity measurement (see Reference 97), SWPF-01 through SWPF-09 which contained  $\text{TiO}_2 > 2.00 \text{ wt\%}$  and  $\text{Al}_2\text{O}_3 < 4.00 \text{ wt\%}$ , and a few viscosity values for other glasses that were 10 poise or less. The individual ES-VSL SWPF glass viscosities are fitted to the Fulcher Equations (see Equation 2) to assess their Newtonian flow behavior in Reference 97. The Fulcher fitting normally does not help determine whether the sample crystallized during the viscosity measurement unless the fit is very non-linear, i.e. SWPF-12, or there is one obvious outlier point. However, the two glasses that gave poor Fulcher fits (SWPF-08 and SWPF-12) were excluded from modeling for other reasons. It is assumed that the remaining glasses used for modeling were not crystallized.

#### 4.3 SWPF ( $\text{TiO}_2$ -only) Viscosity Validation Database

References 82-83 were studies designed to maximize waste loading in defense waste glasses (see Table 6). These glasses span  $\text{TiO}_2$  compositions from 1.25 to 6.76 wt%. These high waste loaded glasses [82-83] are, therefore, used in this study to validate the  $\text{TiO}_2$  term in the  $\text{TiO}_2$ -only viscosity model.

The details of the composition and viscosity measurements for the  $\text{TiO}_2$ -only validation glasses are given in References 82-83 and include dissolution of the glasses by the Process Science Analytical Laboratory (PSAL) using the methods given in ASTM C1463 for dissolution followed by ICP-ES for cations and Ion Chromatography (IC) for anions. The viscosity measurements were made on the SRNL radioactive Harrop viscometer [91,92]. The  $\text{TiO}_2$ -only composition-viscosity validation database is given in Appendix D. Glasses that were omitted as  $\text{TiO}_2$ -only validation data included the following:

- HLW-01 through HLW-06 and FY09EM21-03 which were crystallized
- HLW-15, HLW-18, FY09EM21-05, FY09EM21-08, FY09EM21-11, FY09EM21-14 which contained  $> 2.00 \text{ wt\% TiO}_2$  and  $\text{Al}_2\text{O}_3 < 4.00 \text{ wt\%}$
- FY09EM21-14 which had over 14 wt%  $\text{B}_2\text{O}_3$
- Viscosity values for glasses that were 10 poise or less.

#### 4.4 CST Viscosity Model Database

Table 6 lists the CST viscosity study data as having been used to validate the historic viscosity model and document why a uranium term was not needed in the historic viscosity model. In this study, the CST viscosity data from References 65-69 were used to develop a viscosity model with a  $\text{TiO}_2$ ,  $\text{Nb}_2\text{O}_5$ , and  $\text{ZrO}_2$  term (all species found in crystalline silicotitanate). Many of the CST glasses failed the old ROC limits ( $\leq 2.00 \text{ TiO}_2$  and  $\text{Al}_2\text{O}_3 < 3.00 \text{ wt\%}$ ) and many more failed the higher  $\text{TiO}_2$  ROC limits ( $> 2.00 \text{ wt\% TiO}_2$  and  $\text{Al}_2\text{O}_3 < 4.00 \text{ wt\%}$ ) from Reference 52 on the CST glass compositions. This left only four glasses from these CST studies to use to develop a CST model. This is an insufficient number of glasses to develop a model.

Half of the 58 glass dataset in References 84-87 was used to supplement the CST study glasses. The KT studies in References 84-87 were designed to maximize the amount of  $\text{TiO}_2$  in a glass if the DWPF vitrified combinations of CST and MST. Half of the 58 glasses were selected randomly as CST model data and half were reserved as CST validation data. The glasses given in each data set are shown in Table 7. These glasses span  $\text{TiO}_2$  compositions from 3.03 to 6.62 wt%  $\text{TiO}_2$  (Table 7 and Appendix E).

The details of the composition and viscosity measurements for the CST model glasses are given in References 65-69 and References 84-87 and include dissolution of the glasses by PSAL using the methods given in ASTM C1463 for dissolution followed by ICP-ES for cations and IC for anions. The



viscosity measurements were made on the SRNL radioactive Harrop viscometer [91,92]. The CST composition-viscosity model database is given in Appendix E.

**Table 7. CST Model Data vs. Validation Data Randomly Selected**

CST Model Data Sample Identifications	CST Validation Data Sample Identifications
CST 15	KT04-03
CST 20	KT04-04
CST 26	KT04-05
CST 32	KT04-07
KT04-01	KT06-03
KT04-02	KT06-04
KT04-06	KT06-05
KT04-08	KT06-06
KT04-09	KT06-07
KT04-10	KT06-09
KT06-01	KT06-10
KT06-02	KT06-11
KT06-08	KT06-12
KT06-17	KT06-13
KT06-18	KT06-14
KT07-02	KT06-15
KT07-06	KT06-16
KT07-07	KT07-01
KT07-09	KT07-03
KT07-10	KT07-04
KT08-01	KT07-05
KT08-02	KT07-08
KT08-03	KT08-07
KT08-04	KT08-08
KT08-05	KT08-09
KT08-06	KT10-02
KT08-10	KT10-04
KT10-01	KT10-05
KT10-03	KT10-07
KT10-06	
KT10-08	
KT10-09	
KT10-10	
TiO <sub>2</sub> = 3.03-6.62 wt%	TiO <sub>2</sub> = 4.07-6.53 wt%

#### 4.5 CST Viscosity Validation Database

References 84-87 were studies designed to maximize the amount of TiO<sub>2</sub> in a glass if the DWPF vitrified combinations of CST and MST (Table 6). Half of these glasses were randomly selected to be used as validation data for the CST viscosity model (Table 7). These glasses span TiO<sub>2</sub> compositions from 4.07 to 6.53 wt% TiO<sub>2</sub> (Table 7 and Appendix F). These CST-MST glasses [84-87] are, therefore, used in this

study to validate the  $\text{TiO}_2$  term in the CST viscosity model. This half of the CST-MST glasses [84-87] is also used to validate the  $\text{Nb}_2\text{O}_5$  and  $\text{ZrO}_2$  terms in the CST viscosity model. Additional glasses, such as the West Valley glasses could not be used to validate the  $\text{ZrO}_2$  term as almost all the West Valley glasses contain  $\text{ThO}_2$  (1.80-3.60 wt%) in addition to  $\text{ZrO}_2$  (0.30-5.50 wt%). While the SWPF validation glasses in Appendix D can also be used to validate the CST model these glasses do not contain  $\text{Nb}_2\text{O}_5$  and little  $\text{ZrO}_2$ .

The details of the composition and viscosity measurements for the CST-MST validation glasses are given in References [84-87] and include dissolution of the glasses by PSAL using the methods given in ASTM C1463 for dissolution followed by ICP-ES for cations and IC for anions. The viscosity measurements were made on the SRNL radioactive Harrop viscometer [91,92]. The CST validation composition-viscosity database is given in Appendix F.

## 5.0 SWPF ( $\text{TiO}_2$ -only) Viscosity Model

### 5.1 Evaluation of the SWPF Glasses Against the Historic DWPF Viscosity Model

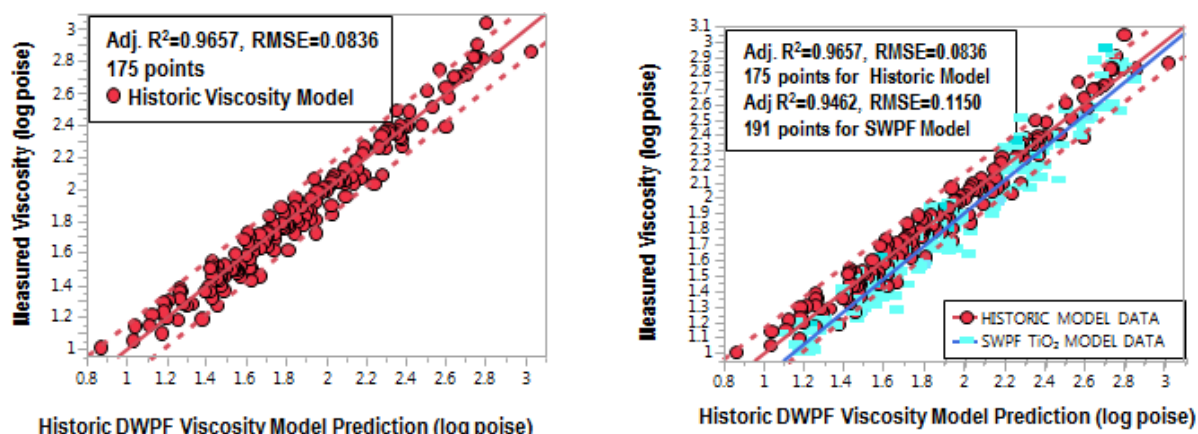
The fit of the historic DWPF viscosity model (from Equation 1 and Equation 3) is shown in Figure 5-1a. It consists of the 175 data points (temperature-viscosity pairs) from 33 different glasses in the historic model database (Appendix A). The model has an adjusted  $R^2$  of 0.9657 and a RMSE of 0.0836.

For the SWPF glass viscosity data given in Appendix C (a pool of 198 temperature-viscosity pairs), three temperature-viscosity pairs were excluded from fitting the data. These three data points had viscosities of <10 poise which is one of the exclusion criteria discussed in Section 2.2. Four points from sample SWPF-12 were removed as this sample was visually inhomogeneous.[94] This left an original SWPF  $\text{TiO}_2$ -only data set of 191 temperature-viscosity pairs. These 191 temperature-viscosity pairs were evaluated against the historic DWPF viscosity model as shown in Figure 5-1b where it can be noted that the SWPF glass viscosities (blue rectangles) do not fit the historic DWPF model. Most of the SWPF  $\text{TiO}_2$  rich glasses lie at or below the U95 confidence band of the historic glass model. This indicates that a  $\text{TiO}_2$  term is needed in the historic viscosity model.

As modeling progressed, an additional thirty six data points (4 points each for glasses SWPF-01 through SWPF-09) were excluded due to the new ROC requirement that the  $\text{Al}_2\text{O}_3$  be  $\geq 4.0$  wt% (see Figure 2-2).[52] However, two of the <10 poise data points were in the SWPF-01 through SWPF-09 dataset. For SWPF-08 and SWPF-12 it was also suspected that these glasses were crystalline before the viscosity measurement was made and this was later confirmed.<sup>f</sup> This left a data modeling pool of 159 temperature-viscosity pairs for 40 of the original 50 glasses which is used in the next section to develop the SWPF  $\text{TiO}_2$ -only viscosity model.

---

<sup>f</sup> preliminary liquidus data indicated that these glasses had crystallized  $\text{Fe}_2\text{O}_3$  and spinel during fabrication,



- (a) Historic DWPF viscosity model (from Equations 1 and 3)
- (b) Historic DWPF viscosity model (from Equations 1 and 3) and data from SWPF Database Overlain

**Figure 5-1. Comparisons of the Historic and SWPF Database Glasses Using the Historic DWPF Viscosity Model (Equations 1 and 3).**

## 5.2 Structural Role of $\text{TiO}_2$ in DWPF Glasses

The historic DWPF viscosity model is a modification of an NBO approach originally developed by White and Minser.[30] While these authors gave mechanistic structural terms for alkali,  $\text{Fe}_2\text{O}_3$ ,  $\text{SiO}_2$ ,  $\text{Al}_2\text{O}_3$ ,  $\text{MgO}$ ,  $\text{CaO}$ , and  $\text{FeO}$ , they did not include +4 charged cations such as  $\text{TiO}_2$  or  $\text{ZrO}_2$ . In the commercial glass industry [99]  $\text{TiO}_2$  is known to decrease melt viscosity which implies that its structural role in glass is one of a bond modifier, ie.,  $\text{TiO}_2$  creates NBOs. Ti acts simultaneously as a network modifier and as a network former because Ti is surrounded by both NBOs and BOs.[100]  $\text{TiO}_4$  polyhedra where Ti is 5-coordinated ( $^{5\text{T}}\text{Ti}$ ) exist in natural melts and these cause heterogeneities in the melt which can lead to crystallization.[100]  $\text{TiO}_2$  is a known crystallizing agent in commercial glasses [99] and HLW defense waste glasses.[101] This is the major reason that a  $\text{TiO}_2$  solubility limit exists in DWPF.[23] The DWPF solubility limit will be redefined once the PCCS model applicability for high  $\text{TiO}_2$  glasses is assessed.

However,  $\text{TiO}_2$  can be tetrahedral ( $^{4\text{T}}\text{Ti}$ ) and substitute for  $\text{SiO}_2$  at temperatures below the glass transition temperature.[99] In addition, Marumo, et al.[102] noted that tetrahedral  $^{4\text{T}}\text{Ti}$  increases with increasing Ti content and octahedral Ti ( $^{6\text{T}}\text{Ti}$ ) is favored at low Ti contents in glass. This is verified in the following sections of this study. For glasses up to ~6 wt%  $\text{TiO}_2$  the Ti is predominately  $^{6\text{T}}\text{Ti}$  and acts as a network modifier creating one NBO. It thus is a positive term in the NBO parameter. At concentrations of  $\text{TiO}_2 \geq 6$  wt% the Ti is predominately  $^{4\text{T}}\text{Ti}$  according to the literature, and the equations developed in the next section for  $\text{TiO}_2$  as a network modifier would have to be modified to account for  $\text{TiO}_2$  being a network former. Thus the  $\text{TiO}_2$  would be a negative term with one BO instead of one NBO. Since this would make the SWPF ( $\text{TiO}_2$ -only) model non-linear, the equations developed in Section 5.3 and validated in Section 5.5 are only considered valid up to a limit of 5.90 wt%  $\text{TiO}_2$  as determined by the validation data in Section 5.5. The exact  $\text{TiO}_2$  concentration at which  $\text{TiO}_2$  switches from a network modifier to a network former lie somewhere between ~6.00 and 8.00 wt%  $\text{TiO}_2$  and additional studies would have to be performed to determine this limit.

## 5.3 Development of the SWPF ( $\text{TiO}_2$ -only) Viscosity Model

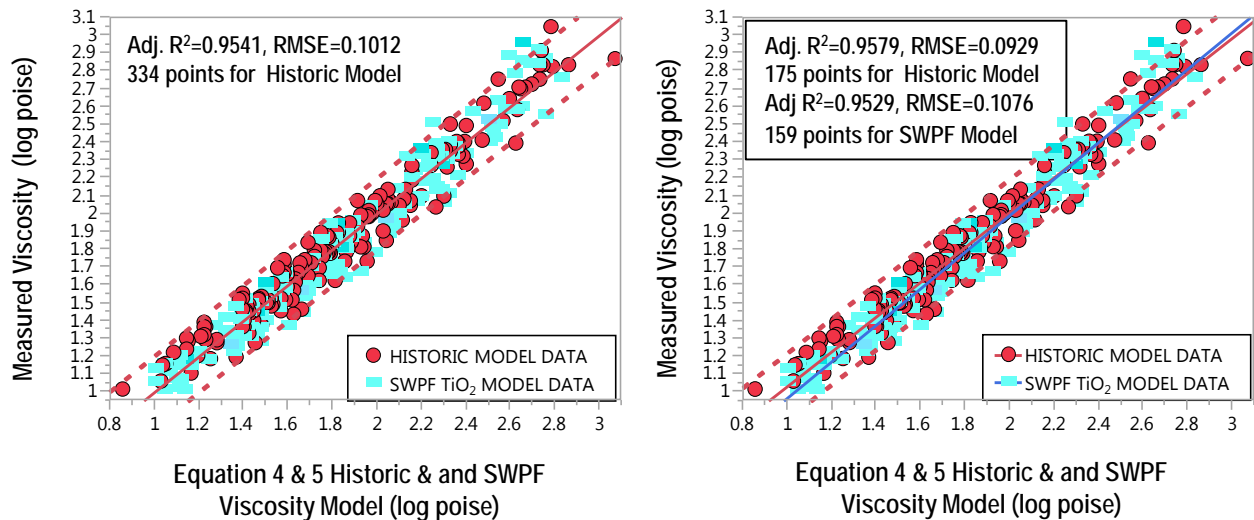
Since  $\text{TiO}_2$ , in the composition range spanned by the SWPF glass viscosity data, acts as a network modifier, it creates one NBO. Therefore, Equation 1 becomes

$$\text{Equation 4} \quad \text{NBO} \equiv \frac{2(\text{Na}_2\text{O} + \text{K}_2\text{O} + \text{Cs}_2\text{O} + \text{Li}_2\text{O} + \text{Fe}_2\text{O}_3 - \text{Al}_2\text{O}_3) + \text{B}_2\text{O}_3 + \text{TiO}_2}{\text{SiO}_2}$$

Fitting the response surface between log viscosity-1/temperature-NBO for the pooled historic and SWPF databases generates the coefficients given in Equation 5. This response surface has 334 data points (temperature-viscosity pair-NBO combinations) and Equation 3 becomes

$$\text{Equation 5} \quad \log \eta(\text{poise}) = -0.606597 + \left( \frac{4587.5797}{T(^{\circ}\text{C})} \right) - (1.711755 * \text{NBO})$$

Figure 5-2a shows how the historic and SWPF glasses overlap one another using Equation 4 and Equation 5 which incorporates the bond breaking caused by concentrations of  $\text{TiO}_2$  up to 5.85 wt%. Application of Equation 4 and Equation 5 to the pooled viscosity dataset as shown in Figure 5-2a gives an adjusted  $R^2=0.9541$  and a RMSE=0.1012. Figure 5-2b shows how each of the datasets (historic vs. SWPF) fit the revised Equation 4 and Equation 5 when analyzed individually. Figure 5-2b indicates that the SWPF viscosity data give about the same adjusted  $R^2$  as the historic data generated by the two commercial glass laboratories (CELS and OCF-SS) but the RMSE is somewhat larger indicating more scatter in the data. The pooled datasets give an overall good fit and  $R^2$  value since potential bias and crystallization (hysteresis) are not known for the SWPF dataset.



(a) Historic and SWPF viscosity model (from Equations 4 and 5) fitted as a pooled dataset

(b) Historic and SWPF viscosity model (from Equations 4 and 5) fitted as separate datasets

Figure 5-2. New SWPF  $\text{TiO}_2$ -only Model fit to Pooled SWPF and Historic Databases and Fit Separately.

The analyzed SWPF glasses contained  $\text{Na}_2\text{O}$  and  $\text{Cs}_2\text{O}$  between 8.03-18.14 wt% and 0.48-1.62 wt%, respectively. This allowed validation of the lumped  $\text{Na}_2\text{O}$  and  $\text{Cs}_2\text{O}$  terms in the historic viscosity model up to these high concentrations.

#### 5.4 Property Acceptable Region (PAR) Assessments for the SWPF ( $\text{TiO}_2$ -only) Viscosity Model

This section provides a closer look at how property-composition models are integrated into DWPF's PCCS, and the information that is necessary to complete that process for the  $\text{TiO}_2$ -only viscosity model. In the DWPF, radioactive sludge is blended with ground glass (frit) in the SME to produce melter feed

slurry. After the SME, the material then passes to the Melter Feed Tank (MFT), which continuously feeds the melter. The melter vitrifies the feed slurry into a molten glass waste form, which is poured into stainless steel canisters for cooling and ultimate storage.

DWPF personnel cannot wait until the melt or waste glass has been made to assess its acceptability, since by then no further changes to either are possible. Therefore, the acceptability decision is made at the SME. The SME is uniquely positioned in the process — it is both the first control point in the process wherein all necessary constituents are present and the last control point at which any change to them can be effected. Thus, the control strategy involves monitoring the blended SME batch.

The monitoring of the SME is accomplished by sampling its contents. For each SME batch, a set of ( $n \geq 4$ ) samples is taken to initiate an acceptability decision. Each of these samples is vitrified and the chemical compositions of the resulting  $n$  glasses are measured. The average of the measured chemical compositions for a minimum of 4 samples is determined, and this average composition serves as the basis for the acceptability decision for the SME batch.

However, the average chemical composition, while necessary, is not sufficient in and of itself, to complete the assessment of the performance of the SME contents against the PCCS constraints. Some of the constraints involve properties (either process or product quality) such as viscosity, liquidus temperature, and durability. These properties cannot be measured in situ, and thus, they must be predicted from models that relate these properties to glass composition. Not only must the model predictions satisfy their corresponding property constraints, but the constraints must also be appropriately met after the applicable modeling uncertainties are introduced into the acceptability decision.

For the constraints involving property-composition models and for most of the other constraints that directly involve composition, the uncertainties associated with the SME samples must also be accounted for as part of the acceptability decision. These uncertainties, the measurement uncertainties, include those related to the collection of the slurry samples in the SME, the preparation of these samples for measurement, and the measurements themselves. Accounting for these uncertainties, while outside of the scope of this effort, is addressed in the technical basis document for PCCS.[103]

A glass composition representing the “average” content of a SME batch is deemed to be within the acceptable operating window for the DWPF if all of the applicable constraints are satisfied, at appropriate confidence levels, after all of the related property modeling and measurement uncertainties are accounted for. Conceptually, there is a layered approach to the acceptability decision. At the first step, the question is, does the average chemical composition representing the SME contents directly or through model predictions satisfy the constraints? If the answer is yes, the composition is said to be within the Expected Property Acceptable Region (EPAR). However, the EPAR does not account for uncertainties in the predicting models. If, after the property model uncertainties are accounted for (to be discussed later), the chemical composition still meets the constraints, then the composition is said to be within the Property Acceptable Region (PAR). Finally, if, after measurement uncertainties are accounted for (to be discussed later), the chemical composition still meets the constraints, then the composition is said to be within the Measurement Acceptable Region (MAR). A composition that is within the MAR for each of the applicable constraints is said to be within the acceptable operating window of the DWPF.

The implementation strategy for integrating the new  $\text{TiO}_2$ -only model into PCCS is similar to the strategy that was utilized for the historical model (please see SME Acceptability Rev 5.[103]) The  $\text{TiO}_2$ -only viscosity-composition model may be expressed as given by:

Equation 6 Viscosity:<sup>††</sup>  $\log \eta = m_v c_v + b_v$

where

$\eta$  is viscosity in poise,

$m_v$  is the estimated slope for this regression model ( $m_v = -1.711755$ )

$b_v$  is the estimated intercept determined from the fitted three-parameter model evaluated at  $T=1150$  °C ( $b_v = 3.382603$ ),

$$c_v = \frac{2(z_{Fe_2O_3} - z_{Al_2O_3} + z_{Cs_2O} + z_{Li_2O} + z_{K_2O} + z_{Na_2O}) + z_{B_2O_3} + z_{TiO_2}}{z_{SiO_2}}, \text{ and}$$

$z_{oxide}$  represents the indicated molar oxide concentration in the glass.

This model can be back-solved (noting the fact that  $m_v$  is negative) to translate the viscosity constraints into constraints on the compositional term,  $c_v$ , as given by:

Equation 7 High Viscosity:

$$\text{high viscosity} \equiv \eta_{hv} \leq 110 \text{ poise} \quad \Rightarrow \quad c_{hv} \geq \left[ \frac{\log(\eta_{hv}) - b_v}{m_v} \right]$$

Equation 8 Low Viscosity:

$$\text{low viscosity} \equiv \eta_{lv} \geq 20 \text{ poise} \quad \Rightarrow \quad c_{lv} \leq \left[ \frac{\log(\eta_{lv}) - b_v}{m_v} \right]$$

The above inequalities describe the region in compositional space where all of the predicted values for viscosity are acceptable. This defines the EPAR for viscosity. The region is denoted as “expected” since it is derived from the fitted line, which is the expected viscosity, based upon the model for a given composition.

The determination of the PAR for this viscosity model is accomplished by accounting for the property model uncertainty in the implementation of the viscosity constraints as was performed in earlier versions of the SME acceptability report for the historic viscosity models. And as before, statistical confidence intervals are used in the determinations of this uncertainty. Specifically, Scheffé simultaneous confidence limits (also called confidence bands [104] and [105]), are used in the development of the PAR’s for the constraints associated with the TiO<sub>2</sub>-only viscosity model as they were for the historical model.

Since the TiO<sub>2</sub>-only viscosity model is of the same form as the historic model, it too includes a linear parameter based upon the inverse temperature (1/T) at which the viscosity ( $\eta$ ) is measured. The complete form of the TiO<sub>2</sub>-only viscosity model may be expressed as:

<sup>††</sup> Actually the viscosity prediction is a three-parameter model including an inverse temperature term. However, this temperature is fixed at 1150°C for DWPF. This allows the viscosity model to be presented as a two-parameter model with the temperature-dependent term included in the pseudo-constant,  $b_v$ .

Equation 9 
$$\log(\eta) = m_v c_v + m_T \frac{1}{T(^{\circ}\text{C})} + b_T.$$

As already indicated in an earlier footnote, for DWPF use, the temperature is fixed at 1150°C. Thus, the predicting relationship for viscosity can be written as:

Equation 10 
$$\log(\eta) = m_v c_v + b_v$$

where  $b_v \equiv \frac{m_T}{T(^{\circ}\text{C})} + b_T$  and  $T(^{\circ}\text{C})$  is 1150°C.

However, the additional parameter must be accounted for when defining the confidence limits for viscosity prediction. The approach used to develop the viscosity PAR is the true one-sided, 100(1-α)% Scheffé-type confidence limit. This leads to the following one-sided, 100(1-α)% Scheffé-type confidence limit to determine the PAR for each viscosity constraint:

Equation 11 
$$\pi = b_T + \left( \frac{m_T}{T^*} \right) + m_v(c^*) + s_r \left\{ \sqrt{p F_{2\alpha}(p, n-p)} \sqrt{\underline{c}_0 (\mathbf{X}^T \mathbf{X})^{-1} \underline{c}_0^T} \right\}$$

where  $\pi$  represents the EPAR for the corresponding constraint (20 P for low viscosity and 110 P for high viscosity),  $s_r$  is the RMSE for the regression fit,  $F_{2\alpha}(p, n-p)$  is the upper 2α% tail of the F distribution with  $p$  degrees of freedom in the numerator and  $n-p$  degrees of freedom in the denominator,  $T^* = 1150^{\circ}\text{C}$ ,  $c^*$  is the compositionally-based term in Equation 6,

$$\underline{c}_0 \equiv \left[ 1, \frac{1}{T^*}, c^* \right] \text{ and } \mathbf{X} \equiv \begin{bmatrix} 1 & \frac{1}{T_1} & c_1 \\ 1 & \frac{1}{T_2} & c_2 \\ \vdots & \vdots & \vdots \\ 1 & \frac{1}{T_n} & c_n \end{bmatrix}.$$

$\mathbf{X}$  is an  $n \times p$  matrix that contains the data for the independent variables from which the regression model was formulated where  $p$  is the number of parameters in the model and  $n$  is the number of observations used in the fitting of the  $\text{TiO}_2$ -only model. Note that the  $\mathbf{X}$  matrix is different for this model as compared to the matrix that was used for the historical model (i.e., the new matrix had 334 observations while the historical model had 173). Thus, the product moment matrix,  $\mathbf{X}^T \mathbf{X}$ , is different for the two models but of dimension 3x3 for both models. The one-sided, 100(1-α)% Scheffé-type confidence limit to determine the PAR for each viscosity constraint may be written as:

Equation 12

$$\pi = b_T + \left( \frac{m_T}{T^*} \right) + m_v(c^*) + s_r \left\{ \sqrt{pF_{2\alpha}(p, n-p)} \sqrt{\begin{bmatrix} 1 & (1/T^*) & c^* \\ c_{0,0} & c_{0,1} & c_{0,2} \\ c_{0,1} & c_{1,1} & c_{1,2} \\ c_{0,2} & c_{1,2} & c_{2,2} \end{bmatrix} \begin{bmatrix} 1 \\ (1/T^*) \\ c^* \end{bmatrix}} \right\},$$

where the inverse of the  $\mathbf{X}^T\mathbf{X}$  matrix is represented by the 3×3 array of  $c$ 's. Since the  $(1/T^*)$  term will be constant for DWPF use, the expression given by Equation 12 can be expanded for each viscosity constraint (i.e., low and high) to a quadratic in  $c^*$  given by  $A(c^*)^2 + B(c^*) + C = 0$  with coefficients given by the set of equations:

Equation 13

$$\begin{aligned} A &\equiv m_v^2 - c_{2,2} [ps_r^2 F_{2\alpha}(p, n-p)] \\ B &\equiv -2 \left\{ m_v (\pi - b_T) + \left( c_{0,2} + \frac{c_{1,2}}{T^*} \right) [ps_r^2 F_{2\alpha}(p, n-p)] \right\} \\ C &\equiv (\pi - b_T)^2 - \left[ c_{0,0} + 2 \left( \frac{c_{0,1}}{T^*} \right) + \frac{c_{1,1}}{(T^*)^2} \right] [ps_r^2 F_{2\alpha}(p, n-p)] \end{aligned}$$

The information from the fitting of the TiO<sub>2</sub>-only viscosity model that is necessary to address its property uncertainty and, thus, to derive its PAR values is provided in Exhibit 1.

Exhibit 1 Information Generated from the Fitting of the TiO<sub>2</sub>-Only Viscosity Model

$p = 3, n = 334, \alpha = 0.05, m = -1.711755, b_T = 3.382603^1, s_r = 0.101351$ , and

$$(\mathbf{X}^T \mathbf{X}) = \begin{bmatrix} 334 & 0.299006 & 322.49187 \\ 0.299006 & 0.000270798 & 0.2899217 \\ 322.49187 & 0.2899217 & 319.71202 \end{bmatrix}$$

For the low viscosity constraint, the roots from the quadratic expression are 1.232996 and 1.200566, and selecting the desired root corresponding to the appropriate one-sided simultaneous confidence interval gives 1.200566 as the limit in composition space for the viscosity model, or

$$\text{Equation 14} \quad \eta = 10^{m_v c_v + b_v} = 10^{-1.711755 \times 1.200566 + 3.382603} = 10^{1.3275} = 21.26$$

(i.e., 21.26 poise at  $T^* = 1150^\circ\text{C}$ ). Only the SiO<sub>2</sub> coefficient in the low viscosity constraint is impacted; that is, the SiO<sub>2</sub> coefficient in the lower viscosity constraint vector is the root from the quadratic

<sup>1</sup> The new melt viscosity model is a three parameter model where the melt temperature is assumed to be 1150°C, and thus the intercept provided is  $b_v = b_T + (m_T/1150) = -0.606597 + (4587.5797/1150) = 3.382603$ .



expression, or  $\underline{a}_{\text{low visc, SiO}_2} = 1.200566$ , while the coefficients of the other oxides are taken directly from their values in Equation 6. The complete  $\underline{a}_{\text{low visc}}$  vector for the TiO<sub>2</sub>-only viscosity model is provided in Table 8.

For the upper viscosity constraint the roots are 0.795480 and 0.770608. The desired root corresponding to the appropriate one-sided simultaneous confidence interval becomes 0.795480, or

$$\text{Equation 15} \quad \eta = 10^{m_v c_v + b_v} = 10^{-1.711755 \times 0.795480 + 3.382603} = 10^{2.02093} = 104.94$$

(i.e., 104.94 poise at  $T^* = 1150^\circ\text{C}$ ). Only the SiO<sub>2</sub> coefficient in the high viscosity constraint is impacted; that is, the SiO<sub>2</sub> coefficient in the high viscosity constraint vector is derived from the root from the quadratic expression, or  $\underline{a}_{\text{high visc, SiO}_2} = -0.79548$ , while the coefficients of the other oxides are taken directly from their values in Equation 6. The complete  $\underline{a}_{\text{high visc}}$  vector for the SWPF TiO<sub>2</sub>-only viscosity model is provided in Table 8 with the SiO<sub>2</sub> coefficients derived in this section highlighted. The constraints are of the form  $\mathbf{z} \bullet \mathbf{a}^T - \beta \geq 0$  in PCCS (see 103).

**Table 8.  $\underline{a}$  Vectors and Offsets for the TiO<sub>2</sub>-Only Viscosity Model Constraints**

	$\underline{z}^T$	Transpose of $\underline{a}$ Vectors for TiO <sub>2</sub> -Only Viscosity Model Constraints	
	Average		
	Molar Oxide		
Oxide	Wt Fraction	$\underline{a}^T_{\text{high visc}}$	$\underline{a}^T_{\text{low visc}}$
Al <sub>2</sub> O <sub>3</sub>	$z_{\text{Al2O3}}$	-2	2
B <sub>2</sub> O <sub>3</sub>	$z_{\text{B2O3}}$	1	-1
BaO	$z_{\text{BaO}}$	0	0
HCOO	$z_{\text{HCOO}}$	0	0
CaO	$z_{\text{CaO}}$	0	0
Ce <sub>2</sub> O <sub>3</sub>	$z_{\text{Ce2O3}}$	0	0
NaCl	$z_{\text{NaCl}}$	0	0
Cr <sub>2</sub> O <sub>3</sub>	$z_{\text{Cr2O3}}$	0	0
Cs <sub>2</sub> O	$z_{\text{Cs2O}}$	2	-2
CuO	$z_{\text{CuO}}$	0	0
NaF	$z_{\text{NaF}}$	0	0
Fe <sub>2</sub> O <sub>3</sub>	$z_{\text{Fe2O3}}$	2	-2
K <sub>2</sub> O	$z_{\text{K2O}}$	2	-2
La <sub>2</sub> O <sub>3</sub>	$z_{\text{La2O3}}$	0	0
Li <sub>2</sub> O	$z_{\text{Li2O}}$	2	-2
MgO	$z_{\text{MgO}}$	0	0
MnO	$z_{\text{MnO}}$	0	0
MoO <sub>3</sub>	$z_{\text{MoO3}}$	0	0
NO <sub>2</sub>	$z_{\text{NO2}}$	0	0
NO <sub>3</sub>	$z_{\text{NO3}}$	0	0
Na <sub>2</sub> O	$z_{\text{Na2O}}$	2	-2
Na <sub>2</sub> SO <sub>4</sub>	$z_{\text{Na2SO4}}$	0	0
Nd <sub>2</sub> O <sub>3</sub>	$z_{\text{Nd2O3}}$	0	0
NiO	$z_{\text{NiO}}$	0	0
P <sub>2</sub> O <sub>5</sub>	$z_{\text{P2O5}}$	0	0
PbO	$z_{\text{PbO}}$	0	0
SiO <sub>2</sub>	$z_{\text{SiO2}}$	-0.79548	1.200566
ThO <sub>2</sub>	$z_{\text{ThO2}}$	0	0
TiO <sub>2</sub>	$z_{\text{TiO2}}$	1	-1
U <sub>3</sub> O <sub>8</sub>	$z_{\text{U3O8}}$	0	0
Y <sub>2</sub> O <sub>3</sub>	$z_{\text{Y2O3}}$	0	0
ZnO	$z_{\text{ZnO}}$	0	0
ZrO <sub>2</sub>	$z_{\text{ZrO2}}$	0	0
	Offset ( $\beta$ )	0	0
		$\beta_{\text{high visc}}$	$\beta_{\text{low visc}}$

The MAR assessment of the TiO<sub>2</sub>-only viscosity model will follow the same approach as was used for the previous viscosity model in Revision 5 of the SME Acceptability report.[103] Thus, completing the assessment of these constraints for a given composition requires that the measurement uncertainty for each of these constraints be accounted for. Since each of the viscosity constraints involves a linear combination of the  $\underline{z}$  vector of component concentrations, the measurement uncertainty can be addressed as described in Appendix B of Reference 103.

The PAR assessment demonstrates that the following operating limits would be imposed on DWPF viscosity using Equation 4 and Equation 5:

20	<	Viscosity	<	110	poise
21.26	<	PAR	<	104.94	poise

### 5.5 Validation of the SWPF (TiO<sub>2</sub>-only) Viscosity Model

References 82-83, two studies which maximized waste loadings in defense waste glasses, (Table 6) were used to validate the SWPF TiO<sub>2</sub>-only viscosity model. The acceptable glasses from these studies span TiO<sub>2</sub> compositions from 1.25 to 6.76 wt% TiO<sub>2</sub>. The acceptable SWPF TiO<sub>2</sub> data spanned 1.90 to 5.85 wt% TiO<sub>2</sub> (Appendix C) and the historic database (Appendix A and Table 2) spanned 0-1.78 wt% TiO<sub>2</sub>. Since the historic and SWPF databases were merged to generate the SWPF (TiO<sub>2</sub>-only) viscosity model the range of TiO<sub>2</sub> is 0-5.85 wt%.

The two high waste loading glass databases used for validation of the SWPF (TiO<sub>2</sub>-only) model span TiO<sub>2</sub> values of 1.25-5.90 wt% in the absence of Nb<sub>2</sub>O<sub>5</sub> and minimal ZrO<sub>2</sub>, i.e., 0.01-0.82 wt% ZrO<sub>2</sub> (Appendix D). Other potential datasets listed in Table 6 included glasses with high Nb<sub>2</sub>O<sub>5</sub> and/or high ZrO<sub>2</sub>, and these were not appropriate validation composition ranges for a model without these oxide components. These high waste loaded glasses [82-83] are, therefore, used in this study to validate the TiO<sub>2</sub> term in the SWPF viscosity model.

Table 6 indicates that the two high level waste loading studies had measured 264 viscosity-temperature pairs. However, 154 viscosity-temperature pairs violated the criteria given in Sections 2.1 or 2.2 and six glasses violated the new ROC requirement of 4.0 wt% Al<sub>2</sub>O<sub>3</sub>. [52] This left 116 viscosity-temperature pairs and these are tabulated in Appendix D. Figure 5-3 shows how 101 viscosity-temperature-NBO combinations fit within the 95% confidence bands of the SWPF TiO<sub>2</sub>-only model generated from Equation 4 and Equation 5. The other five viscosity-temperature-NBO combinations are five viscosity-temperature measurements from the same glass, FY09EM21-15, as identified in Figure 5-3. This glass had only 1.86 wt% TiO<sub>2</sub> but contained 2.27 wt% NiO, 4.35 wt% MnO coupled with 1.34 wt% MgO and 3.33 wt% CaO for a sum of 13.15 wt% XO terms where X=Ni, Mn, Mg, and Ca. Since neither the DWPF historic viscosity model nor the SWPF TiO<sub>2</sub>-only model has a +2 cation NBO term, it is believed that the poor fit of this one glass is due to the sum of the divalent cations and not TiO<sub>2</sub>.

While the validation data only spans from log 1 or 10 poise to log 2.04 or 110 poise this encompasses the DWPF processing range of 20-110 poise. Therefore, the use of Equation 4 and Equation 5 have shown that the TiO<sub>2</sub> term as a network modifier has been validated up to 5.90 wt% TiO<sub>2</sub> the maximum given in the TiO<sub>2</sub> validation database (Appendix D) while the model development showed that Equation 4 and Equation 5 were valid up to 5.85 wt% TiO<sub>2</sub>.

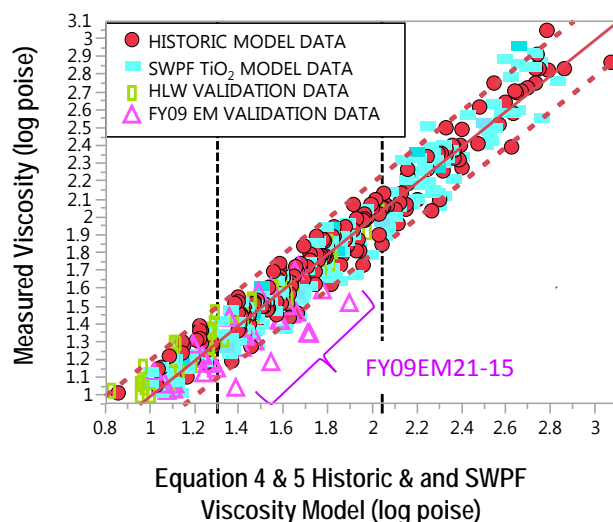


Figure 5-3. Validation Data from Appendix D (116 viscosity-temperature-NBO combinations) overlain on the SWPF (TiO<sub>2</sub>-only) model developed from the SWPF and Historic glass Databases in Appendices B and C (334 viscosity-temperature-NBO combinations). Vertical lines indicate DWPF processing limits.

## 6.0 CST TiO<sub>2</sub>-Nb<sub>2</sub>O<sub>5</sub>-ZrO<sub>2</sub> Viscosity Model

### 6.1 Evaluation of the CST Model Glasses Against the Historic DWPF Viscosity Model

The DWPF CST glasses not only contain TiO<sub>2</sub> but contain Nb<sub>2</sub>O<sub>5</sub> and a ZrO<sub>2</sub> binder. The DWPF validation glasses shown in Table 6 include CST glass viscosity data generated in References 65-69 that are used in this document to generate a CST viscosity model. The CST viscosity model includes the viscosity data from References 65-69 and the SWPF viscosity data generated by ES-VSL which are discussed in Section 5.3, and the historic viscosity data discussed in Section 5.1. Any glasses containing TiO<sub>2</sub> >2.0 wt%, including the CST glasses (TiO<sub>2</sub> up to 6.62 wt% as given in Appendix E) require a TiO<sub>2</sub> term in the DWPF viscosity model as discussed in Section 5.1.

### 6.2 Structural Role of TiO<sub>2</sub>, Nb<sub>2</sub>O<sub>5</sub> and ZrO<sub>2</sub> in DWPF Glasses

The role of TiO<sub>2</sub> in glass was discussed in Section 5.2. TiO<sub>2</sub> was shown to act as a network modifier creating NBOs up to about 6.0 wt% TiO<sub>2</sub>. ZrO<sub>2</sub> is always octahedrally coordinated (<sup>6</sup>Zr or ZrO<sub>6</sub>) and should be a network modifier creating NBO in a similar fashion to TiO<sub>2</sub>. However, Zr-Si correlations are observed in melts studied by X-ray Absorption Near Edge Spectroscopy (XANES), i.e. corner sharing of ZrO<sub>6</sub> octahedra and SiO<sub>4</sub> tetrahedra.[99] Zirconium has a large field strength and a directional bond that strengthens glass structures.[99] Thus ZrO<sub>2</sub> acts like a network former rather than a network modifier and is modeled as such in this study.

The element niobium exists as +2, +4 and +5 valence states. It can form niobium monoxide (NbO), niobium dioxide (NbO<sub>2</sub>), or niobium pentoxide (Nb<sub>2</sub>O<sub>5</sub>). While it appears intuitive that NbO<sub>2</sub>, which is isostructural with TiO<sub>2</sub>, ThO<sub>2</sub>, ZrO<sub>2</sub>, HfO<sub>2</sub> and other fluorite structured oxides, might be the form of niobium in glass, Volf [99] states that Nb is very difficult to reduce to lower oxidation states in glass and occurs solely in its highest oxidation state as Nb<sub>2</sub>O<sub>5</sub>. In the chemical formula for CST, Na<sub>1.5</sub>Nb<sub>0.5</sub>Ti<sub>1.5</sub>O<sub>3</sub>SiO<sub>4</sub>•2H<sub>2</sub>O, the Nb is in the +5 oxidation state as well. So when CST melts into DWPF glass the Nb coordination should remain as a +5 oxidation state.

Niobium is unique in that it shows both ionic and covalent bonding with the covalent bonding being dominant and approaching that of silicon.[99] The coordination number of Nb in glass varies between 6

and 8 and may even be 9. Therefore, it is considered an intermediate glass forming element like other transition elements in the 2<sup>nd</sup> and 3<sup>rd</sup> column of the periodic table. Silicon-29 Magic Angle Spinning Nuclear Magnetic Resonance (MAS NMR) spectra suggest that Nb<sup>5+</sup> ions create cross-links between several oxygen sites, breaking BO bonds to form a range of polyhedra such as [Nb(OM)<sub>6-y</sub>(OSi)<sub>y</sub>] where y varies from 1 to 5 and M can be Na, Ca, or P.[106] Therefore, Nb<sub>2</sub>O<sub>5</sub> is considered to create NBOs in this study, i.e., it is a network modifier.

### 6.3 Development of the CST (TiO<sub>2</sub>-Nb<sub>2</sub>O<sub>5</sub>-ZrO<sub>2</sub>) Viscosity Model

Since TiO<sub>2</sub>, in the composition range spanned by the SWPF and CST glass viscosity data, acts as a network modifier, it creates one NBO per mole. Likewise, Nb<sub>2</sub>O<sub>5</sub> creates 2 NBO per mole, and ZrO<sub>2</sub> creates one BO per mole. Therefore, Equation 1 becomes

$$\text{Equation 16} \quad \text{NBO} \equiv \frac{2(\text{Na}_2\text{O} + \text{K}_2\text{O} + \text{Cs}_2\text{O} + \text{Li}_2\text{O} + \text{Fe}_2\text{O}_3 + \text{Nb}_2\text{O}_5 - \text{Al}_2\text{O}_3) + \text{B}_2\text{O}_3 + \text{TiO}_2 - \text{ZrO}_2}{\text{SiO}_2}$$

The combined CST and randomly selected KT glass viscosity data used to develop a CST model are given in Appendix E. They consist of a pool of 233 temperature-viscosity pairs. When the 233 CST data points are added to the 159 SWPF glass viscosity data points discussed in Section 5.3, and the 175 historic viscosity-temperature pairs discussed in Section 5.1, the CST model database has 557 log viscosity-1/temperature-NBO combinations.

The response surface between log viscosity-1/temperature-NBO for 557 pooled historic, SWPF, and CST databases generates the CST model, i.e., Equation 17.

$$\text{Equation 17} \quad \log \eta(\text{poise}) = -0.629934 + \left( \frac{4547.3573}{T(^{\circ}\text{C})} \right) - (1.622574 * \text{NBO})$$

Figure 6-1 shows how the historic, SWPF, and CST glasses overlap one another using Equation 16 and Equation 17 which incorporate the bond breaking caused by TiO<sub>2</sub> and Nb<sub>2</sub>O<sub>5</sub> and the bond forming tendencies of ZrO<sub>2</sub>. Application of Equation 16 and Equation 17 to the pooled viscosity dataset as shown in Figure 6-1 gives an adjusted R<sup>2</sup>=0.9397 and a RMSE=0.1033 somewhat lower than the corresponding values for the combined historic and SWPF TiO<sub>2</sub>-only model.

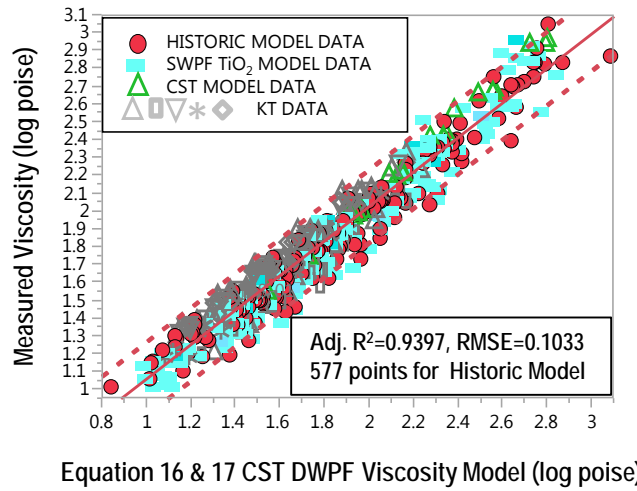


Figure 6-1. CST Viscosity Model with terms for  $\text{TiO}_2$ ,  $\text{Nb}_2\text{O}_5$ , and  $\text{ZrO}_2$ . Note that there were 5 different KT studies and so there are 5 different symbols on the figure but all the KT studies are shaded gray.

The CST model not only covers the  $\text{TiO}_2$  range defined by the CST and randomly selected KT data ( $\text{TiO}_2 = 3.03\text{--}6.62\text{ wt\%}$ ), but covers the combined range of  $\text{TiO}_2$  from being merged with the historic and SWPF viscosity databases (Section 5.3, Appendices B and C) for a combined  $\text{TiO}_2$  range of 0-6.62 wt%  $\text{TiO}_2$ . The CST model covers  $\text{Nb}_2\text{O}_5$  concentrations of 0-1.96 wt% and  $\text{ZrO}_2$  concentrations of 0-1.78 wt%.

#### 6.4 Property Acceptable Region (PAR) Assessments for the CST ( $\text{TiO}_2$ - $\text{Nb}_2\text{O}_5$ - $\text{ZrO}_2$ ) Viscosity Model

A major consideration for the introduction of CST into the DWPF flowsheet is that niobium would become a reportable element in PCCS and that means that the measurement error associated with niobium would have to be known. At present, Nb measurement error is not known and Nb is not a reportable element to the geologic repository. Some Waste Acceptance Product Specifications (WAPS) documentation would have to be changed at the point at which CST is introduced into the DWPF. All of the activities necessary to complete this process are not addressed in this document. This section develops only the implementation strategy for integrating the new CST model into the viscosity evaluation conducted by PCCS. This effort follows the strategy that was utilized above for SWPF  $\text{TiO}_2$ -only viscosity-composition model. The CST viscosity-composition model may be expressed as given by:

Equation 18 Viscosity:<sup>††</sup> 
$$\log \eta = m_v c_v + b_v$$
 where

$\eta$  is viscosity in poise,

$m_v$  is the estimated slope for this regression model ( $m_v = -1.763161$ )

$b_v$  is the estimated intercept determined from the fitted three parameter model evaluated at  $T=1150\text{ }^\circ\text{C}$  ( $b_v = 3.424645$ ),

<sup>††</sup> Actually the viscosity prediction is a three-parameter model including the inverse temperature term. However, this temperature is fixed at  $1150^\circ\text{C}$  for DWPF. This allows the viscosity model to be presented as a two-parameter model with the temperature-dependent term included in the pseudo-constant,  $b_v$ .

$$c_v = \frac{2(z_{Fe_2O_3} - z_{Al_2O_3} + z_{Cs_2O} + z_{Li_2O} + z_{K_2O} + z_{Na_2O}) + z_{B_2O_3} + z_{TiO_2} - z_{ZrO_2}}{z_{SiO_2}}, \text{ and}$$

$z_{\text{oxide}}$  represents the indicated molar oxide concentration in the glass.

This model can be back-solved (noting the negative value for  $m_v$ ) to translate the viscosity constraints into constraints on the compositional term,  $c_v$ , as given by:

Equation 19 High Viscosity:

$$\text{high viscosity} \equiv \eta_{hv} \leq 110 \text{ poise} \quad \Rightarrow \quad c_{hv} \geq \left[ \frac{\log(\eta_{hv}) - b_v}{m_v} \right]$$

Equation 20 Low Viscosity:

$$\text{low viscosity} \equiv \eta_{lv} \geq 20 \text{ poise} \quad \Rightarrow \quad c_{lv} \leq \left[ \frac{\log(\eta_{lv}) - b_v}{m_v} \right]$$

The above inequalities describe the region in compositional space where all of the predicted values for viscosity are acceptable. This defines the EPAR for viscosity. The region is denoted as “expected” since it is derived from the fitted line, which is the expected viscosity, based upon the model for a given composition.

The determination of the PAR for this viscosity model is accomplished by accounting for the property model uncertainty in the implementation of the viscosity constraints. And as before, statistical confidence intervals are used in the determinations of this uncertainty. Specifically, Scheffé simultaneous confidence limits (also called confidence bands [104] and [105]), are used in the development of the PAR’s for the constraints associated with the CST viscosity model as they were for the current model.

Since the CST viscosity model is of the same form as the historic model and the SWPF TiO<sub>2</sub>-only model, it too includes a linear parameter based upon the inverse temperature (1/T) at which the viscosity ( $\eta$ ) is measured. The complete form of the CST viscosity model may be expressed as:

$$\text{Equation 21} \quad \log(\eta) = m_v c_v + m_T \frac{1}{T(^{\circ}\text{C})} + b_T.$$

As already indicated in an earlier footnote, for DWPF use, the temperature is fixed at 1150°C. Thus, the predicting relationship for viscosity can be written as:

$$\begin{aligned} \text{Equation 22} \quad \log(\eta) &= m_v c_v + b_v \\ \text{where } b_v &\equiv \frac{m_T}{T(^{\circ}\text{C})} + b_T \text{ and } T(^{\circ}\text{C}) \text{ is } 1150^{\circ}\text{C}. \end{aligned}$$

However, the additional parameter must be accounted for when defining the confidence limits for viscosity prediction. The approach used to develop the viscosity PAR is the true one-sided, 100(1- $\alpha$ )% Scheffé-type confidence limit. This leads to the following one-sided, 100(1- $\alpha$ )% Scheffé-type confidence limit to determine the PAR for each viscosity constraint:

$$\text{Equation 23} \quad \pi = b_T + \left( \frac{m_T}{T^*} \right) + m_v(c^*) + s_r \left\{ \sqrt{pF_{2\alpha}(p, n-p)} \sqrt{\underline{c}_0 (\mathbf{X}^T \mathbf{X})^{-1} \underline{c}_0^T} \right\}$$

where  $\pi$  represents the EPAR for the corresponding constraint (20 P for low viscosity and 110 P for high viscosity),  $s_r$  is the RMSE for the regression fit,  $F_{2\alpha}(p, n-p)$  is the upper  $2\alpha\%$  tail of the F distribution with  $p$  degrees of freedom in the numerator and  $n-p$  degrees of freedom in the denominator,  $T^* = 1150^\circ\text{C}$ ,  $c^*$  is the compositionally-based term in Equation 18,

$$\underline{c}_0 \equiv \left[ 1, \frac{1}{T^*}, c^* \right] \quad \text{and} \quad \mathbf{X} \equiv \begin{bmatrix} 1 & \frac{1}{T_1} & c_1 \\ 1 & \frac{1}{T_2} & c_2 \\ \vdots & \vdots & \vdots \\ 1 & \frac{1}{T_n} & c_n \end{bmatrix}.$$

$\mathbf{X}$  is an  $n \times p$  matrix that contains the data for the independent variables from which the regression model was formulated where  $p$  is the number of parameters in the model and  $n$  is the number of observations used in the fitting of the CST model. Note that the product moment matrix,  $\mathbf{X}^T \mathbf{X}$ , is different than that for the SWPF  $\text{TiO}_2$ -Only model but of dimension  $3 \times 3$ . The one-sided,  $100(1-\alpha)\%$  Scheffé-type confidence limit to determine the PAR for each viscosity constraint may be written as:

Equation 24

$$\pi = b_T + \left( \frac{m_T}{T^*} \right) + m_v(c^*) + s_r \left\{ \sqrt{pF_{2\alpha}(p, n-p)} \sqrt{\begin{bmatrix} 1 & (1/T^*) & c^* \\ c_{0,0} & c_{0,1} & c_{0,2} \\ c_{0,1} & c_{1,1} & c_{1,2} \\ c_{0,2} & c_{1,2} & c_{2,2} \end{bmatrix} \begin{bmatrix} 1 \\ (1/T^*) \\ c^* \end{bmatrix}} \right\},$$

where the inverse of the  $\mathbf{X}^T \mathbf{X}$  matrix is represented by the  $3 \times 3$  array of  $c$ 's. Since the  $(1/T^*)$  term will be constant for DWPF use, the expression in Equation 24 can be expanded for each viscosity constraint (i.e., low and high) to a quadratic in  $c^*$  given by  $A(c^*)^2 + B(c^*) + C = 0$  with coefficients given by the set of equations:

Equation 25

$$\begin{aligned} A &\equiv m_v^2 - c_{2,2} [ps_r^2 F_{2\alpha}(p, n-p)] \\ B &\equiv -2 \left\{ m_v (\pi - b_T) + \left( c_{0,2} + \frac{c_{1,2}}{T^*} \right) [ps_r^2 F_{2\alpha}(p, n-p)] \right\} \\ C &\equiv (\pi - b_T)^2 - \left[ c_{0,0} + 2 \left( \frac{c_{0,1}}{T^*} \right) + \frac{c_{1,1}}{(T^*)^2} \right] [ps_r^2 F_{2\alpha}(p, n-p)] \end{aligned} \quad (9)$$

The information from the fitting of the CST viscosity model that is necessary to address its property uncertainty and, thus, to derive its PAR values is provided in Exhibit 2.



Exhibit 2 Information Generated from the Fitting of the CST Viscosity Model

$p = 3, n = 557, \alpha = 0.05, m = -1.622574, b_T = 3.32429^2, s_r = 0.103304$ , and

$$(\mathbf{X}^T \mathbf{X}) = \begin{bmatrix} 557 & 0.494583 & 549.0442 \\ 0.494583 & 0.0004429 & 0.488414 \\ 549.0442 & 0.488414 & 552.1812 \end{bmatrix}$$

For the low viscosity constraint, the roots from the quadratic expression are 1.262267 and 1.232882, and selecting the desired root corresponding to the appropriate one-sided simultaneous confidence interval gives 1.232882 as the limit in composition space for the viscosity model, or

Equation 26  $\eta = 10^{m_v c_v + b_v} = 10^{-1.622574 \times 1.232882 + 3.32429} = 10^{1.3238} = 21.08$

(i.e., 21.08 poise at  $T^* = 1150^\circ\text{C}$ ). Only the  $\text{SiO}_2$  coefficient in the low viscosity constraint is impacted; that is, the  $\text{SiO}_2$  coefficient in the lower viscosity constraint vector is the root from the quadratic expression, or  $\underline{a}_{\text{low visc}, \text{SiO}_2} = 1.232882$ , while the coefficients of the other oxides are taken directly from their values in Equation 18. The complete  $\underline{a}_{\text{low visc}}$  vector for the CST viscosity model is provided in Table 9.

For the upper viscosity constraint the roots are 0.801801 and 0.778606. The desired root corresponding to the appropriate one-sided simultaneous confidence interval becomes 0.801801, or

Equation 27  $\eta = 10^{m_v c_v + b_v} = 10^{-1.622574 \times 0.801801 + 3.32429} = 10^{2.0233} = 105.51$

(i.e., 105.51 poise at  $T^* = 1150^\circ\text{C}$ ). Only the  $\text{SiO}_2$  coefficient in the high viscosity constraint is impacted; that is, the  $\text{SiO}_2$  coefficient in the high viscosity constraint vector is derived from the root from the quadratic expression, or  $\underline{a}_{\text{high visc}, \text{SiO}_2} = -0.801801$ , while the coefficients of the other oxides are taken directly from their values in Equation 18. The complete  $\underline{a}_{\text{high visc}}$  vector for the CST viscosity model is provided in Table 9 with the  $\text{SiO}_2$  coefficients derived in this section highlighted as well as the coefficients for  $\text{Nb}_2\text{O}_5$  and  $\text{ZrO}_2$ . The constraints are of the form  $\mathbf{z} \bullet \mathbf{a}^T - \beta \geq 0$  in PCCS (see 103).

<sup>2</sup> The CST viscosity model is a three parameter model where the melt temperature is assumed to be  $1150^\circ\text{C}$ , and thus the intercept provided is  $b_v = b_T + (m_T/1150) = -0.629934 + (4547.357/1150) = 3.32429$ .

**Table 9.  $\underline{a}$  Vectors and Offsets for the CST Viscosity Model Constraints**

	$\underline{z}^T$	Transpose of $\underline{a}$ Vectors for CST Viscosity Model Constraints	
	Average		
	Molar Oxide		
Oxide	Wt Fraction	$\underline{a}^T_{\text{high visc}}$	$\underline{a}^T_{\text{low visc}}$
Al <sub>2</sub> O <sub>3</sub>	$z_{\text{Al}_2\text{O}_3}$	-2	2
B <sub>2</sub> O <sub>3</sub>	$z_{\text{B}_2\text{O}_3}$	1	-1
BaO	$z_{\text{BaO}}$	0	0
HCOO	$z_{\text{HCOO}}$	0	0
CaO	$z_{\text{CaO}}$	0	0
Ce <sub>2</sub> O <sub>3</sub>	$z_{\text{Ce}_2\text{O}_3}$	0	0
NaCl	$z_{\text{NaCl}}$	0	0
Cr <sub>2</sub> O <sub>3</sub>	$z_{\text{Cr}_2\text{O}_3}$	0	0
Cs <sub>2</sub> O	$z_{\text{Cs}_2\text{O}}$	2	-2
CuO	$z_{\text{CuO}}$	0	0
NaF	$z_{\text{NaF}}$	0	0
Fe <sub>2</sub> O <sub>3</sub>	$z_{\text{Fe}_2\text{O}_3}$	2	-2
K <sub>2</sub> O	$z_{\text{K}_2\text{O}}$	2	-2
La <sub>2</sub> O <sub>3</sub>	$z_{\text{La}_2\text{O}_3}$	0	0
Li <sub>2</sub> O	$z_{\text{Li}_2\text{O}}$	2	-2
MgO	$z_{\text{MgO}}$	0	0
MnO	$z_{\text{MnO}}$	0	0
MoO <sub>3</sub>	$z_{\text{MoO}_3}$	0	0
NO <sub>2</sub>	$z_{\text{NO}_2}$	0	0
NO <sub>3</sub>	$z_{\text{NO}_3}$	0	0
Na <sub>2</sub> O	$z_{\text{Na}_2\text{O}}$	2	-2
Na <sub>2</sub> SO <sub>4</sub>	$z_{\text{Na}_2\text{SO}_4}$	0	0
Nb <sub>2</sub> O <sub>5</sub>	$z_{\text{Nb}_2\text{O}_5}$	2	-2
Nd <sub>2</sub> O <sub>3</sub>	$z_{\text{Nd}_2\text{O}_3}$	0	0
NiO	$z_{\text{NiO}}$	0	0
P <sub>2</sub> O <sub>5</sub>	$z_{\text{P}_2\text{O}_5}$	0	0
PbO	$z_{\text{PbO}}$	0	0
SiO <sub>2</sub>	$z_{\text{SiO}_2}$	-0.801801	1.23288
ThO <sub>2</sub>	$z_{\text{ThO}_2}$	0	0
TiO <sub>2</sub>	$z_{\text{TiO}_2}$	1	-1
U <sub>3</sub> O <sub>8</sub>	$z_{\text{U}_3\text{O}_8}$	0	0
Y <sub>2</sub> O <sub>3</sub>	$z_{\text{Y}_2\text{O}_3}$	0	0
ZnO	$z_{\text{ZnO}}$	0	0
ZrO <sub>2</sub>	$z_{\text{ZrO}_2}$	-1	1
	Offset ( $\beta$ )	0	0
		$\beta_{\text{high visc}}$	$\beta_{\text{low visc}}$

Once niobium is introduced into PCCS, the MAR assessment of the CST viscosity model will follow the same approach as was used for the previous viscosity model in Revision 5 of the SME Acceptability report.[103] Thus, completing the assessment of these constraints for a given composition requires that the measurement uncertainty for each of these constraints be accounted for. Since each of the viscosity constraints involves a linear combination of the  $\underline{z}$  vector of component concentrations, the measurement uncertainty can be addressed as described in Appendix B of [103].

The PAR assessment demonstrates that the following operating limits would be imposed on DWPF viscosity using Equation 16 and Equation 17:

20	<	Viscosity	<	110	poise
21.08	<	PAR	<	105.51	poise

### 6.5 Validation of the CST (TiO<sub>2</sub>-Nb<sub>2</sub>O<sub>5</sub>-ZrO<sub>2</sub>) Viscosity Model

In References 84-87 combinations of MST and CST in glass were studied (see Table 6). The CST validation data glass studies are randomly selected from studies KT-04, KT-06, KT-07, KT-08, and KT-10. Several of the other KT studies did not measure viscosity. Table 6 indicates that there are 587 viscosity-temperature measurements available for all the KT studies but the randomly selected 29 of 58 glasses provide 201 viscosity-temperature measurements. In the KT studies not used in this report, concentrations of TiO<sub>2</sub> greater than ~6.00 wt% were examined, the TiO<sub>2</sub> in these glasses was acting as a network former and not a network modifier as discussed in Section 5.2. Thus at high TiO<sub>2</sub> concentrations a different term for TiO<sub>2</sub> would be needed with a different sign (negative) which would make the CST viscosity model non-linear and problematic to program into PCCS. The exact TiO<sub>2</sub> concentrations at which TiO<sub>2</sub> switches from a network modifier to a network former lie somewhere between ~6.00 and 8.00 wt% TiO<sub>2</sub>, and additional studies would have to be performed to determine this limit.

For the CST Model development 182 viscosity-temperature measurements from studies KT-01 through KT-03 were not used in validation of the CST model. The remaining randomly selected KT-04 through KT-10 data span TiO<sub>2</sub> concentrations from 4.17 to 6.53, Nb<sub>2</sub>O<sub>5</sub> concentrations from 0.03 to 2.30, and ZrO<sub>2</sub> concentrations from 0.11 to 2.90. The data are given in Appendix F.

Figure 6-2 shows how the 201 viscosity-temperature-NBO validation combinations fit within the 95% confidence bands of the CST viscosity model generated from Equation 16 and Equation 17. The other seven viscosity-temperature-NBO combinations are viscosity-temperature measurements from the same glass, KT-08-07 as identified in Figure 6-2. This glass had only 4.27 wt% TiO<sub>2</sub>, 0.89 wt% Nb<sub>2</sub>O<sub>5</sub>, and 0.01 wt% ZrO<sub>2</sub>. All the other oxides were in ranges studied and/or bracketed by other glasses in the KT-04 through KT-10 studies. Although the Fulcher fit did not indicate hysteresis, this glass did crystallize during canister centerline cooling curve experiments.[87]

Therefore, the use of Equation 16 and Equation 17 has shown that the TiO<sub>2</sub> term as a network modifier has been validated up to 6.53 wt% for the CST model when coupled with Nb<sub>2</sub>O<sub>5</sub> and ZrO<sub>2</sub> in a DWPF glass. The value of 6.53 wt% for validation data is less than the 6.62 TiO<sub>2</sub> in the CST model data. Both the CST model and validation data, 6.62 and 6.53 wt% TiO<sub>2</sub> respectively, are higher than the 5.90 wt% TiO<sub>2</sub> validated for the SWPF TiO<sub>2</sub>-only model: both the SWPF TiO<sub>2</sub>-only and the CST viscosity models are valid up to ~6-6.5 wt% TiO<sub>2</sub>.

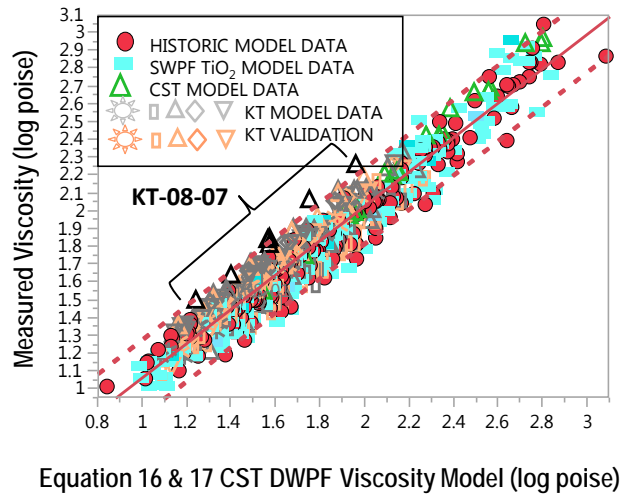


Figure 6-2. Validation Data from Appendix F (201 viscosity-temperature-NBO combinations) overlain on the CST viscosity model developed from the CST, KT (5 different studies shown with 5 different symbols), SWPF, and Historic glass Databases in Appendices B, C, and E (577 viscosity-temperature-NBO combinations).

## 7.0 Conclusions

The DWPF will soon be receiving increased concentrations of TiO<sub>2</sub> enriched wastes from the SWPF. In order to process TiO<sub>2</sub> concentrations >2.0 wt% in the DWPF, new viscosity data were developed over the range of 1.90 to 6.09 wt% TiO<sub>2</sub> and evaluated against the 2005 viscosity model. The SWPF TiO<sub>2</sub>-only model data had to be truncated at 5.85 wt% TiO<sub>2</sub> due to other modeling considerations, i.e. ROC. It was determined that a TiO<sub>2</sub> term was needed in the model to adequately describe the impact of higher TiO<sub>2</sub> concentrations on melt viscosity at 1150°C. Titanium oxide, TiO<sub>2</sub>, acts as a depolymerizing agent in the glass (creating NBO's). Therefore, the SWPF TiO<sub>2</sub>-only containing viscosity model takes the following form:

$$\log \eta(\text{poise}) = -0.606597 + \left( \frac{4587.5797}{T(^{\circ}\text{C})} \right) - (1.711755 * NBO)$$

where 
$$NBO \equiv \frac{2(Na_2O + K_2O + Cs_2O + Li_2O) + 2(Fe_2O_3 - Al_2O_3) + B_2O_3 + TiO_2}{SiO_2}$$

With an adjusted R<sup>2</sup> = 0.9541 and a root mean square error of 0.1012.

This SWPF TiO<sub>2</sub>-only model covers TiO<sub>2</sub> concentrations up to 5.85 wt% and was validated up to TiO<sub>2</sub> concentrations of 5.90 wt% TiO<sub>2</sub> as determined by the validation data.

The new SWPF data used to develop the TiO<sub>2</sub>-only viscosity model (Appendix C) also contained glasses with Cs<sub>2</sub>O up to 1.62 wt%. These new data validated the Cs<sub>2</sub>O term in the historic and TiO<sub>2</sub>-only DWPF viscosity models. The TiO<sub>2</sub>-only model was also shown to be valid (see data in Appendices A, C, and D) up to 4.14 wt% CaO and 2.92 wt% MgO. These wide limits on the amount of CaO and/or MgO that can

be added to future frit compositions are beneficial since CaO is known to suppress nepheline crystallization [38,39,40,107,108] and MgO is known to improve glass durability [109] and to reduce DWPF refractory corrosion and wear.

An alternate viscosity model is also derived for potential future use, should the DWPF ever need to process other titanate containing ion exchange materials, such as crystalline silicotitanate (CST -  $\text{Na}_{1.5}\text{Nb}_{0.5}\text{Ti}_{1.5}\text{O}_3\text{SiO}_4 \cdot 2\text{H}_2\text{O}$ ). The DWPF may receive CST generated by an alternate flowsheet used to pretreat the high-curie fraction of the SRS salt waste. The CST not only contains  $\text{TiO}_2$  but also contains  $\text{Nb}_2\text{O}_5$  and a  $\text{ZrO}_2$  binder where  $\text{TiO}_2$  and  $\text{Nb}_2\text{O}_5$  act to depolymerize the glass (create NBO's) and  $\text{ZrO}_2$  polymerizes the glass (creates BO's). The MST would still be used for  $^{90}\text{Sr}$  removal so this viscosity model would cover future DWPF processing of CST alone or coupled CST-MST flowsheet additions. Therefore, the CST viscosity model takes the following form:

$$\log \eta(\text{poise}) = -0.629934 + \left( \frac{4547.3573}{T(^{\circ}\text{C})} \right) - (1.622574 * \text{NBO})$$

where

$$\text{NBO} \equiv \frac{2 (\text{Na}_2\text{O} + \text{K}_2\text{O} + \text{Cs}_2\text{O} + \text{Li}_2\text{O} + \text{Fe}_2\text{O}_3 + \text{Nb}_2\text{O}_5 - \text{Al}_2\text{O}_3) + \text{B}_2\text{O}_3 + \text{TiO}_2 - \text{ZrO}_2}{\text{SiO}_2}$$

When the SWPF MST glasses ( $\text{TiO}_2=1.90\text{-}5.85$  wt%) and the CST glasses ( $\text{TiO}_2=3.03\text{-}6.62$ ,  $\text{Nb}_2\text{O}_5=0.06\text{-}1.96$  wt% and  $\text{ZrO}_2=0.15\text{-}1.82$  wt%) are combined with the historic DWPF viscosity database ( $\text{TiO}_2=0\text{-}1.78$  wt%), the MST glass data cover a wider range of  $\text{TiO}_2$  than the historic viscosity data but the CST glass data are higher in  $\text{TiO}_2$  content than either of the other model databases. The  $\text{Nb}_2\text{O}_5$  and  $\text{ZrO}_2$  terms are derived solely from the CST data as neither the SWPF-MST viscosity data nor the historic viscosity data contain these species. The CST viscosity model covers up to 2.28 wt% CaO and 2.92 wt% MgO (Appendices A, C, E, and F) and likely is applicable up to 4.14 wt% CaO (Appendix D) as the CST model was not assessed against the  $\text{TiO}_2$  only validation database.

While the  $\text{TiO}_2$ -only viscosity model has been modeled/validated up to  $\sim 6$  wt% (actual of 5.85 wt%  $\text{TiO}_2$ ) and the CST viscosity model has been modeled/validated up to 6.62 wt%  $\text{TiO}_2$ , the role of  $\text{TiO}_2$  as a network breaker switches to a network former by 8.38 wt%  $\text{TiO}_2$ . The exact region at which this switch occurs has not been investigated so the usage of the  $\text{TiO}_2$ -only viscosity model is  $\sim 6$  wt%  $\text{TiO}_2$  and the CST model is  $\sim 6.5$  wt%  $\text{TiO}_2$ .

The ultimate limit on the amount of  $\text{TiO}_2$  that can be accommodated from SWPF will be determined by the three PCCS models, the waste composition of a given sludge batch, the waste loading of the sludge batch, and the frit used for vitrification. Once a component like  $\text{TiO}_2$  is present at larger concentrations than 1-2 wt%, the interactions of that component with other components in the melter feed must be considered simultaneously, i.e. an individual solubility limit cannot be defined to globally account for the interactions with all the remaining sludge/frit composition variables. It is known that  $\text{Ti}^{4+}$  competes with  $\text{Al}^{3+}$  for alkali bonding and it is known that  $\text{Ti}^{4+}$  and  $\text{Fe}^{3+}$  have a coupled impact on their joint solubility in a glass.

## 8.0 Acknowledgements

The authors would like to acknowledge the assistance of all of the authors of the supporting viscosity composition studies including the ES-VSL.

## APPENDIX A. Historic Glass Model Database

Sample ID	Temp (°C)	Visc (poise)	Fe <sup>+2</sup> /ΣFe	Al2O3(v)	B2O3(v)	BaO(v)	CaO(v)	Cr2O3(v)	Cs2O(v)	CuO(v)	FeO(v)	Fe2O3(v)	K2O(v)	La2O3(v)	Li2O(v)	MgO(v)	MnO(v)	Na2O(v)	NiO(v)	SiO2(v)	SrO(v)	TiO2(v)	ZnO(v)	ZrO2(v)	Sum Oxides
AH131AL(1985)	944	562.34	0.02	13.50	10.80	0.00	0.38	0.00	0.00	0.00	0.09	4.57	0.00	0.36	4.09	1.38	2.51	14.10	0.63	46.40	0.00	0.72	0.00	0.34	99.88
	1021	234.42																							
	1098	112.20																							
	1178	58.88																							
	1264	31.62																							
AH131AL(1988)	1020	213.80	0.02	13.50	10.80	0.00	0.38	0.00	0.00	0.00	0.09	4.57	0.00	0.36	4.09	1.38	2.51	14.10	0.63	46.40	0.00	0.72	0.00	0.34	99.88
	1079	120.23																							
	1143	69.18																							
	1200	44.67																							
	1255	30.20																							
	1283	25.12																							
	1079	380.19																							
AH165AL(1988)	1145	208.93	0.06	13.40	7.34	0.00	0.51	0.00	0.00	0.00	0.24	4.57	0.00	0.00	4.20	0.66	2.62	10.60	0.67	53.60	0.00	0.00	0.00	0.79	99.23
	1202	125.89																							
	1259	79.43																							
	1288	64.57																							
	1022	190.55																							
AH165AV(1988)	1082	109.65	0.05	5.17	6.57	0.00	1.04	0.00	0.00	0.00	0.47	11.08	0.00	0.00	5.02	0.66	2.57	9.96	1.01	55.30	0.00	0.00	0.00	0.76	99.66
	1143	64.57																							
	1199	41.69																							
	1255	28.18																							
	1285	23.44																							
	873	741.31																							
AH168AV(1985)	953	245.47	0.06	5.58	10.60	0.00	0.68	0.00	0.00	0.00	0.61	10.51	0.00	0.00	4.24	0.74	2.64	10.10	1.02	51.60	0.00	0.00	0.00	0.69	99.08
	1031	107.15																							
	1107	53.70																							
	1191	28.84																							
	1022	125.89																							
AH168AV(1988)	1084	70.79	0.06	5.58	10.60	0.00	0.68	0.00	0.00	0.00	0.61	10.51	0.00	0.00	4.24	0.74	2.64	10.10	1.02	51.60	0.00	0.00	0.00	0.69	99.08
	1147	41.69																							
	1204	26.92																							
	1260	18.62																							
	1290	15.49																							
	1022	63.10																							
AH168FE(1988)	1082	37.15	0.42	2.47	11.40	0.00	1.35	0.00	0.00	0.00	6.22	9.39	0.00	0.00	4.12	0.71	0.98	10.80	2.82	48.30	0.00	0.00	0.00	0.67	99.92
	1144	22.91																							
	1203	15.85																							
	1259	11.48																							
	1017	812.83																							
AH200AL(1988)	1079	416.87	0.02	13.40	10.20	0.00	0.54	0.00	0.00	0.00	0.07	4.39	3.12	0.00	2.65	1.25	2.49	10.60	0.61	48.40	0.00	1.70	0.00	0.03	99.46
	1143	218.78																							
	1201	134.90																							
	1257	87.10																							
	1286	67.61																							
	916	660.69																							
AH200AV(AH8/1985)	994	251.19	0.04	5.14	10.30	0.00	0.63	0.00	0.00	0.00	0.39	11.47	3.18	0.00	2.68	1.24	2.55	9.77	1.02	49.50	0.00	1.41	0.00	0.02	99.34
	1071	114.82																							
	1148	58.88																							
	1234	31.62																							

39

40



Sample ID	Temp (°C)	Visc (poise)	Fe <sup>2+</sup> /ΣFe	Al <sub>2</sub> O <sub>3</sub> (v)	B <sub>2</sub> O <sub>3</sub> (v)	BaO(v)	CaO(v)	Cr <sub>2</sub> O <sub>3</sub> (v)	Cs <sub>2</sub> O(v)	CuO(v)	FeO(v)	Fe <sub>2</sub> O <sub>3</sub> (v)	K <sub>2</sub> O(v)	La <sub>2</sub> O <sub>3</sub> (v)	Li <sub>2</sub> O(v)	MgO(v)	MnO(v)	Na <sub>2</sub> O(v)	NiO(v)	SiO <sub>2</sub> (v)	SrO(v)	TiO <sub>2</sub> (v)	ZnO(v)	ZrO <sub>2</sub> (v)	Sum Oxides
FRIT 201(1987)	1353	38.90	0.00	0.00	10.50	0.00	0.00	0.00	0.00	0.00	0.00	0.00	0.00	0.00	5.50	1.00	0.00	10.00	0.00	73.00	0.00	0.00	0.00	0.00	100.00
	1382	33.11																							
	1409	28.84																							
	1436	25.12																							
	1491	18.62																							
FRIT 202(1987)	1358	72.44	0.00	0.40	7.81	0.00	0.10	0.00	0.00	0.00	0.00	0.00	0.30	0.00	6.60	1.90	0.00	5.80	0.00	77.04	0.00	0.10	0.00	0.00	100.04
	1384	61.66																							
	1411	52.48																							
	1438	46.77																							
	1466	39.81																							
FRIT 202PHP(1987)	1491	33.88	0.00	4.30	8.60	0.20	1.22	0.07	0.15	0.66	0.00	10.70	5.73	0.00	3.42	2.92	0.00	9.20	0.70	51.20	0.00	1.24	0.00	0.00	100.31
	1091	117.49																							
	1137	77.62																							
	1193	48.98																							
	1249	32.36																							
MAX	1304	22.91	0.47	13.90	12.20	0.20	1.47	0.09	0.15	0.66	7.14	14.20	5.73	0.36	6.96	2.92	3.26	15.80	2.97	77.04	0.07	1.78	0.00	0.99	100.31
	1360	16.60																							
MIN	873	10.23	0.00	0.00	6.41	0.00	0.00	0.00	0.00	0.00	0.00	0.00	0.00	0.00	2.59	0.49	0.00	5.80	0.00	45.60	0.00	0.00	0.00	0.00	98.23

## APPENDIX B. Modeling Constraints

As stated in Section 2.1, various constraints on the compositions of glasses being considered for inclusion in modeling must be applied. The sum of oxides ( $100 \pm 5$  wt%) was mentioned above, as well as the importance that a given glass must be homogeneous, i.e. not phase separated by liquid-liquid amorphous phase separation (APS) due to low  $\text{Al}_2\text{O}_3$  ( $\leq 3.00$  wt%), high  $\text{P}_2\text{O}_5$  ( $\geq 2.25$  wt%), or high  $\text{B}_2\text{O}_3$  ( $\geq 15.00$  wt%) concentrations and not crystallized. The impacts of low  $\text{Al}_2\text{O}_3$ , high  $\text{P}_2\text{O}_5$ , or high  $\text{B}_2\text{O}_3$  on glass durability are discussed below.

### *B.1 The Homogeneity and Low $\text{Al}_2\text{O}_3$ Constraint*

A homogeneity constraint was developed as part of THERMO™ to ensure that DWPF glasses were homogeneous.[18,19] It was noted during the development of THERMO™ that a minimum of 3 wt%  $\text{Al}_2\text{O}_3$  was necessary in high  $\text{Fe}_2\text{O}_3$  containing and high  $\text{Na}_2\text{O}$  containing glasses to avoid amorphous phase separation.[18,19,110] Amorphous phase separation in low  $\text{Al}_2\text{O}_3$  containing glasses is consistent with the known immiscibility gap in the  $\text{Al}_2\text{O}_3$ - $\text{Fe}_2\text{O}_3$ - $\text{Na}_2\text{O}$ - $\text{SiO}_2$  quaternary system that defines the melt surface and crystallization of molten basalt magmas.[111] It is also consistent with known phase separation in  $\text{Na}_2\text{O}$ - $\text{Al}_2\text{O}_3$ - $\text{SiO}_2$  glasses that are known to phase separate when the glasses contain less than ~ 3 wt%  $\text{Al}_2\text{O}_3$ .[112,113]

The homogeneity constraint was implemented in the DWPF PCCS to avoid the possible production of glasses that could be phase separated (liquid-liquid phase separation) and not predictable by the durability models. While the homogeneity constraint was typically an issue at lower waste loadings (WLs), it may impact the operating windows<sup>ξ</sup> for DWPF operations, where the glass forming systems may be limited to lower waste loadings based on fissile or heat load limits. In the Sludge Batch 1b (SB1b) variability study, application of the homogeneity constraint at the MAR limit eliminated much of the potential operating window for DWPF.[114] As a result, Edwards and Brown [115] developed criteria that allowed DWPF to relax the homogeneity constraint from the MAR to the property acceptance region (PAR), which opened up the operating window for DWPF operations. These criteria are defined as:

- (1) use the alumina constraint as currently implemented in PCCS ( $\text{Al}_2\text{O}_3 \geq 3$  wt%) and add a sum of alkali constraint with an upper limit of 19.3 wt% ( $\sum \text{R}_2\text{O} < 19.3$  wt%), or
- (2) adjust the lower limit on the  $\text{Al}_2\text{O}_3$  constraint to 4 wt% ( $\text{Al}_2\text{O}_3 \geq 4$  wt%).

where  $\sum \text{R}_2\text{O}$  is the sum of the concentrations of the alkali oxides, i.e.  $\text{Cs}_2\text{O} + \text{K}_2\text{O} + \text{Li}_2\text{O} + \text{Na}_2\text{O}$ . The alkali and alumina limits in criterion 1 above are those of the Waste Form Compliance Plan (WCP) Purex glass and the criteria are not only to ensure that glasses are not phase separated but to ensure that the glass durability stays well below that of the benchmark EA glass. Recent studies on the long term durability of high alkali versus low alkali glasses has shown that high alkali glasses return to the undesirable accelerated rate of dissolution preferentially to low alkali glasses.[116, 117] Therefore, the implementation of an alkali/alumina constraint for DWPF glasses was prudent.

Historical glasses of interest to DWPF meeting criteria 1 and 2 above were found to be acceptable using a normalized boron release (NL [B]) of 10 g/L as a benchmark. This value was chosen in order to be certain that the boron releases of the study glasses were  $2\sigma$  below that of the EA glass with measurement and analytical uncertainty considered. It should be emphasized that this limit was not empirically derived and was only used as a guide to develop the  $\text{Al}_2\text{O}_3$  and/or sum or alkali criteria. Herman et al. [118] later

<sup>ξ</sup> The WL interval over which a particular glass system is considered to be acceptable based on model predictions.

demonstrated that these criteria could be used to replace the homogeneity constraint for future sludge-only batches.

With the initiation of the ARP and MCU at SRS in 2008, there was a need to revisit the DWPF homogeneity constraint for coupled operations. This constraint was specifically addressed through the variability study for Sludge Batch 5 (SB5).

In addition to variability studies, other studies [119] were conducted to better understand the homogeneity-composition relationship, which is discussed next. Raszewski and Edwards [119] conducted a reduction of constraints (ROC) study for coupled operations (ARP and MCU) and this is discussed in Section 3.0. This constraint was revisited for SWPF coupled operations and the  $\text{Al}_2\text{O}_3$  content in the ROC was found to be too low in high  $\text{TiO}_2$  containing glasses. The higher  $\text{Al}_2\text{O}_3$  ROC limit will be reported and justified in Reference 52.

### *B.2 High $\text{P}_2\text{O}_5$ Constraint*

Glasses were further screened for modeling (see Figure 2-1) and were not modeled if they contained  $>2.25$  wt%  $\text{P}_2\text{O}_5$  (Figure 2-1) as this had been shown to cause lithium phosphate phase separation and compromise glass durability.[120,121,122] High  $\text{P}_2\text{O}_5$  ( $>2.25$  wt%) concentration creates crystalline phosphate phases by crystalline phase separation (CPS). In CPS the two phases, one phosphate rich, co-exist as liquid phases in the melt and the glass cannot be quenched rapidly enough to prevent the phosphate rich liquid from crystallizing.[121, 122]

### *B.3 High $\text{B}_2\text{O}_3$ Constraint*

In 1994 Toven, et. al. [45] demonstrated that various glass durability models, whether based on thermodynamics, enthalpy or structural concepts, did not predict waste glass durability accurately when the composition of the waste glass contained  $>15\%$   $\text{B}_2\text{O}_3$  with little or no  $\text{Al}_2\text{O}_3$ . For these glasses, all the models under-predicted the glass durability significantly. Toven, et. al. [45] attributed the under prediction to phase separation and complete dissolution of a borate rich phase in the glass when the  $\text{Al}_2\text{O}_3$  content was insufficient. This was confirmed by SRNL researchers in 1995 [18,19,110] and a  $\text{B}_2\text{O}_3$  constraint of 14 wt% is imposed to be conservative.

APPENDIX C. SWPF (TiO<sub>2</sub>-only) Glass Database

Sample ID	Temp (iC)	Measured Visc (poise)	Al2O3(v)	B2O3(v)	BaO(v)	CaO(v)	Ce2O3(v)	CoO(v)	Cr2O3(v)	Cs2O(v)	CuO(v)	Fe2O3(v)	K2O(v)	La2O3(v)	Li2O(v)	MgO(v)	MnO(v)	Na2O(v)	NiO(v)	PbO(v)	RuO2(v)	SO4(v)	SiO2(v)	ThO2(v)	TiO2(v)	U3O8(v)	ZnO(v)	ZrO2(v)	Sum Oxides
SWPF-01	947	391.84	3.90	4.54	0.23	0.23	0.19	0.11	0.19	1.19	0.11	13.27	0.22	0.09	6.95	1.85	0.21	7.78	0.00	0.22	0.11	0.39	55.34	0.95	2.05	0.00	0.18	0.24	100.53
	1047	127.47																											
	1145	51.72																											
	1245	25.27																											
SWPF-02	947	380.20	3.87	4.50	0.00	2.11	0.00	0.00	0.00	0.36	0.00	4.98	0.00	0.00	6.91	0.00	4.20	7.76	2.00	0.00	0.09	0.00	55.49	0.86	1.99	4.97	0.00	0.00	100.09
	1047	120.55																											
	1145	48.54																											
	1245	23.55																											
SWPF-03	947	246.81	3.85	4.55	0.00	2.04	0.00	0.00	0.00	0.45	0.00	7.54	0.00	0.00	6.87	1.85	4.07	7.81	0.00	0.00	0.11	0.00	55.32	0.00	6.03	0.00	0.00	0.00	100.49
	1047	78.72																											
	1145	33.39																											
	1245	16.89																											
SWPF-04	947	438.09	3.86	4.54	0.20	2.11	0.30	0.05	0.19	0.69	0.10	4.96	0.24	0.06	6.84	0.00	0.21	7.75	0.00	0.23	0.11	0.32	55.62	0.00	5.90	5.51	0.19	0.21	100.20
	1047	132.21																											
	1145	52.04																											
	1245	25.21																											
SWPF-05	947	135.55	3.72	10.22	0.21	0.25	0.31	0.05	0.19	0.33	0.12	5.12	0.24	0.05	1.06	1.80	4.14	16.18	2.12	0.23	0.09	0.33	39.90	1.00	6.09	6.23	0.20	0.23	100.41
	1047	41.73																											
	1145	17.69																											
	1245	8.95																											
SWPF-06	947	252.75	3.85	10.03	0.00	0.24	0.00	0.00	0.00	0.38	0.00	5.09	0.00	0.00	6.83	0.00	0.21	9.30	0.00	0.00	0.12	0.00	54.89	0.96	1.99	6.03	0.00	0.00	99.92
	1047	84.14																											
	1145	37.05																											
	1245	19.03																											
SWPF-07	947	135.81	3.86	10.01	0.30	0.22	0.40	0.05	0.18	0.45	0.10	4.89	0.22	0.07	6.84	0.00	4.03	7.56	2.00	0.22	0.13	0.32	52.06	0.00	5.96	0.00	0.18	0.23	100.29
	1047	45.95																											
	1145	20.48																											
	1245	10.76																											
SWPF-08	Not measured		3.92	10.12	0.00	0.24	0.00	0.00	0.00	1.15	0.00	15.34	0.00	0.00	0.98	1.84	0.21	8.07	0.00	0.00	0.13	0.00	45.57	0.97	5.86	6.15	0.00	0.00	100.54
	1145	185.32																											
	1245	61.84																											
SWPF-09	947	99.50	3.75	9.99	0.00	2.00	0.00	0.00	0.00	1.24	0.00	4.84	0.00	0.00	6.81	1.87	0.22	7.96	1.94	0.00	0.10	0.00	47.39	0.00	5.69	5.76	0.00	0.00	99.56
	1047	33.73																											
	1145	14.94																											
	1245	7.83																											
SWPF-10	947	320.89	3.81	10.02	0.20	2.05	0.18	0.08	0.19	1.11	0.12	15.51	0.25	0.07	1.05	0.00	4.06	12.43	0.00	0.22	0.11	0.37	40.00	0.00	1.96	5.94	0.19	0.21	100.12
	1047	87.84																											
	1145	33.48																											
	1245	15.87																											
SWPF-11	947	841.21	5.85	10.31	0.00	0.23	0.00	0.00	0.00	1.62	0.00	4.91	0.00	0.00	1.07	0.00	0.21	18.14	1.99	0.00	0.14	0.00	53.72	0.00	1.90	0.00	0.00	0.00	100.08
	1047	244.55																											
	1145	91.30																											
	1245	43.69																											
SWPF-12	947	790.36	13.63	4.51	0.00	0.23	0.00	0.00	0.00	0.33	0.00	14.94	0.00	0.00	7.13	0.00	0.21	8.42	0.00	0.00	0.12	0.00	40.67	0.00	4.63	5.66	0.00	0.00	100.47
	1047	183.75																											
	1145	39.98																											
SWPF-13	947	580.58	13.38	4.57	0.21	0.22	0.19	0.05	0.19	1.11	0.11	4.98	0.23	0.12	6.81	1.92	4.08	8.03	0.00	0.23	0.14	0.32	45.15	0.00	1.95	6.24	0.20	0.22	100.65
	1047	162.39																											

Sample ID	Temp (°C)	Measured Visc (poise)	Al <sub>2</sub> O <sub>3</sub> (v)	B <sub>2</sub> O <sub>3</sub> (v)	BaO(v)	CaO(v)	Ce <sub>2</sub> O <sub>3</sub> (v)	CoO(v)	Cr <sub>2</sub> O <sub>3</sub> (v)	Cs <sub>2</sub> O(v)	CuO(v)	Fe <sub>2</sub> O <sub>3</sub> (v)	K <sub>2</sub> O(v)	La <sub>2</sub> O <sub>3</sub> (v)	Li <sub>2</sub> O(v)	MgO(v)	MnO(v)	Na <sub>2</sub> O(v)	NiO(v)	PbO(v)	RuO <sub>2</sub> (v)	SO <sub>4</sub> (v)	SiO <sub>2</sub> (v)	ThO <sub>2</sub> (v)	TiO <sub>2</sub> (v)	U <sub>3</sub> O <sub>8</sub> (v)	ZnO(v)	ZrO <sub>2</sub> (v)	Sum Oxides
SWPF-14	1145	60.14																											
	1245	27.56																											
	947	355.46																											
	1047	114.44	13.34	10.21	0.31	1.94	0.42	0.04	0.17	0.48	0.09	4.84	0.22	0.06	6.77	1.94	0.19	8.11	0.00	0.23	0.16	0.33	48.36	0.00	1.93	0.00	0.19	0.24	100.57
	1145	47.04																											
SWPF-15	1245	23.35																											
	947	130.24																											
	1047	43.42	13.35	10.14	0.23	1.98	0.24	0.05	0.19	1.26	0.10	4.83	0.22	0.15	6.76	0.00	3.99	8.18	0.00	0.22	0.11	0.30	40.10	0.95	5.85	0.86	0.19	0.23	100.46
	1145	19.02																											
SWPF-16	1245	9.54																											
	947	268.76																											
	1047	85.77	6.62	7.96	0.11	1.04	0.10	0.06	0.11	0.72	0.07	7.64	0.14	0.06	5.46	0.95	1.96	9.75	0.65	0.11	0.13	0.23	49.30	0.37	3.96	2.92	0.10	0.11	100.64
	1145	36.02																											
SWPF-17	1245	17.82																											
	947	718.62																											
	1047	211.47	6.31	5.93	0.06	0.66	0.06	0.04	0.05	1.09	0.04	7.51	0.09	0.03	2.64	1.41	1.17	14.84	0.51	0.06	0.12	0.16	51.02	0.24	4.90	1.52	0.06	0.06	100.56
	1145	81.40																											
SWPF-18	1245	38.05																											
	949	151.47																											
	1049	55.98	6.24	5.89	0.06	0.65	0.06	0.05	0.05	1.09	0.04	7.49	0.08	0.03	5.68	0.47	1.17	15.42	1.47	0.06	0.12	0.18	48.88	0.71	2.92	1.52	0.05	0.05	100.43
	1149	25.85																											
SWPF-19	1248	13.45																											
	947	732.25																											
	1047	209.69	6.28	5.91	0.18	1.55	0.14	0.06	0.14	0.62	0.09	7.50	0.19	0.04	2.65	0.48	3.08	14.23	0.49	0.16	0.13	0.28	51.12	0.24	2.98	1.52	0.14	0.17	100.37
	1145	80.10																											
SWPF-20	1245	37.60																											
	951	159.64																											
	1050	50.68	6.31	5.79	0.19	1.54	0.15	0.10	0.14	0.66	0.08	12.75	0.17	0.04	5.57	1.40	1.16	10.53	0.50	0.16	0.12	0.34	45.12	0.71	4.96	1.48	0.15	0.17	100.31
	1150	22.06																											
SWPF-21	1249	11.35																											
	949	254.38																											
	1049	77.92	6.18	5.78	0.06	1.56	0.06	0.05	0.05	1.02	0.05	8.09	0.09	0.03	2.57	0.47	3.16	15.39	1.50	0.05	0.13	0.18	43.46	0.71	4.97	4.57	0.05	0.05	100.27
	1149	32.17																											
SWPF-22	1248	15.62																											
	949	212.17																											
	1049	71.82	6.18	7.10	0.06	1.54	0.05	0.04	0.05	1.09	0.04	12.84	0.09	0.03	2.61	0.48	3.10	15.33	0.50	0.06	0.12	0.24	43.67	0.27	3.00	1.52	0.05	0.05	100.12
	1149	30.17																											
SWPF-23	1248	14.40																											
	949	227.87																											
	1049	72.40	6.14	8.35	0.17	0.68	0.11	0.06	0.14	0.54	0.10	7.57	0.19	0.09	2.53	1.26	1.20	15.44	0.50	0.17	0.12	0.28	43.70	0.83	4.90	4.53	0.14	0.17	99.90
	1149	31.19																											
SWPF-24	1248	15.82																											
	949	897.81																											
	1049	232.30	6.25	8.55	0.06	0.67	0.06	0.04	0.05	0.99	0.04	12.80	0.10	0.03	2.56	0.46	1.17	10.48	0.50	0.05	0.13	0.20	46.96	0.80	2.93	4.46	0.06	0.05	100.45
	1149	87.61																											
SWPF-25	1248	40.71																											
	947	134.77																											
	1047	45.82	6.17	8.64	0.06	1.61	0.06	0.04	0.06	0.55	0.03	7.48	0.09	0.03	5.52	0.46	3.11	10.34	0.50	0.06	0.11	0.15	45.36	0.81	4.82	4.43	0.05	0.05	100.60
	1145	20.21																											
SWPF-26	1245	10.47																											
	947	136.93																											
	1047	46.33	6.16	8.66	0.06	1.55	0.06	0.04	0.06	1.02	0.05	7.51	0.09	0.03	5.61	1.40	3.13	10.38	1.47	0.06	0.11	0.17	45.23	0.26	2.93	4.45	0.06	0.05	100.58
	1145	20.32																											
SWPF-	1245	10.35																											
SWPF-	949	335.40	10.88	5.74	0.06	0.69	0.07	0.05	0.05	0.59	0.05	7.54	0.10	0.03	5.47	0.49	3.13	10.53	1.45	0.05	0.13	0.17	43.94	0.27	4.86	4.03	0.06	0.05	100.47

Sample ID	Temp (iC)	Measured Visc (poise)	Al2O3(v)	B2O3(v)	BaO(v)	CaO(v)	Ce2O3(v)	CoO(v)	Cr2O3(v)	Cs2O(v)	CuO(v)	Fe2O3(v)	K2O(v)	La2O3(v)	Li2O(v)	MgO(v)	MnO(v)	Na2O(v)	NiO(v)	PbO(v)	RuO2(v)	SO4(v)	SiO2(v)	ThO2(v)	TiO2(v)	U3O8(v)	ZnO(v)	ZrO2(v)	Sum Oxides
27	1049	93.20																											
	1149	36.85																											
	1248	18.51																											
SWPF-28	949	303.41	10.88	5.85	0.06	0.68	0.06	0.04	0.06	1.00	0.04	7.71	0.09	0.03	5.29	1.41	3.17	11.09	0.50	0.05	0.13	0.16	43.76	0.82	2.96	4.59	0.06	0.05	100.53
	1049	91.66																											
	1149	38.21																											
	1248	18.79																											
	949	325.89																											
	1049	99.94																											
SWPF-29	1149	39.63	10.90	5.69	0.18	1.58	0.17	0.08	0.14	1.00	0.08	7.73	0.18	0.12	5.35	0.47	1.19	10.31	0.51	0.17	0.12	0.29	43.89	0.27	4.91	4.52	0.15	0.16	100.16
	1248	19.43																											
	949	698.13																											
SWPF-30	1049	188.65	10.96	8.64	0.18	0.67	0.20	0.07	0.14	1.07	0.09	7.49	0.17	0.07	2.61	0.46	3.05	12.43	0.49	0.16	0.13	0.28	43.88	0.82	4.93	1.52	0.15	0.17	100.83
	1149	70.95																											
	1248	33.45																											
	949	765.07																											
	1049	211.07																											
	1149	73.80																											
SWPF-31	1248	29.70	10.98	8.77	0.06	1.55	0.07	0.04	0.04	0.65	0.03	7.52	0.08	0.03	2.47	1.36	1.17	14.81	1.50	0.05	0.14	0.18	43.72	0.84	3.00	1.53	0.05	0.05	100.69
	951	399.47																											
	1050	126.06																											
	1150	51.20	6.95	5.90	0.11	1.10	0.10	0.04	0.08	0.89	0.06	7.08	0.13	0.03	5.11	0.80	1.85	10.06	0.96	0.10	0.13	0.22	50.74	0.52	4.68	2.63	0.09	0.10	100.44
	1249	25.08																											
	949	218.00																											
SWPF-33	1049	68.03	7.67	8.38	0.11	1.07	0.11	0.05	0.09	0.75	0.08	8.52	0.15	0.03	4.88	0.90	1.89	10.30	0.98	0.11	0.12	0.25	44.80	0.53	3.91	4.66	0.10	0.11	100.55
	1149	29.64																											
	1248	15.15																											
	951	433.62	10.30	6.43	0.10	0.98	0.10	0.05	0.08	0.82	0.06	6.46	0.12	0.06	3.09	1.02	1.92	15.81	0.99	0.10	0.13	0.21	45.65	0.55	3.67	1.58	0.09	0.11	100.48
	1050	139.01																											
	1150	55.70																											
SWPF-34	1249	26.93																											
	951	149.99																											
	1050	48.13																											
SWPF-35	1150	20.61	7.77	8.87	0.10	1.08	0.11	0.04	0.08	0.83	0.07	10.58	0.12	0.03	5.32	1.08	2.49	10.18	0.90	0.11	0.11	0.25	43.62	0.54	4.31	1.92	0.09	0.10	100.69
	1249	10.31																											
	951	384.31																											
SWPF-36	1050	117.67	11.34	6.53	0.13	1.10	0.10	0.06	0.08	0.90	0.06	7.00	0.13	0.04	5.37	1.05	2.02	10.37	1.09	0.10	0.13	0.23	46.39	0.56	4.13	1.27	0.11	0.11	100.40
	1150	46.34																											
	1249	22.89																											
	951	318.06																											
	1050	99.61																											
	1150	41.02																											
SWPF-37	1249	20.18	5.13	7.81	0.11	1.10	0.11	0.05	0.10	0.79	0.07	9.63	0.13	0.04	4.63	0.93	1.84	9.43	1.04	0.11	0.13	0.23	49.68	0.52	3.82	2.78	0.09	0.11	100.41
	951	370.58																											
	1050	111.17																											
SWPF-38	1150	46.40	5.54	7.63	0.10	1.05	0.10	0.04	0.09	0.75	0.07	11.28	0.13	0.03	2.26	1.00	2.27	13.32	0.99	0.10	0.13	0.25	44.93	0.56	4.02	3.63	0.09	0.09	100.43
	1249	23.51																											
	951	213.52																											
	1050	72.96	6.04	5.88	0.10	1.07	0.09	0.06	0.09	0.81	0.05	7.03	0.12	0.04	4.95	0.93	1.74	14.24	0.96	0.09	0.12	0.21	49.39	0.52	3.90	1.76	0.08	0.09	100.37
	1150	32.21																											
	1249	16.51																											
SWPF-40	951	220.34	10.85	7.73	0.13	1.19	0.13	0.04	0.10	0.85	0.07	9.42	0.14	0.03	4.55	1.02	2.72	12.87	0.92	0.11	0.11	0.26	41.65	0.55	3.86	1.40	0.11	0.13	100.96
	1050	68.14																											
	1150	28.51																											
	1249	14.05																											

Sample ID	Temp (iC)	Measured Visc (poise)	Al2O3(v)	B2O3(v)	BaO(v)	CaO(v)	Ce2O3(v)	CoO(v)	Cr2O3(v)	Cs2O(v)	CuO(v)	Fe2O3(v)	K2O(v)	La2O3(v)	Li2O(v)	MgO(v)	MnO(v)	Na2O(v)	NiO(v)	PbO(v)	RuO2(v)	SO4(v)	SiO2(v)	ThO2(v)	TiO2(v)	U3O8(v)	ZnO(v)	ZrO2(v)	Sum Oxides
SWPF-41	951	141.14	5.75	8.36	0.11	1.07	0.10	0.05	0.10	0.86	0.06	6.38	0.12	0.07	5.99	0.95	2.37	11.53	0.99	0.11	0.13	0.22	48.64	0.56	4.06	1.82	0.10	0.11	100.61
	1050	49.83																											
	1150	22.32																											
	1249	11.75																											
SWPF-42	951	696.43	5.91	6.78	0.09	1.00	0.11	0.04	0.08	0.78	0.06	6.21	0.12	0.04	2.26	0.96	1.73	14.48	0.91	0.09	0.13	0.21	50.58	0.58	3.75	3.25	0.09	0.10	100.36
	1050	203.00																											
	1150	77.88																											
	1249	36.88																											
SWPF-43	951	180.07	6.57	5.86	0.09	1.14	0.09	0.05	0.09	0.75	0.06	11.08	0.12	0.06	5.38	1.01	1.97	11.60	0.99	0.10	0.11	0.25	45.68	0.57	3.97	2.68	0.09	0.10	100.46
	1050	58.82																											
	1150	25.42																											
	1249	12.88																											
SWPF-44	951	251.26	6.83	7.24	0.10	1.21	0.11	0.05	0.08	0.76	0.08	6.67	0.13	0.07	5.02	0.96	2.37	10.59	1.01	0.11	0.12	0.23	47.61	0.57	3.98	4.40	0.10	0.11	100.50
	1050	78.34																											
	1150	33.89																											
	1249	16.98																											
SWPF-45	951	616.81	6.67	6.56	0.11	1.09	0.08	0.06	0.08	0.79	0.06	10.26	0.13	0.03	2.35	1.03	1.73	13.83	0.90	0.10	0.13	0.24	48.47	0.49	3.67	1.36	0.09	0.11	100.42
	1050	174.97																											
	1150	67.67																											
	1249	31.71																											
SWPF-46	951	237.69	6.32	6.05	0.10	1.10	0.14	0.06	0.10	0.76	0.08	6.95	0.13	0.05	3.46	0.91	1.81	15.57	1.09	0.11	0.12	0.23	46.22	0.54	3.71	4.52	0.10	0.11	100.34
	1050	79.27																											
	1150	34.27																											
	1249	16.76																											
SWPF-47	951	158.03	7.98	7.80	0.10	1.14	0.10	0.04	0.09	0.76	0.07	6.68	0.13	0.05	4.41	1.14	2.10	13.22	1.09	0.12	0.12	0.23	43.35	0.62	4.76	4.16	0.10	0.11	100.49
	1050	54.28																											
	1150	23.53																											
	1249	11.84																											
SWPF-48	951	377.85	9.28	8.04	0.11	1.13	0.10	0.04	0.06	0.87	0.06	7.18	0.11	0.06	3.75	1.06	2.37	12.47	1.12	0.10	0.13	0.22	46.11	0.59	3.84	1.49	0.09	0.10	100.49
	1050	113.77																											
	1150	46.36																											
	1249	23.17																											
SWPF-49	951	190.48	5.74	8.27	0.13	1.07	0.11	0.06	0.10	0.87	0.06	7.22	0.13	0.04	3.56	0.85	1.75	15.44	0.92	0.12	0.12	0.24	47.29	0.57	3.38	2.10	0.10	0.13	100.37
	1050	64.42																											
	1150	28.30																											
	1249	15.29																											
SWPF-50	951	200.58	11.06	6.23	0.12	1.11	0.09	0.05	0.10	0.76	0.07	6.90	0.14	0.06	5.67	0.97	2.22	12.22	0.89	0.12	0.11	0.24	42.58	0.55	3.66	4.40	0.10	0.11	100.54
	1050	62.92																											
	1150	26.42																											
	1249	13.99																											
MAX*	1249	897.81	13.38	10.31	0.31	2.05	0.42	0.10	0.19	1.62	0.12	15.51	0.25	0.15	6.81	1.94	4.08	18.14	1.99	0.23	0.16	0.37	53.72	0.95	5.85	6.24	0.20	0.24	100.96
MIN*	947	10.31	3.81	4.57	0.00	0.22	0.00	0.00	0.00	0.48	0.00	4.83	0.00	0.00	1.05	0.00	0.19	8.03	0.00	0.00	0.11	0.00	40.00	0.00	1.90	0.00	0.00	0.00	99.90

\*Where max and min refer to the glasses used for modeling and not the glasses excluded

**APPENDIX D. SWPF (TiO<sub>2</sub>-only) Validation Database**

Sample ID	Measured Visc (poise)	Temperature (°C)	Al <sub>2</sub> O <sub>3</sub> (v)	B <sub>2</sub> O <sub>3</sub> (v)	BaO(v)	CaO(v)	CdO(v)	Ce <sub>2</sub> O <sub>3</sub> (v)	Cr <sub>2</sub> O <sub>3</sub> (v)	Cs <sub>2</sub> O(v)	Fe <sub>2</sub> O <sub>3</sub> (v)	La <sub>2</sub> O <sub>3</sub> (v)	Li <sub>2</sub> O(v)	MgO(v)	MnO(v)	Na <sub>2</sub> O(v)	NiO(v)	PbO(v)	SO <sub>3</sub> (v)	SiO <sub>2</sub> (v)	TiO <sub>2</sub> (v)	ZnO(v)	ZrO <sub>2</sub> (v)	Oxide Sum
HWL-01	32.35	1203.00	10.90	7.84	0.09	1.22	0.00	0.23	0.102	0.00	13.74	0.082	5.264	0.187	1.51	10.16	0.45	0.10	0.00	44.12	1.42	0.055	0.22	97.82
	22.01	1258.50																						
	16.39	1301.17																						
	12.03	1352.00																						
	31.73	1203.00																						
	49.93	1149.50																						
	34.35	1201.17																						
HWL-02	23.79	1203.00	12.15	7.11	0.11	1.38	0.00	0.26	0.11	0.00	16.16	0.09	4.66	0.22	1.79	11.27	0.51	0.11	0.00	41.56	1.61	0.062	0.25	99.55
	16.67	1251.00																						
	11.85	1302.50																						
	8.88	1350.83																						
	23.41	1201.17																						
	37.33	1149.00																						
	25.06	1202.50																						
	23.79	1203.00																						
HWL-03	28.09	1201.3	10.83	9.92	0.10	1.21	0.00	0.24	0.10	0.00	13.53	0.09	4.37	0.20	1.49	10.15	0.48	0.10	0.00	42.09	1.47	0.06	0.23	96.79
	20.05	1250.50																						
	14.84	1295.67																						
	10.91	1350.00																						
	28.32	1202.33																						
	43.92	1149.33																						
	30.03	1201.00																						
HWL-04	26.0	1200.50	11.97	9.33	0.11	1.36	0.00	0.26	0.11	0.00	15.28	0.09	4.34	0.21	1.69	11.34	0.49	0.11	0.00	39.10	1.62	0.06	0.25	97.88
	18.21	1250.00																						
	13.31	1299.50																						
	10.16	1348.50																						
	26.77	1201.00																						
	43.04	1148.17																						



Sample ID	Measured Visc (poise)	Temperature (°C)	Al <sub>2</sub> O <sub>3</sub> (v)	B <sub>2</sub> O <sub>3</sub> (v)	BaO(v)	CaO(v)	CdO(v)	Ce <sub>2</sub> O <sub>3</sub> (v)	Cr <sub>2</sub> O <sub>3</sub> (v)	Cs <sub>2</sub> O(v)	Fe <sub>2</sub> O <sub>3</sub> (v)	La <sub>2</sub> O <sub>3</sub> (v)	Li <sub>2</sub> O(v)	MgO(v)	MnO(v)	Na <sub>2</sub> O(v)	NiO(v)	PbO(v)	SO <sub>4</sub> (v)	SiO <sub>2</sub> (v)	TiO <sub>2</sub> (v)	ZnO(v)	ZrO <sub>2</sub> (v)	Oxide Sum
	29.26	1199.83																						
HWL-05	9.09	1303.50	7.03	7.57	0.12	1.58	0.00	0.25	0.13	0.00	16.05	0.09	5.14	0.22	2.03	10.77	0.49	0.11	0.00	45.46	1.23	0.07	0.27	98.78
	6.89	1352.00																						
	17.01	1203.17																						
	25.41	1150.00																						
	38.77	1099.00																						
	61.09	1049.17																						
	27.32	1150.00																						
HWL-06	19.87	1201.00	7.69	7.30	0.12	1.74	0.00	0.27	0.16	0.00	17.62	0.10	4.77	0.24	2.25	11.68	0.57	0.11	0.00	41.82	1.38	0.08	0.30	98.41
	14.33	1252.00																						
	10.56	1303.83																						
	7.970	1351.00																						
	19.61	1201.83																						
	29.50	1148.00																						
	44.37	1099.33																						
	20.64	1201.17																						
HWL-07	18.92	1204.33	6.92	4.90	0.11	1.53	0.00	0.25	0.15	0.00	16.01	0.09	5.10	0.22	2.02	12.17	0.54	0.11	0.00	46.37	1.25	0.07	0.27	98.24
	13.90	1251.00																						
	10.19	1301.00																						
	7.82	1352.00																						
	19.71	1202.00																						
	29.57	1149.50																						
	44.11	1102.00																						
	72.67	1049.00																						
HWL-08	19.94	1203.00	7.78	4.33	0.13	1.77	0.00	0.27	0.15	0.00	16.98	0.11	4.55	0.24	2.19	13.22	0.57	0.12	0.00	42.73	1.37	0.08	0.29	97.07
	14.75	1249.00																						
	10.72	1298.50																						
	8.10	1348.00																						
	19.87	1200.00																						

Sample ID	Measured Visc (poise)	Temperature (°C)	Al2O3(v)	B2O3(v)	BaO(v)	CaO(v)	CdO(v)	Ce2O3(v)	Cr2O3(v)	Cs2O(v)	Fe2O3(v)	La2O3(v)	Li2O(v)	MgO(v)	MnO(v)	Na2O(v)	NiO(v)	PbO(v)	SO4(v)	SiO2(v)	TiO2(v)	ZnO(v)	ZrO2(v)	Oxide Sum
	29.26	1148.33																						
HWL-09	24.26	1201.00	4.53	11.91	0.07	0.84	0.00	0.18	0.08	0.00	10.37	0.06	5.42	0.13	2.84	8.00	0.60	0.10	0.00	49.36	2.25	0.03	0.72	97.58
	17.85	1249.50																						
	13.36	1298.00																						
	10.19	1347.83																						
	23.75	1201.00																						
	35.47	1146.17																						
	52.12	1100.00																						
	82.43	1049.00																						
HWL-10	22.66	1151.50	5.12	11.12	0.09	0.98	0.00	0.20	0.09	0.00	11.73	0.07	5.18	0.16	3.25	8.99	0.66	0.12	0.00	46.26	2.58	0.04	0.82	97.55
	16.03	1203.00																						
	11.90	1252.00																						
	9.04	1302																						
	23.10	1150.67																						
	34.78	1099.50																						
	53.51	1052.00																						
	23.89	1150.00																						
HWL-14	25.34	1147.00	5.86	4.46	0.10	1.14	0.00	0.22	0.09	0.00	13.15	0.08	4.68	0.18	3.78	13.88	0.71	0.12	0.00	44.39	2.82	0.04	0.82	96.64
	16.15	1198.00																						
	11.68	1250.00																						
	8.97	1299.00																						
	23.19	1148.17																						
	34.06	1100.00																						
	23.54	1148.00																						
HWL-15	58.94	1150.00	3.91	12.52	0.07	0.87	0.00	0.21	0.06	0.00	10.53	0.07	4.37	0.14	1.94	7.59	0.27	0.10	0.00	51.83	2.57	0.01	0.53	97.65
	39.78	1201.50																						
	28.50	1251.00																						
	20.45	1301.00																						
	58.67	1149.00																						
	89.67	1100.17																						

Sample ID	Measured Visc (poise)	Temperature (°C)	Al <sub>2</sub> O <sub>3</sub> (v)	B <sub>2</sub> O <sub>3</sub> (v)	BaO(v)	CaO(v)	CdO(v)	Ce <sub>2</sub> O <sub>3</sub> (v)	Cr <sub>2</sub> O <sub>3</sub> (v)	Cs <sub>2</sub> O(v)	Fe <sub>2</sub> O <sub>3</sub> (v)	La <sub>2</sub> O <sub>3</sub> (v)	Li <sub>2</sub> O(v)	MgO(v)	MnO(v)	Na <sub>2</sub> O(v)	NiO(v)	PbO(v)	SO <sub>4</sub> (v)	SiO <sub>2</sub> (v)	TiO <sub>2</sub> (v)	ZnO(v)	ZrO <sub>2</sub> (v)	Oxide Sum
HWL-16	43.05	1150.50	4.45	11.76	0.07	1.00	0.00	0.25	0.08	0.00	11.81	0.08	4.04	0.17	2.19	8.58	0.31	0.12	0.00	48.40	2.92	0.02	0.60	96.94
	28.56	1205.00																						
	20.87	1250.00																						
	14.97	1301.00																						
	42.50	1150.83																						
	64.69	1102.50																						
	107.62	1050.00																						
HWL-17	41.02	1149.50	5.05	10.57	0.09	1.15	0.00	0.28	0.08	0.00	13.61	0.09	3.66	0.19	2.54	9.46	0.36	0.14	0.00	45.73	3.35	0.02	0.70	97.19
	28.43	1200.75																						
	19.60	1247.83																						
	14.30	1297.50																						
	38.75	1149.50																						
	59.53	1099.00																						
	40.01	1148.00																						
HWL-18	39.69	1148.17	3.91	5.55	0.07	0.84	0.00	0.22	0.07	0.00	10.37	0.07	5.72	0.15	1.90	12.36	0.28	0.11	0.00	52.31	2.62	0.02	0.50	97.13
	26.62	1201.00																						
	20.05	1249.50																						
	15.21	1297.50																						
	40.22	1147.83																						
	59.78	1098.00																						
	40.35	1147.67																						
HWL-19	29.14	1150.67	4.48	5.14	0.08	1.01	0.00	0.24	0.09	0.00	11.67	0.08	5.27	0.16	2.23	13.14	0.32	0.12	0.00	49.95	2.93	0.02	0.62	97.65
	20.30	1201.50																						
	14.90	1250.00																						
	11.10	1299.00																						
	28.77	1151.00																						
	42.90	1100.67																						
	66.80	1050.50																						
	29.11	1150.83																						
HWL-	22.93	1153.33	5.08	4.74	0.08	1.16	0.00	0.27	0.10	0.00	13.45	0.09	4.88	0.18	2.53	13.52	0.36	0.13	0.00	46.16	3.28	0.02	0.66	96.81

Sample ID	Measured Visc (poise)	Temperature (°C)	Al2O3(v)	B2O3(v)	BaO(v)	CaO(v)	CdO(v)	Ce2O3(v)	Cr2O3(v)	Cs2O(v)	Fe2O3(v)	La2O3(v)	Li2O(v)	MgO(v)	MnO(v)	Na2O(v)	NiO(v)	PbO(v)	SO4(v)	SiO2(v)	TiO2(v)	ZnO(v)	ZrO2(v)	Oxide Sum
20	15.87	1205.00																						
	11.88	1252.00																						
	8.92	1302.33																						
	23.09	1153.67																						
	34.68	1102.67																						
	23.44	1152.50																						
HLW-21	45.61	1201.00																						
	32.45	1249.50																						
	23.42	1299.00																						
	67.43	1151.00	17.21	8.80	0.09	1.44	0.00	0.09	0.13	0.00	8.77	0.05	4.03	0.19	0.70	14.53	0.14	0.03	0.00	40.22	1.47	0.04	0.22	98.30
	79.36	1100.67																						
	169.30	1050.17																						
	68.69	1150.00																						
HLW-22	70.62	1147.00																						
	46.74	1199.00																						
	32.91	1246.50																						
	23.67	1295.00	18.99	7.90	0.10	1.61	0.00	0.10	0.16	0.00	9.69	0.05	3.72	0.21	0.79	15.70	0.16	0.04	0.00	37.38	1.66	0.05	0.24	98.73
	70.68	1148.00																						
	84.08	1098.00																						
	185.76	1046.33																						
FY09E M21-02	11.99	1151.50																						
	8.61	1202.5																						
	12.00	1151.00	4.11	5.18	0.08	0.01	0.25	0.36	0.01	0.13	20.23	0.09	4.03	1.46	0.26	17.05	0.01	0.18	0.49	40.38	2.06	0.13	0.20	96.70
	17.35	1100.50																						
	12.47	1150.00																						
FY09E M21-03	9.50	1145.00																						
	6.91	1197.00																						
	9.50	1146.00	6.934	4.629	0.006	0.02	0.01	0.01	0.015	0.01	13.22	0.01	6.74	1.415	4.58	14.58	0.01	0.01	0.08	40.11	4.98	0.01	0.01	97.36
	13.21	1095.83																						
	9.50	1146.00																						

Sample ID	Measured Visc (poise)	Temperature (°C)	Al <sub>2</sub> O <sub>3</sub> (v)	B <sub>2</sub> O <sub>3</sub> (v)	BaO(v)	CaO(v)	CdO(v)	Ce <sub>2</sub> O <sub>3</sub> (v)	Cr <sub>2</sub> O <sub>3</sub> (v)	Cs <sub>2</sub> O(v)	Fe <sub>2</sub> O <sub>3</sub> (v)	La <sub>2</sub> O <sub>3</sub> (v)	Li <sub>2</sub> O(v)	MgO(v)	MnO(v)	Na <sub>2</sub> O(v)	NiO(v)	PbO(v)	SO <sub>4</sub> (v)	SiO <sub>2</sub> (v)	TiO <sub>2</sub> (v)	ZnO(v)	ZrO <sub>2</sub> (v)	Oxide Sum
FY09E M21-05	45.03	1148.50	3.69	4.33	0.01	4.11	0.01	0.01	0.02	0.01	13.35	0.01	3.95	0.01	0.25	9.95	2.29	0.01	0.07	49.74	5.83	0.01	0.01	97.64
	30.74	1199.00																						
	21.20	1251.00																						
	15.04	1304.00																						
	43.57	1150.50																						
FY09E M21-06	10.90	1148.50	4.44	11.48	0.07	0.03	0.25	0.34	0.19	0.13	5.19	0.09	3.85	0.01	4.51	14.80	2.39	0.19	0.43	42.95	5.90	0.01	0.01	97.25
	8.15	1200.25																						
	10.98	1150.00																						
	15.13	1100.00																						
	11.06	1150.00																						
FY09E M21-07	4.70	1150.5	4.814	13.70	0.01	3.97	0.01	0.01	0.01	0.01	16.84	0.01	3.87	1.37	4.43	12.83	0.06	0.01	0.07	33.16	1.99	0.01	0.01	97.16
	3.73	1201.00																						
	4.70	1151.50																						
	6.49	1101.00																						
	4.70	1151.50																						
FY09E M21-08	10.19	1151.50	3.26	4.83	0.01	0.52	0.01	0.01	0.16	0.01	20.16	0.01	6.73	1.38	1.16	9.66	0.02	0.01	0.07	42.73	5.95	0.01	0.01	96.67
	7.53	1201.50																						
	10.03	1151.50																						
	14.18	1101.17																						
	10.11	1151.00																						
FY09E M21-09	15.99	1153.00	12.97	9.54	0.01	3.01	0.01	0.01	0.14	0.01	10.53	0.01	6.79	0.01	1.68	10.08	0.59	0.01	0.07	40.43	2.49	0.01	0.01	98.38
	11.56	1203.00																						
	8.47	1254.67																						
	15.83	1153.00																						
	23.04	1102.50																						
	15.91	1153.00																						
FY09E M21-11	17.49	1150.00	3.23	4.28	0.07	4.03	0.25	0.33	0.02	0.12	5.99	0.08	5.49	1.35	4.41	12.29	0.01	0.18	0.45	47.71	6.76	0.13	0.19	97.37
	12.65	1200.00																						
	9.37	1251.00																						
	17.49	1150.00																						

Sample ID	Measured Visc (poise)	Temperature (°C)	Al <sub>2</sub> O <sub>3</sub> (v)	B <sub>2</sub> O <sub>3</sub> (v)	BaO(v)	CaO(v)	CdO(v)	Ce <sub>2</sub> O <sub>3</sub> (v)	Cr <sub>2</sub> O <sub>3</sub> (v)	Cs <sub>2</sub> O(v)	Fe <sub>2</sub> O <sub>3</sub> (v)	La <sub>2</sub> O <sub>3</sub> (v)	Li <sub>2</sub> O(v)	MgO(v)	MnO(v)	Na <sub>2</sub> O(v)	NiO(v)	PbO(v)	SO <sub>4</sub> (v)	SiO <sub>2</sub> (v)	TiO <sub>2</sub> (v)	ZnO(v)	ZrO <sub>2</sub> (v)	Oxide Sum
	25.75	1099.00																						
	17.73	1149.00																						
FY09E M21-12	17.08	1154.50	4.57	5.23	0.01	0.01	0.01	0.01	0.02	0.01	15.37	0.01	6.62	0.01	3.81	9.81	1.69	0.01	0.07	46.26	1.99	0.01	0.01	95.50
	12.02	1205.00																						
	8.82	1257.00																						
	16.80	1153.33																						
	24.94	1102.00																						
	17.37	1152.67																						
FY09E M21-14	15.19	1148.83	3.217	14.97	0.08	0.04	0.25	0.34	0.14	0.13	19.62	0.09	4.34	0.01	0.24	9.77	0.01	0.19	0.43	39.42	5.60	0.13	0.19	99.20
	11.02	1199.50																						
	15.13	1150.00																						
	21.95	1099.00																						
	15.29	1149.33																						
FY09E M21-15	22.36	1154.00	5.55	4.60	0.10	3.33	0.21	0.35	0.14	0.13	7.92	0.09	5.89	1.34	4.35	9.94	2.27	0.18	0.44	49.35	1.86	0.13	0.19	98.35
	15.58	1206.00																						
	11.27	1258.00																						
	22.35	1154.83																						
	33.54	1103.00																						
	22.73	1153.50																						
FY09E M21-16	21.57	1148.50	3.74	6.62	0.08	3.84	0.23	0.35	0.15	0.13	8.74	0.09	3.99	1.41	0.25	15.27	2.34	0.19	0.43	48.08	1.97	0.14	0.20	98.21
	15.29	1202.00																						
	10.66	1259.67																						
	21.46	1150.83																						
	32.01	1098.33																						
	21.88	1148.83																						
FY09E M21-17	9.80	1152.33	7.67	4.80	0.09	0.11	0.23	0.37	0.01	0.14	13.81	0.10	7.00	0.01	0.48	15.03	0.01	0.21	0.49	41.29	6.13	0.14	0.21	98.36
	7.14	1204.00																						
	9.79	1154.50																						
	13.62	1103.33																						
	9.79	1154.50																						

Sample ID	Measured Visc (poise)	Temperature (°C)	Al <sub>2</sub> O <sub>3</sub> (v)	B <sub>2</sub> O <sub>3</sub> (v)	BaO(v)	CaO(v)	CdO(v)	Ce <sub>2</sub> O <sub>3</sub> (v)	Cr <sub>2</sub> O <sub>3</sub> (v)	Cs <sub>2</sub> O(v)	Fe <sub>2</sub> O <sub>3</sub> (v)	La <sub>2</sub> O <sub>3</sub> (v)	Li <sub>2</sub> O(v)	MgO(v)	MnO(v)	Na <sub>2</sub> O(v)	NiO(v)	PbO(v)	SO <sub>4</sub> (v)	SiO <sub>2</sub> (v)	TiO <sub>2</sub> (v)	ZnO(v)	ZrO <sub>2</sub> (v)	Oxide Sum
	9.80	1152.33																						
FY09E M21-18	54.07	1146.00	11.07	4.86	0.08	0.40	0.20	0.35	0.02	0.12	6.67	0.09	5.33	0.01	0.65	16.11	0.01	0.19	0.43	49.74	1.96	0.12	0.20	98.61
	38.27	1199.75																						
	19.17	1296.50																						
	50.57	1151.00																						
FY09E M21-19	26.51	1154.50	5.84	4.58	0.01	4.07	0.01	0.01	0.02	0.01	4.98	0.01	3.97	0.01	0.25	16.72	0.90	0.01	0.07	51.45	5.85	0.01	0.01	98.74
	18.68	1207.00																						
	13.36	1263.33																						
	26.42	1156.17																						
	39.21	1103.33																						
	26.80	1154.00																						
FY09E M21-20	27.67	1152.67	6.16	5.41	0.01	0.01	0.01	0.01	0.16	0.01	11.39	0.01	4.02	1.18	0.24	16.95	2.31	0.01	0.07	47.87	1.98	0.01	0.01	97.79
	19.47	1203.50																						
	13.72	1260.00																						
	27.59	1152.33																						
	40.79	1101.00																						
	27.98	1152.00																						
FY09E M21-21	6.19	1153.00	4.861	8.95	0.08	0.01	0.28	0.36	0.19	0.13	18.84	0.09	6.88	0.01	0.82	14.42	0.01	0.21	0.47	39.15	1.98	0.13	0.20	98.07
	4.76	1204.00																						
	6.22	1154.66																						
	8.52	1103.00																						
	6.35	1154.00																						
FY09E M21-25	29.21	1143.00	6.41	4.98	0.01	4.14	0.01	0.01	0.16	0.01	7.53	0.01	4.01	0.01	4.61	15.40	0.01	0.01	0.07	48.83	2.01	0.01	0.01	98.22
	20.42	1199.00																						
	14.43	1256.00																						
	29.09	1150.00																						
FY09E M21-27	16.06	1154.33	7.29	6.87	0.04	1.79	0.14	0.18	0.09	0.07	12.69	0.05	4.95	0.67	2.20	12.63	1.13	0.10	0.25	43.05	3.89	0.07	0.11	98.25
	11.63	1205.00																						

Sample ID	Measured Visc (poise)	Temperature (°C)	Al <sub>2</sub> O <sub>3</sub> (v)	B <sub>2</sub> O <sub>3</sub> (v)	BaO(v)	CaO(v)	CdO(v)	Ce <sub>2</sub> O <sub>3</sub> (v)	Cr <sub>2</sub> O <sub>3</sub> (v)	Cs <sub>2</sub> O(v)	Fe <sub>2</sub> O <sub>3</sub> (v)	La <sub>2</sub> O <sub>3</sub> (v)	Li <sub>2</sub> O(v)	MgO(v)	MnO(v)	Na <sub>2</sub> O(v)	NiO(v)	PbO(v)	SO <sub>4</sub> (v)	SiO <sub>2</sub> (v)	TiO <sub>2</sub> (v)	ZnO(v)	ZrO <sub>2</sub> (v)	Oxide Sum
	16.17	1154.00																						
	23.83	1103.00																						
	16.45	1154.00																						
MAX*	107.62	1347.83	12.97	11.91	0.13	4.14	0.25	0.36	0.19	0.13	20.23	0.11	6.79	1.46	4.61	17.05	2.39	0.19	0.49	51.45	5.90	0.14	0.82	98.74
MIN*	10.19	1049.00	3.74	4.33	0.01	0.01	0.00	0.01	0.01	0.00	4.98	0.01	3.66	0.01	0.24	8.00	0.01	0.01	0.00	40.38	1.25	0.01	0.01	95.50

\*Where max and min refer to the glasses used for modeling and not the glasses excluded



APPENDIX E. CST (TiO<sub>2</sub>-Nb<sub>2</sub>O<sub>5</sub>-ZrO<sub>2</sub>) Glass Model Database

Sample ID	Temp (°C)	Measured Visc (poise)	Al <sub>2</sub> O <sub>3</sub> (v)	B <sub>2</sub> O <sub>3</sub> (v)	BaO (v)	CaO(v)	Ce <sub>2</sub> O <sub>3</sub> (v)	Cr <sub>2</sub> O <sub>3</sub> (v)	CuO(v)	Fe <sub>2</sub> O <sub>3</sub> (v)	K <sub>2</sub> O(v)	La <sub>2</sub> O <sub>3</sub> (v)	Li <sub>2</sub> O(v)	MgO(v)	MnO(v)	Na <sub>2</sub> O(v)	Nb <sub>2</sub> O <sub>5</sub> (v)	NiO(v)	PbO(v)	SO <sub>4</sub> (v)	SiO <sub>2</sub> (v)	ThO <sub>2</sub> (v)	TiO <sub>2</sub> (v)	U <sub>3</sub> O <sub>8</sub> (v)	ZnO (v)	ZrO <sub>2</sub> (v)	Oxide Sum
CST 01	1197.00	48.88	2.74	8.25	0.00	0.91	0.00	0.14	0.08	9.72	0.19	0.00	4.71	0.06	1.83	8.87	0.66	0.85	0.00	0.00	55.39	0.00	2.03	2.02	0.00	0.41	98.85
	1141.00	75.70																									
	1088.00	121.82																									
	1035.00	211.70																									
	982.00	391.25																									
CST 07	1195.50	50.34	2.94	7.79	0.00	0.98	0.00	0.13	0.07	11.25	0.09	0.00	4.05	0.09	1.93	8.97	0.70	0.88	0.00	0.00	53.43	0.00	1.81	2.86	0.00	0.64	98.61
	1140.00	78.05																									
	1087.00	126.73																									
	1034.00	217.55																									
	980.50	401.17																									
CST 08	1192.50	45.31	2.96	7.24	0.00	0.93	0.00	0.12	0.08	11.14	0.09	0.00	4.17	0.09	1.89	8.45	1.28	0.87	0.00	0.00	52.27	0.00	2.68	3.04	0.00	1.14	98.43
	1138.50	70.75																									
	1085.50	115.38																									
	1032.00	200.04																									
	979.50	370.70																									
CST 09	1197.00	38.98	2.83	7.10	0.00	0.99	0.00	0.13	0.08	11.98	0.12	0.00	3.72	0.09	1.91	8.73	1.92	0.89	0.00	0.00	50.40	0.00	3.81	2.51	0.00	1.66	98.88
	1142.50	60.12																									
	1088.50	99.37																									
	1035.50	173.61																									
	982.00	324.34																									
CST 10	1199.00	42.20	2.82	7.33	0.00	0.97	0.00	0.12	0.07	10.48	0.09	0.00	4.26	0.09	1.96	9.05	0.74	0.87	0.00	0.00	52.45	0.00	2.43	3.65	0.00	0.64	98.01
	1146.00	64.62																									
	1094.00	103.29																									
	1036.50	177.95																									
	983.00	323.51																									
CST 11	1198.50	37.11	2.89	7.71	0.00	1.01	0.00	0.12	0.06	11.91	0.09	0.00	3.98	0.09	2.00	9.05	1.41	0.93	0.00	0.00	52.49	0.00	3.53	2.50	0.00	1.17	100.94
	1145.00	57.32																									
	1089.00	92.77																									
	1035.50	160.56																									
	982.50	295.24																									
CST 12	1197.50	33.97	3.00	7.53	0.00	1.02	0.00	0.14	0.09	11.70	0.09	0.00	3.91	0.10	1.87	8.66	2.03	0.92	0.00	0.00	49.47	0.00	4.50	2.65	0.00	1.64	99.32

Sample ID	Temp (°C)	Measured Visc (poise)	Al <sub>2</sub> O <sub>3</sub> (v)	B <sub>2</sub> O <sub>3</sub> (v)	BaO (v)	CaO(v)	Ce <sub>2</sub> O <sub>3</sub> (v)	Cr <sub>2</sub> O <sub>3</sub> (v)	CuO(v)	Fe <sub>2</sub> O <sub>3</sub> (v)	K <sub>2</sub> O(v)	La <sub>2</sub> O <sub>3</sub> (v)	Li <sub>2</sub> O(v)	MgO(v)	MnO(v)	Na <sub>2</sub> O(v)	Nb <sub>2</sub> O <sub>5</sub> (v)	NiO(v)	PbO(v)	SO <sub>4</sub> (v)	SiO <sub>2</sub> (v)	ThO <sub>2</sub> (v)	TiO <sub>2</sub> (v)	U <sub>3</sub> O <sub>8</sub> (v)	ZnO (v)	ZrO <sub>2</sub> (v)	Oxide Sum
	1145.00	52.92																									
	1088.50	86.87																									
	1035.50	150.16																									
	982.50	283.45																									
CST 06	1199.00	42.81	2.60	7.53	0.00	0.88	0.00	0.17	0.10	10.46	0.21	0.00	4.22	0.07	1.64	8.67	1.92	0.82	0.00	0.00	51.73	0.00	5.08	2.16	0.00	1.06	99.33
	1143.50	66.59																									
	1089.00	108.50																									
	1035.50	188.65																									
CST 14	983.00	353.10	3.90	7.40	0.00	1.21	0.00	0.15	0.09	13.87	0.18	0.00	4.01	0.08	2.30	9.65	1.32	1.08	0.00	0.00	50.58	0.00	2.91	3.22	0.00	1.26	103.22
	1197.00	35.82																									
	1142.50	55.08																									
	1088.50	90.10																									
CST 15	1036.00	156.54	4.00	6.58	0.00	1.22	0.00	0.15	0.09	13.19	0.17	0.00	3.97	0.07	2.49	9.53	1.96	1.13	0.00	0.00	49.59	0.00	3.94	2.84	0.00	1.78	102.70
	983.00	379.17																									
	1198.00	36.61																									
	1142.00	57.62																									
CST 12c	1088.50	95.92	3.01	6.60	0.00	0.92	0.00	0.17	0.10	11.23	0.19	0.00	3.89	0.07	2.06	8.75	1.89	0.96	0.00	0.00	48.19	0.00	5.05	2.32	0.00	1.33	96.73
	1200.00	34.54																									
	1144.00	53.57																									
	1091.00	87.94																									
CST 20	1037.50	152.89	6.28	8.54	0.00	0.54	0.00	0.10	0.05	7.16	0.18	0.00	4.40	0.15	1.95	8.76	1.27	0.32	0.00	0.00	55.85	0.00	3.08	0.72	0.00	0.93	100.28
	984.00	286.43																									
	1200.00	102.49																									
	1148.00	162.38																									
CST 26	1096.00	268.02	6.82	7.68	0.00	0.52	0.00	0.12	0.04	7.84	0.18	0.00	4.19	0.15	2.16	8.64	1.27	0.35	0.00	0.00	54.76	0.00	3.03	0.61	0.00	0.94	99.29
	1043.00	471.58																									
	991.00	894.41																									
	1200.00	100.55																									
	1147.00	161.21	6.82	7.68	0.00	0.52	0.00	0.12	0.04	7.84	0.18	0.00	4.19	0.15	2.16	8.64	1.27	0.35	0.00	0.00	54.76	0.00	3.03	0.61	0.00	0.94	99.29
	1090.50	267.88																									
	1037.00	474.04																									

Sample ID	Temp (iC)	Measured Visc (poise)	Al <sub>2</sub> O <sub>3</sub> (v)	B <sub>2</sub> O <sub>3</sub> (v)	BaO (v)	CaO(v)	Ce <sub>2</sub> O <sub>3</sub> (v)	Cr <sub>2</sub> O <sub>3</sub> (v)	CuO(v)	Fe <sub>2</sub> O <sub>3</sub> (v)	K <sub>2</sub> O(v)	La <sub>2</sub> O <sub>3</sub> (v)	Li <sub>2</sub> O(v)	MgO(v)	MnO(v)	Na <sub>2</sub> O(v)	Nb <sub>2</sub> O <sub>5</sub> (v)	NiO(v)	PbO(v)	SO <sub>4</sub> (v)	SiO <sub>2</sub> (v)	ThO <sub>2</sub> (v)	TiO <sub>2</sub> (v)	U <sub>3</sub> O <sub>8</sub> (v)	ZnO (v)	ZrO <sub>2</sub> (v)	Oxide Sum
	984.00	892.81																									
CST 32	1200.50	104.09	8.01	6.95	0.00	0.54	0.00	0.12	0.06	8.44	0.21	0.00	3.98	0.18	2.63	8.73	1.28	0.42	0.00	0.00	52.57	0.00	3.10	1.04	0.00	0.97	99.22
	1145.00	166.82																									
	1092.00	279.30																									
	1039.00	498.98																									
	986.00	950.84																									
KT04-01	1145.67	54.96	6.03	5.91	0.07	0.98	0.27	0.07	0.06	11.71	0.04	0.09	3.52	0.15	1.93	13.03	0.95	0.33	0.13	0.00	47.90	0.00	4.48	0.00	0.01	0.83	98.51
	1200.00	36.20																									
	1252.50	25.06																									
	1147.50	52.38																									
	1097.00	79.48																									
	1046.00	129.80																									
KT04-02	1146.50	53.16	5.46	5.87	0.07	0.99	0.28	0.08	0.05	11.34	0.04	0.06	3.57	0.16	1.73	14.07	1.05	0.19	0.11	0.00	48.65	0.00	4.61	0.00	0.04	0.94	99.37
	1148.00	45.28																									
	1203.00	30.55																									
	1254.00	21.78																									
	1149.33	45.61																									
	1099.00	69.54																									
KT04-06	1048.00	113.58	7.65	5.99	0.07	1.05	0.10	0.08	0.07	8.97	0.17	0.03	3.55	0.10	1.19	13.68	0.95	0.15	0.06	0.00	49.45	0.00	4.51	0.00	0.08	0.88	98.75
	1148.00	46.38																									
	1147.50	72.29																									
	1202.33	47.53																									
	1254.50	32.92																									
	1150.00	71.41																									
KT04-08	1100.00	110.09	5.38	5.95	0.08	0.87	0.08	0.10	0.05	9.23	0.12	0.03	3.54	0.11	0.96	15.43	1.26	0.59	0.06	0.00	49.66	0.00	5.13	0.00	0.04	1.05	99.73
	1048.50	183.10																									
	1149.83	72.94																									
	1148.00	45.60																									
	1201.17	31.48																									
	1254.00	22.75																									

Sample ID	Temp (°C)	Measured Visc (poise)	Al <sub>2</sub> O <sub>3</sub> (v)	B <sub>2</sub> O <sub>3</sub> (v)	BaO (v)	CaO(v)	Ce <sub>2</sub> O <sub>3</sub> (v)	Cr <sub>2</sub> O <sub>3</sub> (v)	CuO(v)	Fe <sub>2</sub> O <sub>3</sub> (v)	K <sub>2</sub> O(v)	La <sub>2</sub> O <sub>3</sub> (v)	Li <sub>2</sub> O(v)	MgO(v)	MnO(v)	Na <sub>2</sub> O(v)	Nb <sub>2</sub> O <sub>5</sub> (v)	NiO(v)	PbO(v)	SO <sub>4</sub> (v)	SiO <sub>2</sub> (v)	ThO <sub>2</sub> (v)	TiO <sub>2</sub> (v)	U <sub>3</sub> O <sub>8</sub> (v)	ZnO (v)	ZrO <sub>2</sub> (v)	Oxide Sum
KT04-09	1149.83	43.32	5.96	5.99	0.07	1.04	0.19	0.07	0.07	12.35	0.13	0.07	3.52	0.11	0.55	14.21	0.82	0.48	0.12	0.00	48.30	0.00	5.03	0.00	0.05	0.74	99.86
	1205.50	29.00																									
	1257.17	20.80																									
	1152.50	43.58																									
	1102.00	66.35																									
	1050.67	107.86																									
	1151.33	44.66																									
KT04-10	1146.00	48.57	5.93	5.91	0.08	1.01	0.25	0.08	0.05	13.31	0.05	0.08	3.53	0.12	0.35	13.37	0.77	0.48	0.13	0.00	47.95	0.00	4.74	0.00	0.04	0.73	98.96
	1200.00	32.81																									
	1252.00	23.09																									
	1147.83	48.47																									
	1097.00	74.69																									
	1046.00	122.52																									
	1146.83	50.28																									
KT06-01	1150.00	32.46	5.81	8.27	0.04	1.01	0.20	0.10	0.04	8.94	0.13	0.06	3.55	0.10	1.33	12.56	0.59	0.59	0.10	0.15	47.57	0.00	6.05	0.00	0.05	0.61	98.05
	1201.00	22.15																									
	1247.00	15.98																									
	1149.00	32.58																									
	1107.00	46.24																									
	1050.83	77.87																									
	1151.00	32.43																									
KT06-02	1147.33	46.78	9.79	8.29	0.02	1.82	0.10	0.05	0.05	7.15	0.06	0.03	3.51	0.04	1.09	12.50	0.06	1.13	0.05	0.15	46.88	0.00	6.08	0.00	0.04	0.15	99.04
	1198.83	31.53																									
	1246.00	22.48																									
	1145.00	47.68																									
	1103.67	67.59																									
	1047.50	114.80																									
	1147.33	38.46																									
KT06-08	1148.33	54.14	7.35	4.84	0.02	1.11	0.11	0.06	0.03	11.04	0.06	0.03	5.38	0.05	1.27	10.07	0.54	0.44	0.06	0.15	50.51	0.00	6.28	0.00	0.03	0.61	100.04
	1200.33	41.84																									
	1246.67	25.25																									
	1148.00	53.80																									
	1107.00	77.29																									
	1051.00	132.45																									

Sample ID	Temp (iC)	Measured Visc (poise)	Al <sub>2</sub> O <sub>3</sub> (v)	B <sub>2</sub> O <sub>3</sub> (v)	BaO (v)	CaO(v)	Ce <sub>2</sub> O <sub>3</sub> (v)	Cr <sub>2</sub> O <sub>3</sub> (v)	CuO(v)	Fe <sub>2</sub> O <sub>3</sub> (v)	K <sub>2</sub> O(v)	La <sub>2</sub> O <sub>3</sub> (v)	Li <sub>2</sub> O(v)	MgO(v)	MnO(v)	Na <sub>2</sub> O(v)	Nb <sub>2</sub> O <sub>5</sub> (v)	NiO(v)	PbO(v)	SO <sub>4</sub> (v)	SiO <sub>2</sub> (v)	ThO <sub>2</sub> (v)	TiO <sub>2</sub> (v)	U <sub>3</sub> O <sub>8</sub> (v)	ZnO (v)	ZrO <sub>2</sub> (v)	Oxide Sum
	1149.33	54.41																									
KT06-14	1149.00	45.89	12.13	8.25	0.03	2.17	0.12	0.06	0.02	8.36	0.06	0.03	5.43	0.06	0.46	9.45	0.10	0.14	0.06	0.15	44.91	0.00	6.20	0.00	0.02	1.84	100.05
	1200.00	30.35																									
	1246.00	21.40																									
	1146.00	46.51																									
	1106.67	66.33																									
	1049.50	115.94																									
	1148.00	46.21																									
KT06-17	1148.00	54.08	12.05	4.80	0.02	2.28	0.11	0.06	0.03	8.64	0.08	0.03	6.60	0.08	0.43	9.43	0.07	0.13	0.06	0.15	47.40	0.00	6.06	0.00	0.02	1.71	100.23
	1200.00	35.41																									
	1246.00	25.23																									
	1147.00	54.35																									
	1107.00	77.75																									
	1048.67	135.54																									
	1148.00	54.00																									
KT07-02	1144.67	46.83	5.36	6.13	0.06	0.98	0.28	0.10	0.05	11.21	0.03	0.06	3.47	0.15	1.71	14.15	1.01	0.18	0.11	0.37	48.51	0.00	4.29	0.00	0.03	0.95	99.18
	1197.67	31.03																									
	1245.00	21.98																									
	1145.00	46.83																									
	1105.00	66.49																									
	1048.00	110.34																									
	1148.33	46.10																									
KT07-06	1147.50	73.92	7.39	5.74	0.06	1.00	0.11	0.14	0.05	9.10	0.12	0.03	3.29	0.10	1.19	13.48	0.95	0.15	0.06	0.37	48.94	0.00	4.27	0.00	0.07	0.91	97.51
	1199.00	48.95																									
	1244.00	34.65																									
	1143.50	75.92																									
	1103.83	108.03																									
	1047.17	189.33																									
	1146.83	74.13																									
KT07-07	1146.00	50.55	5.67	5.87	0.07	0.93	0.08	0.15	0.05	9.32	0.08	0.03	3.40	0.11	0.72	14.02	1.13	0.62	0.07	0.39	48.94	0.00	4.77	0.00	0.08	1.03	97.53
	1198.00	33.57																									
	1245.00	26.73																									
	1145.00	51.51																									
	1104.33	73.06																									

62

Sample ID	Temp (iC)	Measured Visc (poise)	Al <sub>2</sub> O <sub>3</sub> (v)	B <sub>2</sub> O <sub>3</sub> (v)	BaO (v)	CaO(v)	Ce <sub>2</sub> O <sub>3</sub> (v)	Cr <sub>2</sub> O <sub>3</sub> (v)	CuO(v)	Fe <sub>2</sub> O <sub>3</sub> (v)	K <sub>2</sub> O(v)	La <sub>2</sub> O <sub>3</sub> (v)	Li <sub>2</sub> O(v)	MgO(v)	MnO(v)	Na <sub>2</sub> O(v)	Nb <sub>2</sub> O <sub>5</sub> (v)	NiO(v)	PbO(v)	SO <sub>4</sub> (v)	SiO <sub>2</sub> (v)	ThO <sub>2</sub> (v)	TiO <sub>2</sub> (v)	U <sub>3</sub> O <sub>8</sub> (v)	ZnO (v)	ZrO <sub>2</sub> (v)	Oxide Sum
	1101.00	54.88																									
	1049.83	89.54																									
	1152.50	35.40																									
KT08-04	1150.50	55.20	5.28	5.98	0.07	0.92	0.24	0.09	0.05	11.79	0.22	0.07	3.44	0.14	1.04	13.88	0.92	0.19	0.09	0.26	50.81	0.24	4.26	0.24	0.08	0.74	101.03
	1201.50	38.48																									
	1253.00	27.50																									
	1151.00	55.25																									
	1099.50	85.12																									
	1048.50	139.77																									
	1150.50	55.97																									
KT08-05	1151.00	76.37	7.22	6.01	0.07	0.98	0.17	0.13	0.05	9.65	0.24	0.07	3.46	0.15	1.02	13.99	0.98	0.14	0.12	0.26	51.93	0.02	4.35	0.49	0.04	0.91	102.45
	1202.50	51.29																									
	1253.17	38.00																									
	1151.50	79.13																									
	1099.50	132.61																									
	1048.00	216.09																									
	1151.00	79.94																									
KT08-06	1152.50	66.19	7.60	6.01	0.07	1.04	0.13	0.13	0.05	8.94	0.27	0.04	3.43	0.11	1.17	13.75	0.94	0.17	0.12	0.26	52.52	.0.02	4.21	0.77	0.08	0.86	102.68
	1203.83	43.96																									
	1255.50	30.26																									
	1153.00	65.42																									
	1101.50	103.69																									
	1049.50	174.40																									
KT08-10	1149.33	65.28	5.34	5.98	0.07	0.93	0.23	0.09	0.04	12.11	0.22	0.07	3.45	0.11	0.36	12.60	0.64	0.46	0.16	0.27	50.70	0.02	3.93	4.54	0.05	0.62	102.98
	1200.50	47.04																									
	1251.00	37.05																									
	1150.00	66.96																									
	1097.67	107.54																									
	1046.33	176.99																									
	1149.50	69.89																									
KT10-01	1147.67	36.14	5.50	4.98	0.06	0.88	0.25	0.09	0.04	10.91	0.04	0.08	5.39	0.14	1.78	11.29	1.35	0.30	0.13	0.00	48.24	0.00	5.98	0.00	0.01	1.17	98.59
	1200.33	24.25																									
	1247.00	17.56																									
	1146.50	36.94																									

64



Sample ID	Temp (°C)	Measured Visc (poise)	Al <sub>2</sub> O <sub>3</sub> (v)	B <sub>2</sub> O <sub>3</sub> (v)	BaO (v)	CaO(v)	Ce <sub>2</sub> O <sub>3</sub> (v)	Cr <sub>2</sub> O <sub>3</sub> (v)	CuO(v)	Fe <sub>2</sub> O <sub>3</sub> (v)	K <sub>2</sub> O(v)	La <sub>2</sub> O <sub>3</sub> (v)	Li <sub>2</sub> O(v)	MgO(v)	MnO(v)	Na <sub>2</sub> O(v)	Nb <sub>2</sub> O <sub>5</sub> (v)	NiO(v)	PbO(v)	SO <sub>4</sub> (v)	SiO <sub>2</sub> (v)	ThO <sub>2</sub> (v)	TiO <sub>2</sub> (v)	U <sub>3</sub> O <sub>8</sub> (v)	ZnO (v)	ZrO <sub>2</sub> (v)	Oxide Sum
	1141.83	34.17																									
	1102.00	48.02																									
	1045.67	81.75																									
	1145.00	33.76																									
MAX	1257.17	950.84	12.13	8.54	0.08	2.28	0.30	0.15	0.09	13.35	0.27	0.09	6.60	0.18	2.63	15.43	1.96	1.13	0.21	0.39	55.85	0.89	6.62	4.54	0.08	1.84	103.08
MIN	983.00	15.14	4.00	4.68	0.00	0.52	0.00	0.05	0.02	7.15	0.03	0.00	3.29	0.04	0.34	8.64	0.06	0.13	0.00	0.00	45.91	0.00	3.03	0.00	0.00	0.15	96.97

\*Where max and min refer to the glasses used for modeling and not the glasses excluded

## APPENDIX F. CST Glass Validation Database (KT-04 to KT-10 Studies)

Sample ID	Temp (°C)	Measured Visc (poise)	Al2O3(v)	B2O3(v)	BaO(v)	CaO(v)	Ce2O3(v)	Cr2O3(v)	CuO(v)	Fe2O3(v)	K2O(v)	La2O3(v)	Li2O(v)	MgO(v)	MnO(v)	Na2O(v)	Nb2O5(v)	NiO(v)	PbO(v)	SO4(v)	SiO2(v)	ThO2(v)	TiO2(v)	U3O8(v)	ZnO(v)	ZrO2(v)	Oxide SUM
KT04-03	1151.00	32.99	4.79	5.93	0.07	1.03	0.24	0.08	0.05	11.60	0.05	0.06	3.55	0.15	1.84	14.44	1.04	0.29	0.11	0.00	48.90	0.00	4.47	0.00	0.04	0.92	99.66
	1205.67	20.65																									
	1258.50	13.57																									
	1150.50	32.85																									
	1099.00	51.88																									
	1048.00	85.53																									
	1150.50	33.08																									
KT04-04	1148.00	48.92	5.21	5.87	0.06	0.92	0.19	0.08	0.06	11.75	0.05	0.06	3.53	0.15	1.03	13.71	0.97	0.15	0.08	0.00	49.51	0.00	4.53	0.00	0.07	0.83	98.83
	1203.00	32.87																									
	1256.00	23.11																									
	1149.50	49.08																									
	1097.67	75.39																									
	1045.00	124.32																									
	1147.33	51.04																									
KT04-05	1142.50	70.46	7.19	6.00	0.07	0.96	0.14	0.15	0.06	9.44	0.09	0.06	3.53	0.16	1.00	13.42	1.02	0.12	0.06	0.00	49.99	0.00	4.58	0.00	0.04	0.94	99.01
	1196.50	45.34																									
	1249.50	31.88																									
	1144.00	68.65																									
	1093.00	107.88																									
	1041.00	173.75																									
	1142.00	71.55																									
KT04-07	1145.00	52.04	5.96	5.93	0.07	0.93	0.08	0.11	0.04	9.40	0.11	0.03	3.55	0.11	0.71	14.28	1.12	0.62	0.06	0.00	49.28	0.00	5.00	0.00	0.08	0.99	98.48
	1199.00	35.29																									
	1251.00	25.21																									
	1145.67	52.17																									
	1093.83	79.37																									
	1041.17	129.90																									
	1142.00	53.58																									
KT06-03	1150.00	37.34	5.70	4.76	0.05	1.23	0.20	0.10	0.04	9.15	0.13	0.06	4.74	0.10	1.33	12.48	0.58	0.59	0.10	0.15	50.68	0.00	6.14	0.00	0.05	0.73	99.09
	1201.33	25.31																									
	1249.00	18.06																									
	1148.00	37.52																									
	1108.00	52.43																									
	1052.00	88.03																									

Sample ID	Temp (°C)	Measured √isc (poise)	Al2O3(v)	B2O3(v)	BaO(v)	CaO(v)	Ce2O3(v)	Cr2O3(v)	CuO(v)	Fe2O3(v)	K2O(v)	La2O3(v)	Li2O(v)	MgO(v)	MnO(v)	Na2O(v)	Nb2O5(v)	NiO(v)	PbO(v)	SO4(v)	SiO2(v)	ThO2(v)	TiO2(v)	U3O8(v)	ZnO(v)	ZrO2(v)	Oxide SUM
	1150.00	37.23																									
KT06-04	1148.50	61.95	10.02	4.91	0.02	1.84	0.09	0.05	0.04	7.39	0.07	0.02	4.78	0.04	1.12	11.22	0.08	1.13	0.05	0.15	50.24	0.00	6.21	0.00	0.04	0.19	99.68
	1201.17	40.71																									
	1247.00	28.97																									
	1147.00	61.97																									
	1107.00	88.20																									
	1050.00	152.60																									
	1150.00	61.26																									
KT06-05	1148.00	49.40	7.46	8.44	0.02	1.18	0.11	0.06	0.02	11.46	0.07	0.03	4.22	0.07	1.21	9.99	0.51	0.40	0.05	0.15	47.68	0.00	6.06	0.00	0.03	0.59	99.81
	1201.00	32.72																									
	1247.00	23.31																									
	1147.50	49.26																									
	1107.67	69.78																									
	1051.33	119.43																									
	1149.00	49.19																									
KT06-06	1148.17	41.61	5.72	8.58	0.02	1.10	0.11	0.06	0.03	12.93	0.06	0.03	4.22	0.05	1.31	9.93	0.54	0.45	0.06	0.15	49.00	0.00	6.28	0.00	0.02	0.61	101.28
	1200.00	27.83																									
	1247.00	19.81																									
	1147.00	41.31																									
	1107.00	58.12																									
	1050.50	99.17																									
	1149.00	41.64																									
KT06-07	1149.00	58.53	9.77	8.14	0.05	0.74	0.23	0.10	0.03	6.93	0.11	0.07	4.17	0.12	3.53	10.02	0.09	0.12	0.11	0.15	47.05	0.00	6.18	0.00	0.05	1.54	99.30
	1201.00	38.39																									
	1247.00	27.22																									
	1149.00	60.00																									
	1108.00	87.25																									
	1052.00	153.58																									
	1150.00	60.33																									
KT06-09	1149.33	37.91	5.71	4.86	0.02	1.11	0.11	0.05	0.02	12.28	0.07	0.03	5.42	0.05	1.24	10.54	0.51	0.40	0.05	0.15	49.96	0.00	6.17	0.00	0.02	0.58	99.35
	1201.33	25.50																									
	1247.00	17.56																									
	1148.00	36.56																									
	1108.00	51.35																									
	1049.50	88.52																									

Sample ID	Temp (tC)	Measured √isc (poise)	Al2O3(v)	B2O3(v)	BaO(v)	CaO(v)	Ce2O3(v)	Cr2O3(v)	CuO(v)	Fe2O3(v)	K2O(v)	La2O3(v)	Li2O(v)	MgO(v)	MnO(v)	Na2O(v)	Nb2O5(v)	NiO(v)	PbO(v)	SO4(v)	SiO2(v)	ThO2(v)	TiO2(v)	U3O8(v)	ZnO(v)	ZrO2(v)	Oxide SUM
	1149.00	36.81																									
KT06-10	1149.00	52.92	9.89	4.99	0.05	0.76	0.21	0.10	0.06	7.37	0.13	0.06	5.31	0.11	3.59	10.77	0.08	0.11	0.11	0.15	48.73	0.00	6.23	0.00	0.07	1.45	100.32
	1200.00	34.99																									
	1247.00	24.47																									
	1147.00	53.50																									
	1106.67	76.30																									
	1049.83	132.53																									
1149.17	52.69																										
KT06-11	1149.00	40.31	5.57	8.39	0.02	1.09	0.10	0.05	0.04	14.62	0.07	0.03	4.16	0.05	1.24	9.14	0.48	0.39	0.05	0.15	47.54	0.00	6.20	0.00	0.03	0.55	99.98
	1200.00	27.02																									
	1246.00	19.09																									
	1146.00	40.30																									
	1106.00	57.08																									
	1050.00	97.55																									
1149.00	40.53																										
KT06-12	1150.83	26.23	6.50	8.31	0.10	1.21	0.42	0.18	0.07	10.38	0.27	0.13	5.30	0.25	0.52	9.22	2.22	0.15	0.21	0.15	44.85	0.00	6.11	0.00	0.11	2.09	98.72
	1201.33	17.59																									
	1247.17	12.49																									
	1147.00	26.67																									
	1107.00	37.84																									
	1048.67	66.42																									
1150.00	26.09																										
KT06-13	1147.00	46.70	9.98	8.56	0.07	0.74	0.29	0.14	0.04	7.44	0.17	0.09	5.36	0.15	3.47	9.08	0.03	0.11	0.14	0.15	49.00	0.00	6.08	0.00	0.07	0.11	101.28
	1199.17	31.22																									
	1245.00	22.40																									
	1145.83	46.91																									
	1106.00	66.05																									
	1049.00	111.85																									
1148.00	47.45																										
KT06-15	1147.00	32.56	6.56	4.77	0.11	1.07	0.43	0.17	0.09	10.54	0.24	0.13	6.57	0.23	0.53	9.76	2.30	0.16	0.22	0.15	47.45	0.00	5.95	0.00	0.12	2.06	99.62
	1200.00	21.31																									
	1246.00	15.15																									
	1145.00	32.01																									
	1106.00	45.88																									
	1050.50	78.79																									

Sample ID	Temp (iC)	Measured Visc (poise)	Al2O3(v)	B2O3(v)	BaO(v)	CaO(v)	Ce2O3(v)	Cr2O3(v)	CuO(v)	Fe2O3(v)	K2O(v)	La2O3(v)	Li2O(v)	MgO(v)	MnO(v)	Na2O(v)	Nb2O5(v)	NiO(v)	PbO(v)	SO4(v)	SiO2(v)	ThO2(v)	TiO2(v)	U3O8(v)	ZnO(v)	ZrO2(v)	Oxide SUM
	1148.00	32.13																									
KT06-16	1149.00	46.37	10.04	4.87	0.07	0.75	0.28	0.12	0.05	7.34	0.17	0.08	6.61	0.15	3.53	9.49	0.08	0.10	0.14	0.15	50.79	0.00	6.20	0.00	0.08	0.18	101.28
	1201.00	30.70																									
	1246.00	22.31																									
	1146.00	47.07																									
	1107.00	65.62																									
	1049.33	112.76																									
	1149.83	45.86																									
KT06-18	1148.00	58.91	5.68	4.89	0.02	1.12	0.10	0.05	0.05	14.65	0.08	0.03	4.80	0.05	1.17	9.40	0.49	0.39	0.05	0.15	50.72	0.00	6.08	0.00	0.03	0.56	100.55
	1199.00	38.77																									
	1245.00	27.15																									
	1145.00	58.60																									
	1106.00	83.36																									
	1048.00	147.66																									
KT07-01	1144.00	49.12	5.77	5.97	0.06	1.01	0.28	0.10	0.06	11.68	0.03	0.09	3.47	0.15	1.93	13.01	0.90	0.33	0.15	0.37	45.99	0.00	4.17	0.00	0.01	0.83	96.37
	1196.33	32.32																									
	1244.00	22.74																									
	1143.83	48.59																									
	1104.00	68.89																									
	1046.50	119.06																									
	1145.00	48.69																									
KT07-03	1146.00	41.23	4.53	6.00	0.06	1.02	0.25	0.12	0.05	11.21	0.03	0.06	3.45	0.15	1.81	13.85	1.04	0.31	0.12	0.38	48.29	0.00	4.20	0.00	0.03	0.97	97.94
	1199.00	27.30																									
	1246.00	19.59																									
	1144.00	41.61																									
	1104.00	58.66																									
	1046.67	100.33																									
	1147.67	40.71																									
KT07-04	1148.00	48.50	5.19	5.98	0.06	0.91	0.22	0.09	0.05	11.84	0.03	0.06	3.49	0.15	1.07	13.79	0.93	0.15	0.09	0.38	48.40	0.00	4.36	0.00	0.07	0.87	98.19
	1199.67	32.03																									
	1246.00	22.73																									
	1146.00	48.68																									
	1105.50	69.07																									
	1048.83	119.68																									
	1148.50	48.44																									

Sample ID	Temp (tC)	Measured Visc (poise)	Al2O3(v)	B2O3(v)	BaO(v)	CaO(v)	Ce2O3(v)	Cr2O3(v)	CuO(v)	Fe2O3(v)	K2O(v)	La2O3(v)	Li2O(v)	MgO(v)	MnO(v)	Na2O(v)	Nb2O5(v)	NiO(v)	PbO(v)	SO4(v)	SiO2(v)	ThO2(v)	TiO2(v)	U3O8(v)	ZnO(v)	ZrO2(v)	Oxide SUM
KT07-05	1148.00	70.84	7.02	6.14	0.06	1.10	0.15	0.14	0.05	9.56	0.07	0.06	3.47	0.16	1.03	13.62	1.04	0.11	0.06	0.37	49.95	0.00	4.32	0.00	0.06	0.99	99.54
	1198.50	47.08																									
	1244.00	33.15																									
	1144.00	72.61																									
	1103.17	104.60																									
	1047.00	184.81																									
	1146.17	72.87																									
KT07-08	1147.00	41.45	5.09	6.07	0.07	0.90	0.08	0.11	0.04	9.13	0.07	0.03	3.44	0.11	0.96	14.93	1.28	0.59	0.07	0.38	48.51	0.00	4.89	0.00	0.04	1.11	97.89
	1198.00	27.95																									
	1244.33	19.99																									
	1143.67	42.32																									
	1103.67	59.57																									
	1047.00	101.61																									
	1146.67	41.48																									
KT08-07	1150.50	66.11	5.35	6.06	0.07	0.84	0.11	0.13	0.04	8.32	0.27	0.04	3.55	0.10	0.65	13.75	0.89	0.57	0.06	0.26	47.21	0.02	4.27	3.73	0.07	0.77	97.13
	1201.50	44.71																									
	1252.83	31.89																									
	1151.50	69.74																									
	1099.50	118.53																									
	1048.50	184.55																									
	1150.50	71.45																									
KT08-08	1150.00	55.75	4.59	5.89	0.06	0.74	0.10	0.09	0.05	7.94	0.25	0.03	3.47	0.09	0.82	14.02	1.11	0.51	0.12	0.26	48.67	0.02	4.18	5.22	0.04	0.90	99.16
	1201.00	38.28																									
	1252.50	27.25																									
	1150.83	58.87																									
	1099.50	93.69																									
	1048.00	157.42																									
	1150.50	60.23																									
KT08-09	1153.00	49.77	5.21	6.02	0.07	0.92	0.20	0.09	0.04	10.73	0.28	0.07	3.51	0.10	0.50	13.01	0.65	0.45	0.13	0.26	45.67	0.02	4.20	4.86	0.04	0.57	97.59
	1204.00	32.97																									
	1255.67	22.95																									
	1153.50	49.30																									
	1101.50	77.38																									
	1050.00	128.26																									
	1153.00	49.72																									

Sample ID	Temp (iC)	Measured Visc (poise)	Al2O3(v)	B2O3(v)	BaO(v)	CaO(v)	Ce2O3(v)	Cr2O3(v)	CuO(v)	Fe2O3(v)	K2O(v)	La2O3(v)	Li2O(v)	MgO(v)	MnO(v)	Na2O(v)	Nb2O5(v)	NiO(v)	PbO(v)	SO4(v)	SiO2(v)	ThO2(v)	TiO2(v)	U3O8(v)	ZnO(v)	ZrO2(v)	Oxide SUM
KT10-02	1141.17	34.46	4.93	4.89	0.06	0.89	0.26	0.08	0.03	10.35	0.04	0.05	5.34	0.14	1.55	11.95	1.30	0.17	0.10	0.00	49.90	0.00	5.95	0.00	0.03	1.14	99.16
	1194.00	23.10																									
	1241.00	16.33																									
	1139.67	34.50																									
	1099.00	48.89																									
	1041.83	83.29																									
	1142.67	33.89																									
KT10-04	1148.00	36.06	4.66	4.97	0.05	0.81	0.19	0.09	0.04	10.78	0.03	0.05	5.40	0.14	0.98	11.60	1.41	0.14	0.08	0.00	49.90	0.00	5.96	0.00	0.07	1.20	98.56
	1201.00	24.24																									
	1247.50	17.48																									
	1148.00	36.06																									
	1108.00	50.47																									
	1051.00	85.40																									
	1150.50	35.53																									
KT10-05	1148.00	48.58	6.44	4.81	0.05	0.87	0.13	0.13	0.03	8.74	0.07	0.05	5.39	0.14	0.92	11.70	1.47	0.10	0.05	0.00	50.27	0.00	6.10	0.00	0.03	1.30	98.79
	1200.17	32.39																									
	1247.00	23.17																									
	1147.00	48.93																									
	1106.33	69.69																									
	1050.00	119.45																									
	1148.67	48.69																									
KT10-07	1152.67	37.97	5.37	4.83	0.06	0.83	0.07	0.14	0.05	8.59	0.08	0.03	5.34	0.11	0.67	12.43	1.60	0.54	0.06	0.00	50.06	0.00	6.53	0.00	0.08	1.32	98.79
	1204.33	25.71																									
	1250.00	18.64																									
	1149.00	38.84																									
	1109.00	54.35																									
	1052.00	92.90																									
	1152.00	38.23																									
MAX*	1258.50	184.81	10.04	8.58	0.11	1.84	0.43	0.18	0.09	14.62	0.28	0.13	6.61	0.25	3.59	14.93	2.30	1.13	0.22	0.38	50.79	0.02	6.53	5.22	0.12	2.09	101.28
MIN*	1041.00	12.49	4.53	4.76	0.02	0.74	0.07	0.05	0.02	6.93	0.03	0.02	3.44	0.04	0.50	9.08	0.03	0.10	0.05	0.00	44.85	0.00	4.17	0.00	0.01	0.11	96.37

\*Where max and min refer to the glasses used for modeling and not the glasses excluded

## **DISTRIBUTION**

D.E. Dooley, 999-W  
A.P. Fellingner, 773-42A  
C.C. Herman, 773-A  
J.W. Amoroso, 999-W  
J.M. Bricker, 704-S  
C.L. Crawford, 773-42A  
R.E. Edwards, 766-H  
T.B. Edwards, 999-W  
B.P. Enevoldsen, 704-5Z  
T.L. Fellingner, 766-H  
K.M. Fox, 999-W  
E.J. Freed, 704-S  
C.M. Jantzen, 773-A  
F.C. Johnson, 999-W  
B.T. Geyer, 704-72S  
J.M. Gillam, 766-H  
B.A. Hamm, 766-H  
E.W. Holtzscheiter, 766-H  
J.F. Iaukea, 704-27S  
C.J. Martino, 773-42A  
J.M. Pareizs, 773-A  
D.K. Peeler, PNNL  
J.W. Ray, 704-27S  
M.A. Rios-Armstrong, 766-H  
H.B. Shah, 766-H  
M.E. Stone, 999-W  
J.R. Vitali, 704-30S  
D.L. McClane, 999-W  
C.L. Trivelpiece, 999-W



## 9.0 References

- 1 C.M. Jantzen, **"Systems Approach to Nuclear Waste Glass Development,"** J. Non-Cryst Solids, 84 [1-3], 215-225 (1986).
- 2 C.M. Jantzen, **"Relationship of Glass Composition to Glass Viscosity, Resistivity, Liquidus Temperature, and Durability: First Principles Process-Product Models for Vitrification of Nuclear Waste,"** Proceedings of the 5th International Symposium on Ceramics in Nuclear Waste Management, G.G. Wicks, D.F. Bickford, and R. Bunnell (Eds.), American Ceramic Society, Westerville, OH, 37-51 (1991).
- 3 C.M. Jantzen and K.G. Brown, **"Statistical Process Control of Glass Manufactured for the Disposal of Nuclear and Other Wastes,"** Am. Ceramic Society Bulletin, 72, 55-59 (May, 1993).
- 4 **"Preliminary Technical Data Summary for the Defense Waste Processing Facility, Stage 1,"** U.S. DOE Report DPSTD-80-38, E.I. duPont deNemours & Co., Savannah River Plant, Aiken, SC (September, 1980).
- 5 A. Applewhite-Ramsey, K.Z. Wolf, and M.J. Plodinec, **"EPA Tests of Simulated DWPF Waste Glass,"** Ceramic Transactions, V.29, A.K. Varshneya, D.F. Bickford, and P.P. Bihuniak (Eds.), Amer. Ceramic Society, Westerville, OH, 515-522 (1993).
- 6 C.M. Jantzen, J.B. Pickett, and I. Joseph, I., **"Toxic Characteristic Leaching Procedure (TCLP) Testing of Waste Glass and K-3 Refractory: Revisited,"** Environmental Issues and Waste Management Technologies in the Ceramic and Nuclear Industries V, G. T. Chandler (Eds.), Ceramic Transactions, V. 107, 271-280 (2000).
- 7 M.M. Reigel, **"Literature Review: Assessment of DWPF Melter and Melter Off-gas System Lifetime,"** SRNL-STI-2014-00134 (July 2015).
- 8 C.M. Jantzen, K.J. Imrich, K.G. Brown, and J.B. Pickett, **"High Chrome Refractory Characterization: Part I. Impact of Melt REDuction/Oxidation (REDOX) on the Corrosion Mechanism in Radioactive Waste Glass Melters,"** International Journal of Applied Glass Science, 6[2], 137-157 (2015).
- 9 C.M. Jantzen, K.J. Imrich, K.G. Brown, and J.B. Pickett, **"High Chrome Refractory Characterization: Part II. Accumulation of Spinel Corrosion Deposits in Radioactive Waste Glass Melters,"** International Journal of Applied Glass Science, 6[2], 158-171 (2015)
- 10 C.M. Jantzen and M.J. Plodinec, **"Composition and Redox Control of Waste Glasses-Recommendation for Process Control Limit,"** U.S. DOE Report DPST-86-773 (1986).
- 11 H.D. Schreiber and A.L. Hockman, **"Redox Chemistry in Candidate Glasses for Nuclear Waste Immobilization,"** J. Am. Ceram. Soc., 70[8], 591-594 (1987).
- 12 C.M. Jantzen, **"Verification and Standardization of Glass Redox Measurement for DWPF,"** U.S. DOE Report DPST- 89-222 (1989).
- 13 C.M. Jantzen, J.R. Zamecnik, D.C. Koopman, C.C. Herman, and J.B. Pickett, **"Electron**

- Equivalents Model for Controlling REDuction/OXidation (REDOX) Equilibrium During High Level Waste (HLW) Vitrification,”** U.S. DOE Report WSRC-TR-2003-00126, Rev.0 (May 2003).
- 14 C.M. Jantzen and F.C. Johnson, **“Impacts of Antifoam Additions and Argon Bubbling on Defense Waste Processing Facility (DWPF) REDuction/OXidation (REDOX),”** SRNL-STI-2011-00652 (April 2012).
  - 15 R.L. Postles and K.G. Brown, **“The DWPF Product Composition Control System (PCCS) at Savannah River: Statistical Process Control Algorithm,”** Ceramic Transactions, 23, American Ceramic Society, Westerville, OH, 559-568 (1991).
  - 16 C.M. Jantzen, **“Method for Controlling Glass Viscosity (VISCOMP™).”** U.S. Patent #5,102,439, (April, 1992).
  - 17 C.M. Jantzen **“The Impacts of Uranium and Thorium on the Defense Waste Processing Facility (DWPF) Viscosity Model,”** U.S. DOE Report WSRC-TR-2004-00311 (2005).
  - 18 C.M. Jantzen, K.G. Brown, T.B. Edwards, and J.B. Pickett, **“Method of Determining Glass Durability (THERMO™),”** U.S. Patent #5,846,278, (December 1998).
  - 19 C.M. Jantzen, J.B. Pickett, K.G. Brown, T.B. Edwards, and D.C. Beam, **“Process/Product Models for the Defense Waste Processing Facility (DWPF): Part I. Predicting Glass Durability from Composition Using a Thermodynamic Hydration Energy Reaction Model (THERMO™),”** U.S. DOE Report WSRC-TR-93-0672, Westinghouse Savannah River Co., Savannah River Technology Center, Aiken, SC, 464p. (1995).
  - 20 K.G. Brown, C.M. Jantzen, and G. Ritzhaupt, **“Relating Liquidus Temperature to Composition for Defense Waste Processing Facility (DWPF) Process Control,”** U.S. DOE Report WSRC-TR-2001-00520, Rev. 0, Westinghouse Savannah River Company, Aiken, SC (October 2001).
  - 21 C.M. Jantzen and Brown, K.G. **“Predicting the Spinel-Nepheline Liquidus for Application to Nuclear Waste Glass Processing: Part I. Primary Phase Analysis, Liquidus Measurement, and Quasicrystalline Approach,”** J. Am. Ceramic Soc., 90 [6], 1866-1879 (2007).
  - 22 C.M. Jantzen and Brown, K.G. **“Predicting the Spinel-Nepheline Liquidus for Application to Nuclear Waste Glass Processing: Part II. Quasicrystalline Freezing Point Depression Model,”** J. Am. Ceramic Soc. 90 [6], 1880-1891 (2007).
  - 23 T.H. Lorier and C.M. Jantzen, **“Evaluation of the TiO<sub>2</sub> Limit for DWPF Glass,”** U.S. DOE Report WSRC-TR-2003-00396 (October 2003).
  - 24 J.E. Miller and N.E. Brown, **“Development and Properties of Crystalline Silicotitanate (CST) Ion Exchangers for Radioactive Waste Applications,”** U.S. Govt. Report SAND97-0771, Sandia National Laboratory, Albuquerque, NM (April 1997).
  - 25 J.L. Krumhansl, P.C. Zhang, C.Jove-Colon, H.L. Anderson, R.C. Moore, F.M. Salas, T.M. Nenoff, D.A. Lucero, **“A Preliminary Assessment of IE-911 Column Pretreatment Options,”** U.S. DOE Report SAND2001-1002, Sandia National Laboratory, Albuquerque, NM (April 2001).

- 26 M.E. Smith, **“Reevaluation of DWPF High Viscosity Constraint: STRC ITS Position,”** SRT-GFM-99-0011 (April 30, 1999).
- 27 M.J. Plodinec, **“Rheology of Glasses Containing Crystalline Material,”** Advances in Ceramics, V. 20, Nuclear Waste Management II, D.E. Clark, W.B. White, and A.J. Machiels (Eds.), Am. Ceram. Soc., Westerville, OH, 117-124 (1986).
- 28 G.W. Scherer, **“Editorial Comments on a Paper by Gordon S. Fulcher,”** J. Am. Ceram. Soc, 75 [5], 1060-1062 (1992).
- 29 ASTM C965. **“Standard Practice for Measuring Viscosity of Glass Above the Softening Point,”** Annual Book of ASTM Standards, Vol. 15.02, (2012).
- 30 W.B. White and D.G. Minser, **“Raman Spectra and Structure of Natural Glasses,”** J. Non-Cryst. Solids, 67, 45-59 (1984).
- 31 E.T. Turkdogan, **Physicochemical Properties of Molten Slags and Glasses**, The Metals Society, London (1983).
- 32 B.O. Mysen, D. Virgo, C.M. Scarfe, and D.J. Cronin, **“Viscosity and Structure of Iron- and Aluminum-Bearing Calcium Silicate Melts at 1 Atm.,”** Am. Mineralogist, 70, 487-498 (1985).
- 33 B.M.J. Smets and D.M. Krol, **“Group III Ions in Sodium Silicate Glass. Part 1. X-ray Photoelectron Spectroscopy Study,”** Phys. Chem. Glasses, 25 [5], 113-118 (1984).
- 34 W.L. Konijnendijk, **“Structural Differences Between Borosilicate and Aluminosilicate Glasses Studied by Raman Scattering,”** Glastechn. Ber. 48 [10], 216-218 (1975).
- 35 T. Furukawa and W.B. White, **“Raman Spectroscopic Investigation of Sodium Borosilicate Glass Structure,”** J. Mat. Sci., 16, 2689-2700 (1981).
- 36 M. Tomozawa and S. Sridharan, **“Viscosity Increase of Phase-Separated Borosilicate Glasses,”** J. Am. Ceram. Soc. 75[11], 3103-10 (1992).
- 37 D.K. Peeler and T.B. Edwards, **“Impact of Thorium on PCCS Predictions Within the Frit 418 – SB6 System,”** SRNL-L3100-2010-00099 (2010).
- 38 K.M. Fox, et al., **“Refinement of the Nepheline Discriminator: Results of a Phase I Study,”** U.S. DOE Report WSRC-STI-2007-00659, Westinghouse Savannah River Co., Aiken, SC (November 2007).
- 39 K.M. Fox and T.B. Edwards, **“Refinement of the Nepheline Discriminator: Results of a Phase II Study,”** U.S. DOE Report SRNS-STI-2008-00099, Savannah River Nuclear Solutions, Aiken, SC (October 2008).
- 40 K.M. Fox and T.B. Edwards, **“Experimental Results of the Nepheline Phase III Study,”** U.S. DOE Report SRNS-STI-2009-00608, Savannah River Nuclear Solutions, Aiken, SC (October 2009).

- 41 D.K. Peeler and T.B. Edwards, **“Integration of SWPF into DWPF Flowsheet: Gap Analysis and Test Matrix Development,”** U.S. DOE Report SRNL-STI-2014-00578, Savannah River Nuclear Solutions, Aiken, SC (December 2014).
- 42 D.K. Peeler, T.B. Edwards, and C.M. Jantzen, **“Task Technical and Quality Assurance Plan for SWPF Integration into the DWPF – Glass Property / Model Impacts,”** U.S. DOE Report SRNL-RP-2014-00348, Savannah River National Laboratory, Aiken, South Carolina (2014).
- 43 SAS Institute, Inc., JMP Pro Version 11.2.1, SAS Institute, Inc., Cary, NC (2014).
- 44 C.M. Jantzen, **“Verification of Glass Composition and Strategy for SGM and DWPF Glass Composition Determination,”** U.S. DOE Report DPST-86-708, E.I. DuPont deNemours & Co., Aiken, SC (1986).
- 45 I. Tovená, T. Advocat, D. Ghaleb, E. Vernaz and F. Larche, **“Thermodynamic and Structural Models Compared with the Initial Dissolution Rates of SON Glass Samples,”** Sci. Basis for Nucl. Waste Mgt., XVII, A. Barkatt and R.A. Van Konynenburg (Eds.), Mat. Res. Soc., Pittsburgh, PA, 595-602 (1994).
- 46 B.C. Bunker, G.W. Arnold, D.E. Day and P.J. Bray, **“The Effect of Molecular Structure on Borosilicate Glass Leaching,”** J. Non-Cryst. Solids, **87**, 226-253 (1986).
- 47 C.M. Jantzen, K.G. Brown, and J.B. Pickett, **“Durable Glass for Thousands of Years,”** International Journal of Applied Glass Science, **1** [1], 38-62 (2010).
- 48 W. Zheng, M. Lin, J. Cheng, **“Effect of Phase Separation on the Crystallization and Properties of Lithium Aluminosilicate Glass-ceramics,”** Glass Physics and Chemistry, **39** [2], 142-149 (2013).
- 49 D.K. Peeler and T.B. Edwards, **“Impact of REDOX on Glass Durability: The Glass Selection Process,”** U.S. DOE Report WSRC-TR-2004-00135, Rev.0, Westinghouse Savannah River Co., Aiken, SC (March 2004).
- 50 D.K. Peeler and T.B. Edwards, **“Impact of REDOX on Glass Durability: Experimental Results,”** U.S. DOE Report WSRC-TR-2004-00313, Rev. 0, Westinghouse Savannah River Co., Aiken, SC (June 2004).
- 51 A.D. Cozzi, T.B. Edwards, D.K. Peeler, and D.R. Best, **“The Impact of REDOX on Durability for Sludge Batch 2,”** U.S. DOE Report WSRC-TR-2003-00246, Rev. 0, Westinghouse Savannah River Co., Aiken, SC (May 2003).
- 52 C.M. Jantzen, C.L. Trivelpiece, and T.B. Edwards, **“Defense Waste Processing Facility (DWPF) Durability and Reduction of Constraints (ROC) Assessments for High TiO<sub>2</sub> Containing Glasses,”** SRNL-STI-2016-00115 (2016).
- 53 F.C. Raszewski and T.B. Edwards, **“Reduction of Constraints for Coupled Operations,”** U.S. DOE Report SRNL-STI-2009-00465, Revision 0, Savannah River National Laboratory, Aiken, SC, (2009).

- 54 D.K. Peeler and T.B. Edwards, **"SWPF Glass Test Matrix,"** U.S. DOE Memorandum SRNL-L3100-2014-00189, Savannah River National Laboratory, Aiken, SC (August 29, 2014).
- 55 C.M. Jantzen and T.B. Edwards, **"Product/Process Models for the Defense Waste Processing Facility (DWPF): Model Ranges and Validation Ranges for Future Processing"** U.S. DOE Report SRNL-STI-2014-00320, Rev. 0 (September 2015).
- 56 C.M. Jantzen, **"Characterization of Defense Waste Processing Facility (DWPF) Startup Frit,"** U.S. DOE Report WSRC-RP-89-18, Westinghouse Savannah River Co., Aiken, SC (1989).
- 57 J.V. Crum, R.L. Russell, M.J. Schweiger, D.E. Smith, J.D. Vienna, T.B. Edwards, D.K. Peeler, R. F. Schumacher, and R.J. Workman, **"DWPF Startup Frit Viscosity Measurement Round Robin Results,"** PNNL Report (2001).
- 58 D.K. Peeler, T.B. Edwards, R.J. Workman, and I.A. Reamer, **"The Impact of Waste Loading on Viscosity in the Frit 418-SB3 System,"** U.S. DOE Report WSRC-TR-2004-00429, Rev. 0, Westinghouse Savannah River Co., Aiken, SC (August 2004).
- 59 S.L. Marra, and C.M. Jantzen, **"Characterization of Projected DWPF Glasses Heat Treated to Simulate Canister Centerline Cooling,"** U.S. DOE Report WSRC-TR-92-142, Westinghouse Savannah River Co., Savannah River Technology Center, Aiken, SC (May, 1992).
- 60 C.M. Jantzen, N.E. Bibler, D.C. Beam, C.L. Crawford, C.L., S.L. Marra, A.A. Ramsey, and M.A. Pickett, **"Development and Characterization of the Defense Waste Processing Facility (DWPF) Waste Compliance Plan (WCP) Glasses,"** US DOE Report WSRC-TR-93-181, Westinghouse Savannah River Co., Savannah River Technology Center, Aiken, SC (in preparation 2006). (See also reference 63).
- 61 T.B. Edwards, J.R. Harbour, R.F. Schumacher, and R.J. Workman, **"Measurement of DWPF Glass Viscosity – Final Report,"** U.S. DOE Report WSRC-RP-99-01053, Westinghouse Savannah River Co., Aiken, SC (November 1999).
- 62 C.M. Jantzen, **"Sharp-Shurtz (Owens Corning Fiberglass) Data on DWPF Glass,"** DWPT-QA-90-1025 (WSRC-NB-90-394).
- 63 P. R. Hrma, G. F. Peipel, M. J. Schweiger, D. E. Smith, D. S. Kim, P. E. Redgate, J. D. Vienna, C. A. LoPresti, D. B. Simpson, D. K. Peeler, and M. H. Langowski, **"Property/Composition Relationships for Hanford High-Level Waste Glasses Melting at 1150°C, Vols. 1 and 2";** U.S. DOE Report PNL-10359, Battelle Memorial Institute, Pacific Northwest Laboratory, Richland, WA, (December 1994).
- 64 P.D. Soper and D.F. Bickford, **"Physical Properties of Frit 165/Waste Glasses,"** U.S. DOE Report DPST-82-899, E.I. DuPont deNemours & Co., Savannah River Laboratory, Aiken, SC (October 5, 1982).
- 65 T.B. Edwards, J.R. Harbour, and R.J. Workman, **"Summary of Results for CST Glass Study: Composition and Property Measurements,"** U.S. DOE WSRC-TR-99-00324, Westinghouse Savannah River Co., Aiken, SC (September 1999).

- 66 T.B. Edwards, J.R. Harbour, and R.J. Workman, **“Composition and Property Measurements for CST Phase 1 Glasses,”** U.S. DOE WSRC-TR-99-00245, Westinghouse Savannah River Co., Aiken, SC (July 1999).
- 67 T.B. Edwards, J.R. Harbour, and R.J. Workman, **“Composition and Property Measurements for CST Phase 2 Glasses,”** U.S. DOE WSRC-TR-99-00289, Westinghouse Savannah River Co., Aiken, SC (August 1999).
- 68 T.B. Edwards, J.R. Harbour, and R.J. Workman, **“Composition and Property Measurements for CST Phase 3 Glasses,”** U.S. DOE WSRC-TR-99-00291, Westinghouse Savannah River Co., Aiken, SC (August 1999).
- 69 T.B. Edwards, J.R. Harbour, and R.J. Workman, **“Composition and Property Measurements for CST Phase 4 Glasses,”** U.S. DOE WSRC-TR-99-00293, Westinghouse Savannah River Co., Aiken, SC (August 1999).
- 70 T.B. Edwards, J.R. Harbour, and R.J. Workman, **“Summary of Results for PHA Glass Study: Composition and Property Measurements,”** U.S. DOE WSRC-TR-99-00332, Westinghouse Savannah River Co., Aiken, SC (September 1999).
- 71 T.B. Edwards, J.R. Harbour, and R.J. Workman, **“Composition and Property Measurements for PHA Phase 1 Glasses,”** U.S. DOE WSRC-TR-99-00262, Westinghouse Savannah River Co., Aiken, SC (August 1999).
- 72 T.B. Edwards, J.R. Harbour, and R.J. Workman, **“Composition and Property Measurements for PHA Phase 1 Glasses,”** U.S. DOE WSRC-TR-99-00290, Westinghouse Savannah River Co., Aiken, SC (August 1999).
- 73 T.B. Edwards, J.R. Harbour, and R.J. Workman, **“Composition and Property Measurements for PHA Phase 3 Glasses,”** U.S. DOE WSRC-TR-99-00292, Westinghouse Savannah River Co., Aiken, SC (August 1999).
- 74 T.B. Edwards, J.R. Harbour, and R.J. Workman, **“Composition and Property Measurements for PHA Phase 4 Glasses,”** U.S. DOE WSRC-TR-99-00294, Westinghouse Savannah River Co., Aiken, SC (August 1999).
- 75 P.B. Macedo, S.M. Finger, A.A. Barkatt, I.L. Pegg, X. Feng, and W.P. Freeborn, **“Durability Testing with West Valley Borosilicate Glass Composition – Phase II,”** DOE/NE/44139-48 (June 1988).
- 76 D. McPherson, I. Joseph, A. Mathur, C. Capozzi, S. Armstrong, and L.D. Pye, **“The Influence of Waste Variability on the Properties and Phase Stability of West Valley Reference Glass,”** U.S. DOE Report DOE/NE/44139-29 (September 1987).
- 77 C.M. Jantzen, K.G. Brown, J.B. Pickett, and G.L. Ritzhaupt, **“Crystalline Phase Separation in Phosphate Containing Waste Glasses: Relevance to INEEL HAW,”** WSRC-TR-2000-00339 (September 2000).

- 78 D.K. Peeler and T.B. Edwards, **“The Impact of Higher Waste Loading on Glass Properties: The Effects of Uranium and Thorium,”** U.S. DOE Report WSRC-TR-2003-00386, Rev. 0, Westinghouse Savannah River Co., Aiken, SC (September 2003).
- 79 C.M. Jantzen and J.B. Pickett, **“M-Area Mixed Waste Glasses: II. Durability and Viscosity Testing of High Aluminum and Uranium Containing Borosilicate Waste Glasses,”** U.S. DOE Report SRNL-STI-2011-00702, Savannah River National Laboratory, Aiken, SC (2015).
- 80 P. Hrma, J. D. Vienna, M. Mika, J. V. Crum, and G. F. Piepel, **“Liquidus Temperature Data for DWPF Glass,”** U.S. DOE Report PNNL-11790, Pacific Northwest National Laboratory, Richland, WA (1999).
- 81 K.M. Fox and T.B. Edwards, **“Summary of FY11 Sulfate Retention Studies for Defense Waste Processing Facility Glass,”** U.S. DOE Report SRNL-STI-2012-00152, Savannah River National Laboratory, Aiken, SC (2012).
- 82 F.C. Raszewski, T.B. Edwards, and D.K. Peeler, **“Matrix 2 Results of the FY07 Enhanced DOE High-Level Waste Melter Throughput Studies at SRNL,”** U.S. DOE Report SRNS-STI-2008-00055, Rev. 0, Savannah River National Laboratory, Aiken, SC (2008).
- 83 F.C. Raszewski and T.B. Edwards, **“Results of the FY09 Enhanced DOE High-Level Waste Melter Throughput Studies at SRNL,”** U.S. DOE Report, SRNL-STI-2009-00778, Rev. 0, Savannah River National Laboratory, Aiken, SC (2010).
- 84 K.M. Fox and T.B. Edwards, **“Impacts of Small Column Ion Exchange Streams on DWPF Glass Formulation: KT01, KT02, KT03, and KT04-Series Glass Compositions,”** U.S. DOE Report SRNL-STI-2010-00566, Savannah River National Laboratory, Aiken, SC (2010).
- 85 K.M. Fox and T.B. Edwards, **“Impacts of Small Column Ion Exchange Streams on DWPF Glass Formulation: KT05 and KT06-Series Glass Compositions,”** U.S. DOE Report SRNL-STI-2010-00687, Savannah River National Laboratory, Aiken, SC (2010).
- 86 K.M. Fox and T.B. Edwards, **“Impacts of Small Column Ion Exchange Streams on DWPF Glass Formulation: KT07-Series Glass Compositions,”** U.S. DOE Report SRNL-STI-2010-00759, Savannah River National Laboratory, Aiken, SC (2010).
- 87 K.M. Fox and T.B. Edwards, **“Impacts of Small Column Ion Exchange Streams on DWPF Glass Formulation: KT08, KT09, and KT10-Series Glass Compositions,”** U.S. DOE Report SRNL-STI-2011-00178, Savannah River National Laboratory, Aiken, SC (2011).
- 88 C.A. Cicero and J.M. Pareizs, **“Viscosity Data from DWPF REDOX Studies,”** U.S. DOE Report SRT-GFM-97-003, Rev. 1, Westinghouse Savannah River Co., Aiken, SC (February 1997).
- 89 J.V. Crum, T.B. Edwards, R.L. Russell, P.J. Workman, M.J. Schweiger, R.F. Schumacher, D.E. Smith, D.K. Peeler, and J.D. Vienna, **“DWPF Startup Frit Viscosity Measurement Round Robin Results,”** J. Am. Ceram. Soc. 95[7], 2196-2205 (2012).
- 90 C.A. Cicero, **“Viscosity Data from DWPF REDOX Studies,”** Memorandum, SRT-GFM-97-003, Rev. 1, Westinghouse Savannah River Co., Aiken, SC (February, 1997).

- 91 R.F. Schumacher, **“Testing of Harrop Viscometer for Viscosity Determinations,”** U.S. DOE Report, WSRC-TR-2000-0097, Westinghouse Savannah River Co., Aiken, SC (April 2000).
- 92 T.B. Edwards, J.R. Harbour, R.F. Schumacher, and R.J. Workman, **“Measurement of DWPF Glass Viscosity – Final Report,”** U.S. DOE Report WSRC-RP-99-01053, Westinghouse Savannah River Co., Aiken, SC (November 1999).
- 93 D.F. Bickford, A.A. Applewhite-Ramsey, C.M. Jantzen, and K.G. Brown, **“Control of Radioactive Waste Glass Melters: I, Preliminary General Limits at Savannah River,”** J. Am. Ceram. Soc, 73 [10] 2896-2902 (1990).
- 94 W.K. Kot and I.L. Pegg, **“Letter Report Fabrication of High-Titanium Glasses to Support Salt Waste Processing Facility (SWPF) Gap Analysis Study,”** VSL-15L3500-1 (March 20, 2015).
- 95 C.M. Jantzen, N.E. Bibler, D.C. Beam, and M.A. Pickett, **“Characterization of the Defense Waste Processing Facility (DWPF) Environmental Assessment (EA) Glass Standard Reference Material,”** U.S. DOE Report WSRC-TR-92-346, Rev. 1, Westinghouse Savannah River Company, Aiken, SC (1993).
- 96 C.M. Jantzen, N.E. Bibler, D.C. Beam, and M.A. Pickett, **“Development and Characterization of the Defense Waste Processing Facility (DWPF) Environmental Assessment (EA) Glass Standard Reference Material,”** Environmental and Waste Management Issues in the Ceramic Industry, Ceramic Transactions, 39, American Ceramic Society, Westerville, OH, 313-322 (1994).
- 97 T.B. Edwards and K.M. Fox, **“Evaluations of the Measurements of Chemical Composition, Viscosity, and Density of the SWPF Study Glasses with High Concentrations of Titanium,”** U.S. DOE Report SRNL-TR-2016-00094 (2016).
- 98 W.K. Kot and I.L. Pegg, **“Letter Report Measurements of Glass Density and Melt Viscosity to Support Salt Waste Processing Facility (SWPF) Gap Analysis Study,”** VSL-15L3500-2 (August 28, 2015).
- 99 M.B. Volf, **“Chemical Approach to Glass,”** Glass Science and Technology, V. 7, Elsevier Science Publishing Co., Inc, New York, 594 pp (1984).
- 100 G.E. Brown, Jr., F. Farges, and G. Calas, **“X-Ray Scattering and X-Ray Spectroscopy Studies of Silicate Melts,”** Structure, Dynamics and Properties of Silicate Melts, J.F. Stebbins, P.F. McMillan, and D.B. Dingwell (Eds.), Reviews in Mineralogy, V.32, 317-410 (1995).
- 101 M.J. Plodinec, **“Improved Glass Compositions for Immobilization of SRP Waste,”** Sci. Basis for Nuclear Waste Management, II, J.M. Clyde Northrup, Jr., Plenum Press, New York, 223-229 (1980).
- 102 F. Marumo, Y. TTabira, T. Mabuckhi, and H. Morikawa, **“Coordination of Transition Metals in Amorphous Silicates,”** in Dynamic Processes of Material Transport and Transformation in the Earth’s Interior, F. Marumo (Ed.) 53-65, Terra Scientific, Tokyo (1990).
- 103 K.G. Brown, R.L. Postles, and T.B. Edwards, **“SME Acceptability Determination for DWPF Process Control,”** WSRC-TR-95-00364, Revision 5 (September 2006).



- 104 H. Scheffé, “**The Analysis of Variance**,” John Wiley & Sons, New York (1959).
- 105 N.R. Draper, and H. Smith, “**Applied Regression Analysis**,” Second Edition John Wiley & Sons, New York (1981).
- 106 J.H. Lopes, A. Magalhaes, I.O. Mazali, and C.A. Bertran, “**Effect of Niobium Oxide on the Structure and Properties of Melt-Derived Bioactive Glasses**,” J. Am. Ceram. Soc. 97[12], 3843-3852 (2014).
- 107 K.M. Fox and T.B. Edwards, “**Refinement of the Nepheline Discriminator: Results of a Phase II Study**,” SRNS-STI-2008-00099 (October 2008).
- 108 J.W. Amoroso, “**The Impact of Kinetics on Nepheline Formation in Nuclear Waste Glass**,” SRNL-STI-2011-00051 (March 2011).
- 109 T. Advocat, J.L. Crovisier, J.L. Dussossoy, and E. Vernaz, “**Effects of MgO on the Short and Long-Term Stability of R7T7 and M7 Nuclear Waste Glass in Aqueous Media**,” Sci. Basis of Nuclear Waste Management, MRS Proceeding Vol. 294, 177-182 (1993).
- 110 C.M. Jantzen and K.G. Brown, “**Impact of Phase Separation on Waste Glass Durability**,” Environmental Issues and Waste Management Technologies in the Ceramic and Nuclear Industries, V, G. T. Chandler (Eds.), Ceramic Transactions, V. 107, 289-300 (2000).
- 111 D.K. Bailey and J.F. Schairer, “**The System  $\text{Na}_2\text{O}-\text{Al}_2\text{O}_3-\text{Fe}_2\text{O}_3-\text{SiO}_2$  at 1 Atmosphere, and the Petrogenesis of Alkaline Rocks**,” Journal of Petrology, 7[1], 114-170 (1966).
- 112 I. M.H. Hager and W. Hinz, “**Beitrag zur Phasentrennung in Glasern der Systemme  $\text{Na}_2\text{O}-\text{SiO}_2-\text{B}_2\text{O}_3$  and  $\text{Na}_2\text{O}-\text{SiO}_2-\text{Al}_2\text{O}_3$** ,” Silikatechnik, 18 [11], 360 (1967).
- 113 J.A. Topping and M.K. Murthy, “**Effect of Small Additions of  $\text{Al}_2\text{O}_3$  and  $\text{Ga}_2\text{O}_3$  on the Immiscibility Temperature of  $\text{Na}_2\text{O}-\text{SiO}_2$  Glasses**,” J. Am. Ceram. Soc., 56[5] 270-275 (1973).
- 114 K.G. Brown and T.B. Edwards, “**Definition of the DWPF Homogeneity Constraint**,” U.S. DOE Report WSRC-TR-95-0060, Westinghouse Savannah River Company, Aiken, SC (1995).
- 115 T.B. Edwards and K.G. Brown, “**Evaluating the Glasses Batched for the Tank 42 Variability Study**,” Westinghouse Savannah River Company, Aiken, SC, SRT-SCS-98-017, Revision 0 (1998).
- 116 C.M. Jantzen, C.L. Crawford, J.M. Pareizs, and J.B. Pickett, “**Accelerated Leach Testing of GLASS (ALTGLASS): I. The Database and Definition of High Level Waste (HLW) Glass Hydrogels**” (accepted to International Journal of Applied Glass Science SRNL-STI-2014-00274).
- 117 C.M. Jantzen, C.L. Crawford, J.M. Pareizs, and J.B. Pickett, “**Accelerated Leach Testing of GLASS (ALTGLASS): II. Mineralization of Hydrogels by Leachate Strong Bases**” (accepted to International Journal of Applied Glass Science SRNL-STI-2014-00381).
- 118 C.C. Herman, T.B. Edwards, D.M. Marsh, and R.J. Workman, “**Reduction of Constraints: Phase 2 Experimental Assessment for Sludge-Only Processing**,” U.S. DOE Report WSRC-TR-2002-00482, Revision 0, Savannah River National Laboratory, Aiken, SC (2002).

- 119 F.C. Raszewski and T.B. Edwards, **“Reduction of Constraints for Coupled Operations,”** U.S. DOE Report SRNL-STI-2009-00465, Revision 0, Savannah River National Laboratory, Aiken, SC, (2009).
- 120 C.M. Jantzen, **“Phosphate Additions to Borosilicate Waste Glass Cause Phase Separation,”** U.S. DOE Report DPST-86-389, E.I. DuPont deNemours & Co., Savannah River Laboratory, Aiken, SC (1986).
- 121 C.M. Jantzen, K.G. Brown, and J.B. Pickett, **“Impact of Phase Separation on Durability in Phosphate Containing Borosilicate Waste Glass for INEEL,”** Environmental Issues and Waste Management Technologies, D.R. Spearing, G.L. Smith, and R.L. Putnam (Eds.), Ceramic Transactions, V. 119, Amer. Ceram. Soc., Westerville, OH, VI, 271-280 (2001).
- 122 C.M. Jantzen, K.G. Brown, J.B. Pickett, and G.L. Ritzhaupt, **“Crystalline Phase Separation in Phosphate Containing Waste Glasses: Relevance to INEEL HAW,”** WSRC-TR-2000-00339 (September 2000).